
Read the Docs Template Documentation

Release 1.0

Read the Docs

Aug 15, 2019

Contents

1	Introduction	1
2	Fundamentals	3
2.1	Near-Field and Far-Field	3
2.2	Electromagnetic Spectrum	3
2.3	Antenna Types	7
2.4	Magnetic Testing	10
2.5	VLF & LF Antenna	10
2.6	Shielding	11
3	Small Loops	13
3.1	Introduction	13
3.2	Radiated Fields	14
3.3	Loop Geometry	15
3.4	Impedance of a Small Loops	15
3.5	Receiving Signal	16
3.6	Signal to Noise Ratio (SNR)	16
4	EM Modeling	21
4.1	Magnetic Dipole Moment	21
4.2	Effective Height (Length)	24
4.3	Directivity and Efficiency	25
4.4	Quality Factor	30
4.5	Losses	30
4.6	Near field Propagation	32
4.7	Antenna Gain	33
5	Circuit Modeling	35
5.1	Complete Model	35
5.2	Circuit Model of Loop Antennas	37
5.3	Radiation Resistance	42
5.4	Coil Resistance	42
5.5	Coil Inductance	46
5.6	Coil capacitance	51
5.7	Impedance Matching	51
5.8	Self Resonance Frequency	53

6	Magnetic Core Loops	55
6.1	Introduction	55
6.2	History	59
6.3	Radiated Fields	61
6.4	Magnetic Cores	61
6.5	Demagnetization Factor	65
6.6	Induced Voltage and Power	71
6.7	Core Loss	73
6.8	Radiation Resistance	74
6.9	Relative Effective Permeability	75
7	Applications	79
7.1	Biomedical Implant	79
7.2	Magnetometer	79
7.3	Marker Beacon	80
7.4	Radio Direction Finder	80
7.5	Radio Receiver Antenna	80
7.6	Real-time Locating System	81
7.7	RFID	81
7.8	Underwater Loop Antenna	81
7.9	Wireless Power Transfer	82
8	Eddy Currents	85
8.1	Multifield Eddy Current Effect	85
9	Electric Dipole Antennas	87
9.1	Circuit Model of Dipole Antenna	87
10	Fundamental Limit	89
11	Lossy Medium	91
11.1	Power Loss	91
12	Magnetically Shielded Wire	93
13	Mutual Inductance	95
14	Nomenclature	97
14.1	Derivations from other quantities	98
15	Abbreviations	99
16	References	101
17	Fingerprints of Papers	103
18	Dictionary	105
18.1	Aperture (of an antenna)	105
18.2	Balanced Line	105
18.3	Balun	106
18.4	Chu Limit	106
18.5	Coupling Coefficient	106
18.6	Like and Unlike Antennas	106
18.7	Magnetic susceptibility	106
18.8	Modal Analysis	107
18.9	Orthogonal Signals	107

18.10 Torquer	107
18.11 Unbalanced Line	107
19 Useful Links	109
20 Journals	111
Bibliography	113

In the case of loop antennas, the dipole consists of a usually circular or rectangular current loop which acts like a coil and functions in response to the magnetic component of the electromagnetic field [49].

A small loop (circular or square) is equivalent to an infinitesimal magnetic dipole whose axis is perpendicular to the plane of the loop. That is, the fields radiated by an electrically small circular or square loop are of the same mathematical form as those radiated by an infinitesimal magnetic dipole [8].

Loop antennas can be separated into two categories: small loops and large loops, as seen in Fig. 1.1.

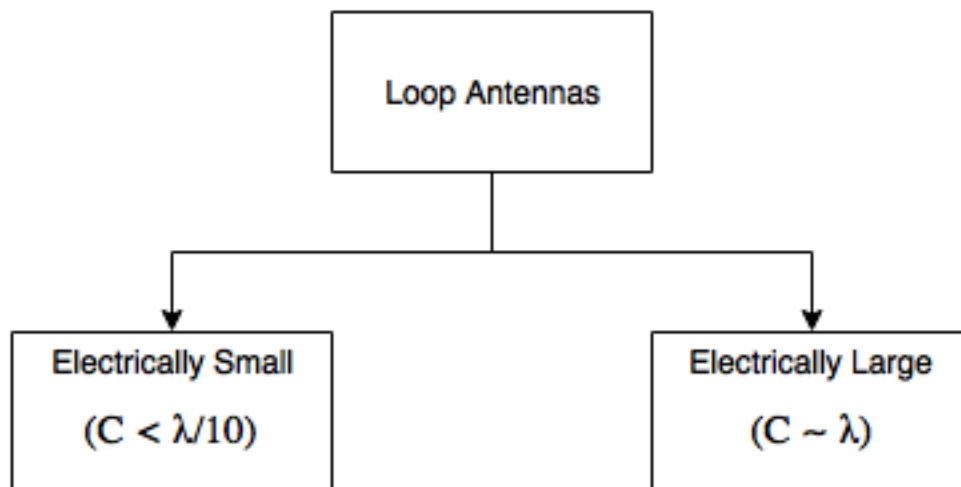


Fig. 1.1: : Loop Antennas

- **Electrically small loops:** overall length (circumference) less than about one-tenth of a wavelength.
 - Small radiation resistance that are usually smaller than their loss resistances. They are very poor radiators and usually in the receiving mode [8].

- The radiation resistance of the loop can be increased by increasing (electrically) its perimeter and/or the number of turns. Another way is to insert a ferrite core [8].
- In view of their small dimensions the current in the entire loop can be regarded as locally constant. Consequently, they generate the same sort of field as a Hertzian dipole, i.e. a very short electrical antenna on which the current distribution is a function of position to an equally small extent [49]. The field pattern of electrically small antennas of any shape is similar to that of an infinitesimal dipole [8].
- Used as probes for field measurements, directional antennas for radiowave navigation [8].
- **Electrically large loops:** circumference is about a free-space wavelength.
 - Used primarily in directional arrays.
 - To achieve such directional pattern characteristics, the circumference (perimeter) of the loop should be about one free-space wavelength.

They have become less significant as transmitting antennas for frequencies below 30 MHz. An exception to this is the tuned transmitting loop, which can be equipped with a remotely controlled capacitor to make a resonant circuit (a receiving loop can be provided with additional selectivity and sensitivity in the same way). However, such loops are extremely narrowband systems and therefore have to be retuned whenever the frequency is changed [49].

2.1 Near-Field and Far-Field

Far-field and near-field describe fields around any electromagnetic source such as antennas. Therefore, two regions and a boundary between them exist around an antenna. Sometimes near-field is divided into two sub-regions. These two- and three-region models are shown Fig. 2.1. Furthermore, various far field definitions can be found in the literature depending on the application area. Fig. 2.2 shows the definitions of near- and far-field boundary. A good discussion about near- and far-field definitions can be read in [12].

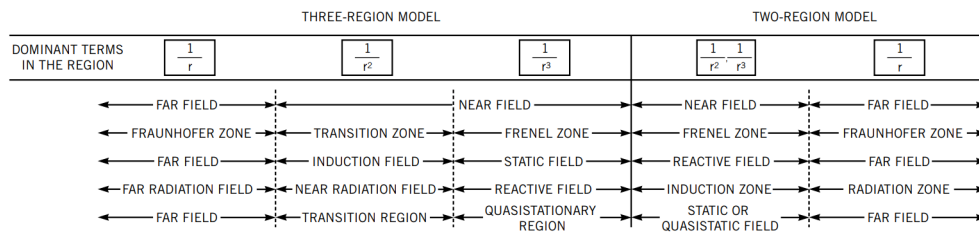


Fig. 2.1: : Two- and three-region models.

2.2 Electromagnetic Spectrum

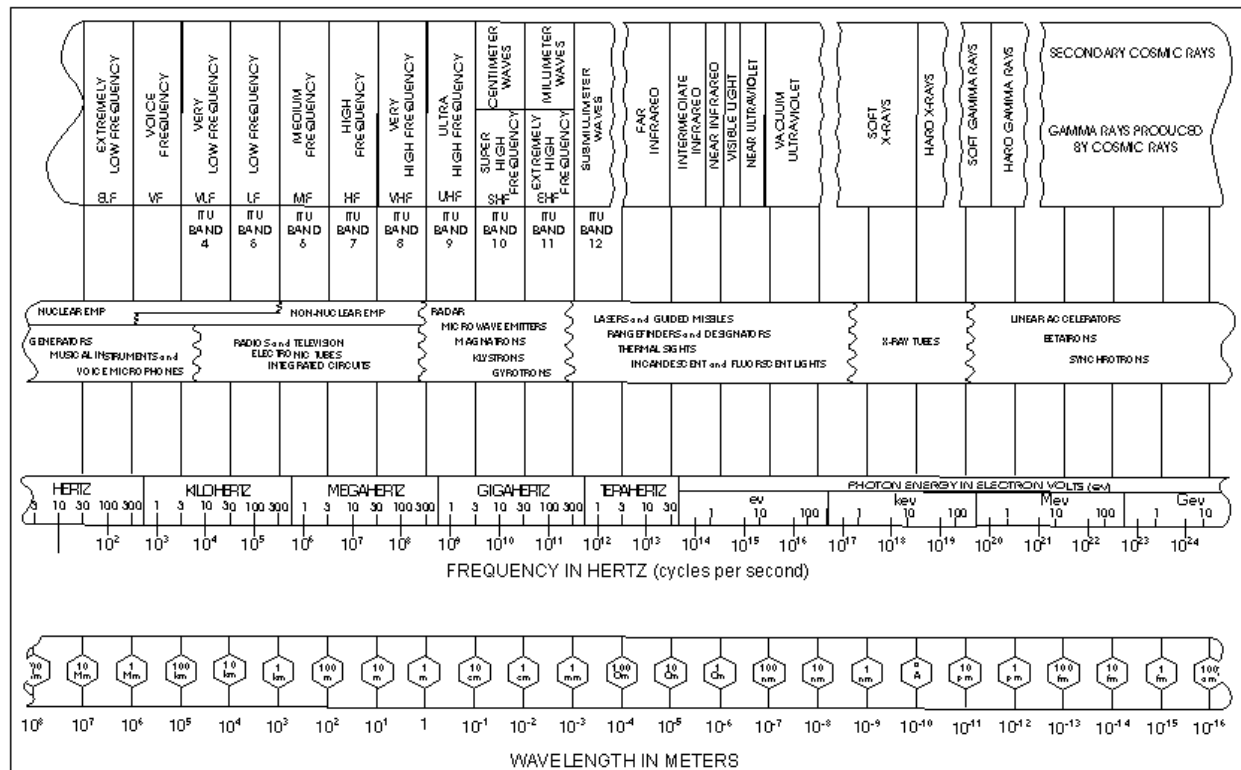
The electromagnetic spectrum is the range of frequencies (the spectrum) of electromagnetic radiation and their respective wavelengths and photon energies [64].

2.2.1 Radio Spectrum

International Telecommunication Union (ITU) divides the radio spectrum into 12 bands, each beginning at a wavelength which is a power of ten ($10^{\sup:n}$) metres, with corresponding frequency of $3 \times 10^{\sup:8n}$ hertz, and each covering a decade of frequency or wavelength [68].

Definition for shielding	Remarks	Reference
$\lambda/2\pi$	1/r terms dominant	Ott, White
$5\lambda/2\pi$	Wave impedance=377 Ω	Kaiser
For antennas		
$\lambda/2\pi$	1/r terms dominant	Krause
3λ	D not $\gg \lambda$	Fricitti, White, Mil-STD-449C
$\lambda/16$	Measurement error<0.1 dB	Krause, White
$\lambda/8$	Measurement error<0.3 dB	Krause, White
$\lambda/4$	Measurement error<1 dB	Krause, White
$\lambda/2\pi$	Satisfies the Rayleigh criteria	Berkowitz
$\lambda/2\pi$	For antennas with $D \ll \lambda$ and printed-wiring-board traces	White, Mardiguian
$2D^2/\lambda$	For antennas with $D \gg \lambda$	White, Mardiguian
$2D^2/\lambda$	If transmitting antenna has less than 0.4D of the receiving antenna	MIL-STD 462
$(d+D)^2/\lambda$	If $d > 0.4D$	MIL-STD 462
$4D^2/\lambda$	For high-accuracy antennas	Kaiser
$50D^2/\lambda$	For high-accuracy antennas	Kaiser
$3\lambda/16$	For dipoles	White
$(D^2+d^2)/\lambda$	If transmitting antenna is 10 times more powerful than receiving antenna, D	MIL-STD-449D

Fig. 2.2: : Definitions of near- and far-field boundary.



electromagnetic spectrum

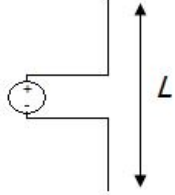
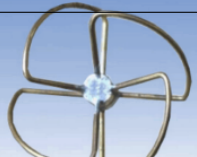
Fig. 2.3: : Electromagnetic Spectrum.

Table 2.1: Radio spectrum bands and example uses.

Band name	Abbreviation	Frequency	Wavelength	Example Uses
Extremely low frequency	ELF	3–30 Hz	100,000–10,000 km	Communication with submarines
Super low frequency	SLF	30–300 Hz	10,000–1,000 km	Communication with submarines
Ultra low frequency	ULF	300–3,000 Hz	1,000–100 km	Submarine communication, communication within mines
Very low frequency	VLF	3–30 kHz	100–10 km	Navigation, time signals, submarine communication, wireless heart rate monitors, geophysics
Low frequency	LF	30–300 kHz	10–1 km	Navigation, time signals, AM longwave broadcasting (Europe and parts of Asia), RFID, amateur radio
Medium frequency	MF	300–3,000 kHz	1,000–100 m	AM (medium-wave) broadcasts, amateur radio, avalanche beacons
High frequency	HF	3–30 MHz	100–10 m	Shortwave broadcasts, citizens band radio, amateur radio and over-the-horizon aviation communications, RFID, over-the-horizon radar, automatic link establishment (ALE) / near-vertical incidence skywave(NVIS) radio communications, marine and mobile radio telephony
Very high frequency	VHF	30–300 MHz	10–1 m	FM, television broadcasts, line-of-sight ground-to-aircraft and aircraft-to-aircraft communications, land mobile and maritime mobile communications, amateur radio, weather radio
Ultra high frequency	UHF	300–3,000 MHz	1–0.1 m	Television broadcasts, microwave oven, microwavedevices/communications, radio astronomy, mobile phones, wireless LAN, Bluetooth, ZigBee, GPS and two-way radios such as land mobile, FRS and GMRSradios, amateur radio, satellite radio, Remote control Systems, ADSB
Super high frequency	SHF	3–30 GHz	100–10 mm	Radio astronomy, microwave devices/communications, wireless LAN, DSRC, most modern radars, communications satellites, cable and satellite television broadcasting, DBS, amateur radio, satellite radio
Extremely high frequency	EHF	30–300 GHz	10–1 mm	Radio astronomy, high-frequency microwave radio relay, microwave remote sensing, amateur radio, directed-energy weapon, millimeter wave scanner, wireless LAN (802.11ad)
Terahertz or Tremendously high frequency	THz or THF	300–3,000 GHz	1–0.1 mm	Experimental medical imaging to replace X-rays, ultrafast molecular dynamics, condensed-matter physics, terahertz time-domain spectroscopy, terahertz computing/communications, remote sensing

2.3 Antenna Types

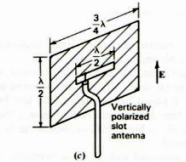
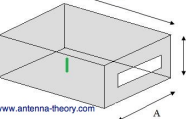
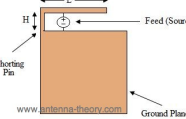
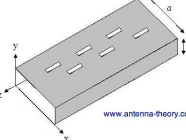
2.3.1 Wire Antennas

<p>Short Dipole The simplest of all antennas. It is simply an open-circuited wire, fed at its center. The words “short” or “small” imply “relative to a wavelength” size of the dipole antenna does not matter.</p>	
<p>Dipole Two monopoles facing away from each other. Used to create a powerful signal in restricted space.</p>	
<p>Half-Wave Dipole Special case of the dipole antenna. Length of this dipole antenna is equal to a half-wavelength.</p>	
<p>Broadband (Wideband) Dipoles Broadband by increasing the radius A of the dipole.</p>	
<p>Monopole (Whip) Works best for narrow range and can be collapsible. Used on small radios and vehicles.</p>	
<p>Folded Dipole Folded dipole forms a closed loop.</p>	
<p>Loop Works like a dipole and reaches multiple frequencies. Commonly used for TV and RFID systems.</p>	
<p>2.3. Antenna Types</p>	

2.3.2 Log-Periodic Antennas

<p>Bow Tie Another type of dipole. Angles can be set to work well with different frequencies. Similar radiation pattern to the dipole antenna, and will have vertical polarization</p>	
<p>Log-Periodic Tooth</p>	
<p>Log-Periodic Dipole Array (LPDA)</p>	

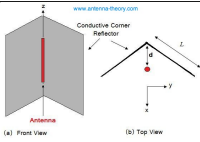
2.3.3 Aperture Antennas

<p>Slot</p>	
<p>Cavity-Backed Slot</p>	
<p>Inverted-F</p>	
<p>Slotted Waveguide</p>	
<p>Horn</p>	
<p>Vivaldi</p>	
<p>Telescopes (Eye)</p>	

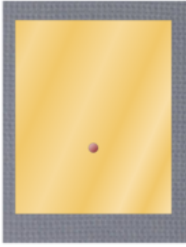
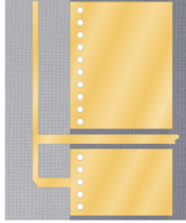
2.3.4 Travelling Wave Antennas

<p>Helical</p>	
<p>Yagi-Uda Ideal for long distance directional applications Can reach multiple frequencies</p>	
<p>Spiral</p>	

2.3.5 Reflector Antennas

<p>Corner Reflector</p>	
<p>Parabolic Reflector (Dish)</p>	

2.3.6 Microstrip Antennas

Rectangular Microstrip (Patch)	
Planar Inverted-F (PIFA)	

2.3.7 Other Antennas

NFC	
Fractal	
Wearable	

2.4 Magnetic Testing

There is a standart about expressing symbols and definitions relating to magnetic testing. Dictionary style definitions of terms are good organized and some important notes clarify complicated issues [3].

2.5 VLF & LF Antenna

VLF (Very Low Frequency) Band take place from 3kHz to 30 kHz in the frequency spectrum [18].

Advantages	Disadvantages
EM waves penetrate more than higher frequencies such as in the sea water	High background noise levels
Low atmospheric attenuation	Communication needs large amount of power at the output of the transmitter
Appropriate for long range communication	
Diffraction around objects that would block higher frequencies	
Less prone to multipath	

VLF antennas operate on VLF band. They are electrically small and this simplifies analysis. They are physically large structures. In other words, they generally have a number of towers that 200-300 m high and cover areas of up to a square kilometer or more. The VLF antennas support worldwide communication [18].

The VLF antennas have some problems that listed below [18]:

- Bandwidth is less than 200 Hz.
- Small radiation resistance.
- They are expensive structures.
- Antenna system covers a large area.
- Designing an efficient transmitting antenna is difficult.
- High power levels are needed for transmission.

Marris produced a ferrite core loopstick antenna for receiving application as shown in Fig. 2.4. He said VLF antenna but operating frequency band is 50 kHz to 195 kHz, so it was a LF antenna. MMG F14 grade nickel-zinc material was used. The antenna compared with a traditional 20 x 1.25 cm diameter loopstick and he noted that increased signal strength and reduced noise [39].

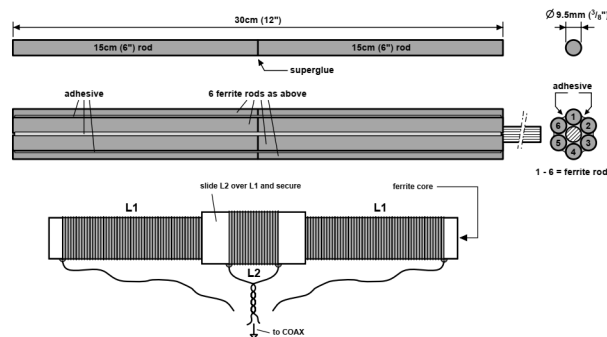


Fig. 2.4: : Loopstick antenna.

1939 The Screened Loop Aerial

2.6 Shielding

A practical version of a single-winding loop for test purposes is shown in Fig. 4.12. As a protection against electric field effects, the actual winding is additionally surrounded by a tubular metal shield that must have a slot at one point in order not to short-circuit the magnetic field [49]

Buie investigated the design and construction of a shielded receiving loop antenna. The designed antenna had approximately 60% increase in effective height and a 3 dB increase in terminal voltage over a conventional loop antenna. Capacitive loading of the shield gap was optimized at 14 - 34 kHz band and results were presented. In addition, optimum number of turns were optimized [10].

Patents

Year	Name	Patent Number
1942	Loop antenna	US2292182
1961	Electrostatically-shielded loop antenna	US2981950

2.6.1 Magnetic Shielding

Magnetic shielding can be made three different ways: high-permeability magnetic material, thick-walled conducting material or active compensation. Heinonen et. al., investigated a thick-walled conducting enclosure for biomagnetic measurements [25].

Commonly, high-permeability μ -metal is used on the magnetically shielded enclosures and it is convenient from DC to radio-frequencies. However, μ -metal is very sensitive to mechanical vibrations and degradation of permeability in mechanical stress.

The advantages of thick-walled conducting material are low price, easy and rigid construction. Its main disadvantage is that the attenuation is zero for static field and increasing function of frequency [25].

The small word means that the antenna is actually electrically small. The most commonly used electrical small definition is that the maximum size of the antenna is less than one-tenth of the wavelength. For loop antennas, it means that the diameter is smaller than one-tenth of the wavelength ($D \leq \lambda/10$).

In the case of loop antennas, the dipole consists of a usually circular or rectangular current loop which acts like a coil and functions in response to the magnetic component of the electromagnetic field [44].

A small loop (circular or square) is equivalent to an infinitesimal magnetic dipole whose axis is perpendicular to the plane of the loop. That is, the fields radiated by an electrically small circular or square loop are of the same mathematical form as those radiated by an infinitesimal magnetic dipole [8].

Breed carried out an article on electrically small antennas. Here, the electrically small antenna was defined and then the application areas were explained in detail. Starting with radiation resistance, then other loss parameters that affect efficiency were mentioned. The important points to be considered when impedance matching were indicated [9].

3.1 Introduction

The most convenient geometrical arrangement for the field analysis of a loop antenna is to position the antenna symmetrically on the $x - y$ plane, at $z = 0$. The wire is assumed to be very thin and the current is assumed to be constant. A constant current distribution is accurate only for a loop antenna with a very small circumference [8].

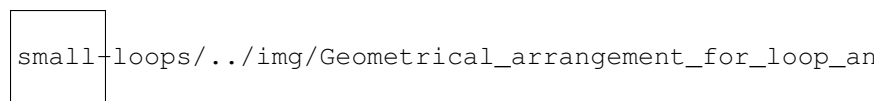


Fig. 3.1: : Geometrical arrangement for loop antenna analysis

In the analysis of radiation problems, the usual procedure is to specify the sources and then require the fields radiated by the sources. It is a very common practice in the analysis procedure to introduce auxiliary functions, known as vector potentials, which will aid in the solution of the problems. The most common vector potential functions are the A (magnetic vector potential) and F (electric vector potential). While it is possible to determine the E and H fields directly from the source-current densities J and M , as shown in Fig. 3.1, it is usually much simpler to find the

auxiliary potential functions first and then determine the E and H . This two-step procedure is also shown in Fig. 3.1 [8].

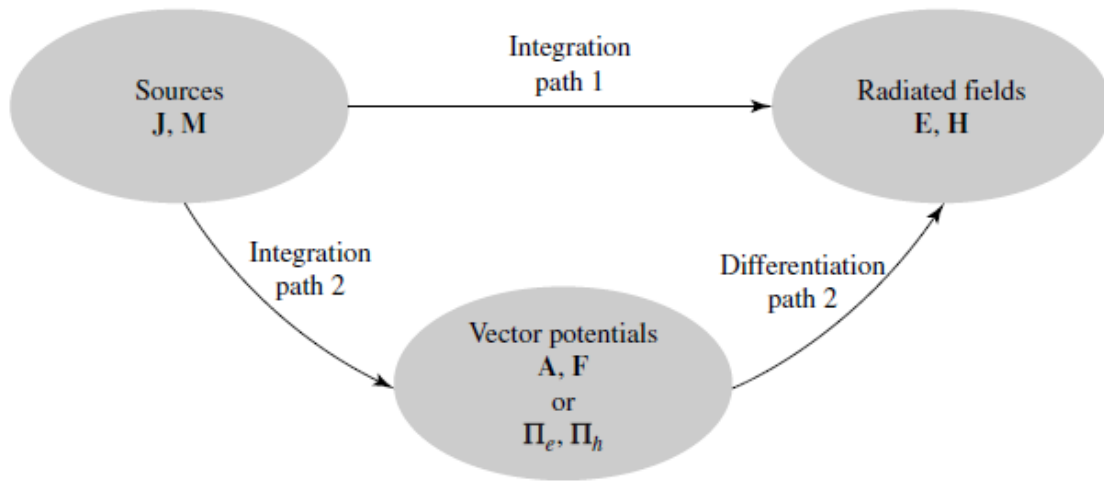


Figure 3.1 Block diagram for computing fields radiated by electric and magnetic sources.

Fig. 3.2: : Block diagram for computing fields radiated by electric and magnetic sources.

Defining properties for an electrically small antenna are low directivity, low input resistance, high input reactance and low radiation efficiency [Stutzman and Thiele, 2012].

In practice, a dipole antenna is usually operated at or near its first resonant frequency. However, electrically small antennas, such as active receiving antennas, operate well below the resonant frequency [58].

3.2 Radiated Fields

A small loop in which loop current is everywhere in phase can be expressed a magnetic dipole with dipole moment M . All the electromagnetic field components of the magnetic dipole are proportional to the M when the loop current varies sinusoidally. These fields vary with distance R as k^2/R for the radiation or far field components, as k/R^2 for the transition field components, and as $1/R^3$ for the induction or reactive field components. If the wavelength λ , and any one of the three field components are given, the remaining components may be calculated. Alternately, if the M is given, all three field components may be calculated [57].

3.2.1 Thin Wire, Constant Current, Small Circumference

The wire is assumed to be very thin and the current spatial distribution is given by $I_\phi = I_0$ where I_0 is a constant. Although this type of current distribution is accurate only for a loop antenna with a very small circumference, a more complex distribution makes the mathematical formulation quite cumbersome [8].

$$\vec{A} = j \frac{k\mu a^2 I_0 \sin \theta}{4r} \left[1 + \frac{1}{jkr} \right] e^{-jkr} \vec{a}_\phi \quad (3.1)$$

$$\begin{aligned}
 E_r &= 0 \\
 E_\theta &= 0
 \end{aligned}
 \tag{3.2}$$

$$E_\phi = \eta \frac{(ka)^2 I_0 \sin \theta}{4r} \left[1 + \frac{1}{jkr} \right] e^{-jkr}$$

$$H_r = j \frac{ka^2 I_0 \cos \theta}{2r^2} \left[1 + \frac{1}{jkr} \right] e^{-jkr}$$

$$H_\theta = -\frac{(ka)^2 I_0 \sin \theta}{4r} \left[1 + \frac{1}{jkr} - \frac{1}{(kr)^2} \right] e^{-jkr}
 \tag{3.3}$$

$$H_\phi = 0$$

3.3 Loop Geometry

3.3.1 Dimensions

3.3.2 Coil cross-section advantage/disadvantage

Circular	Rectangular

Others

Fundamental characteristics of the loop antenna radiation pattern (far field) are largely independent of the loop shape [Donohoe, ECE4990 Lecture Notes].

The far fields of an electrically small loop antenna are dependent on the loop area but are independent of the loop shape [Donohoe, ECE4990 Lecture Notes].

For any of the shapes given, there is less than 1% deviation between demagnetization factors of polygonal and circular cylinders for aspect ratios l_r/d_r above unity. For acicular particles ($l_r/d_r \sim 6.0$) this deviation is less than 0.25% even for the most radical shape, the triangular cross-section [Moskowitz and Della Torre, 1966].

Size and shape of coils affect their high frequency resistance very broadly. Cross section of coil had little effect on the observed resistance [Witzig, 1947].

3.4 Impedance of a Small Loops

3.4.1 Over a Conducting Medium

In 1973 Wait and Spies investigated low-frequency input impedance of a circular loop over a conducting medium as shown in Fig. 3.3. Impedance equation was given and calculated numerically. The impedance of the loop was analysed in terms of wire and loop radius, skin depth and loop height from ground. The limiting value of R for the rate of loop radius to skin depth (a/δ) tending towards infinity was noted [62].

The self resonance frequency (SRF) can be obtained by finding the frequency in which $\text{Im}(Z) = 0$ [14].

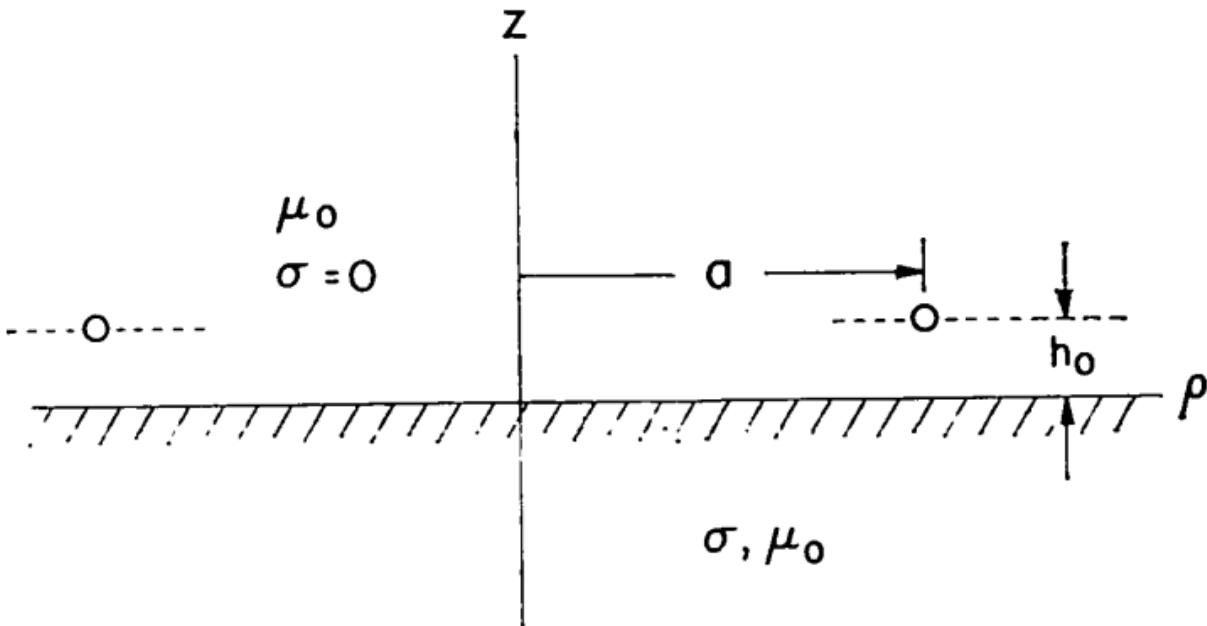


Fig. 3.3: : Side view of circular loop over the conducting earth.

3.5 Receiving Signal

Especially in metal detection systems, transmitter and receiver antennas are used together. Analyzing the signals generated by the receiver antenna is also an important issue.

Bai and Bai investigated an algorithm of digital metal detecting signal processing for the estimation of the size and type of metal that used in food safety and industrial production. In the absence of metal, it receives the induced signal as the reference vector and produces quadrature synchronous signal $\sin \omega t$ and $\cos \omega t$ then multiply to demodulation [7].

3.6 Signal to Noise Ratio (SNR)

The minimum signal that can produce a useful output from a radio receiver is determined by the output signal-to-noise ratio [CIA, 1957].

Table 3.1: Noise Sources [CIA, 1957]

Externally Generated	Internally Generated
Atmospheric (electrical storms)	Antenna ohmic resistance (thermal)
Cosmic (extra-terrestrial radiation)	Coupling circuit resistance (thermal)
Man-made static	First amplifier or mixer (short noise)
Precipitation static	
Radiation resistance (thermal)	

Belrose gives the SNR formula of a loaded-loop antenna [1]:

$$SNR = \frac{66.3NA\mu_{rod}E}{\sqrt{b}} \sqrt{\frac{Qf}{L}}$$

where E is the field strength, L is loop inductance, N is number of turns, Q is the loaded Q of the loop, μ_{rod} is the permeability of the rod, b is the receiver bandwidth, and A is the loop area.

Note: Higher sensitivity can also be obtained (especially at frequencies below 500 kHz) by bunching ferrite cores together to increase the loop area over that which would be possible with a single rod [1].

3.6.1 Rx

Laurent and Carvalho gave the signal to noise ratio of a receiving [Laurent and Carvalho, 1962].

$$\frac{S}{N} = \frac{EmA_r}{C} \left[\mu_{cer} + \left(\frac{d_c^2}{d_r^2} - 1 \right) \right] \sqrt{\frac{\omega_0 Q_L}{4KT \Delta f d_c \mu_c F}}$$

- E magnitude of the electric field intensity vector
- m modulation index
- A_r area of the rod
- C total tuning capacitance
- ω_0 resonance frequency
- $Q_L = \omega_0 \frac{R_p R_L}{R_p + R_L} C$
- $K = 1.38 \times 10^{-23}$ Boltzmann's constant [Joules/Kelvin]
- T Temperature in degrees Kelvin
- Δf 3 db bandwidth of the device
- $\mu_c = L_2/L_1$ coefficient of change in inductance when the rod is inserted
- F form factor (geometry of the coil)

Fratianni obtained the optimum signal to noise ratio equation for a transformer coupled loop system and direct coupled loop system [Fratianni, 1948]

3.6.2 Transformer coupled

$$\psi = \frac{7.94 \times 10^9}{(\Delta f)^{1/2}} E \left(\frac{Q_2}{X_{L_0}} \right)^{1/2} \frac{k_1}{\left[\left(\frac{L_0}{L_p} + \frac{L_p}{L_0} + 2 \right) + k_1^2 \left(\frac{Q_2}{Q_0} + \frac{Q_2 L_p}{Q_p L_0} \right) \right]^{1/2}}$$

Fig. 3.4: : ex17.

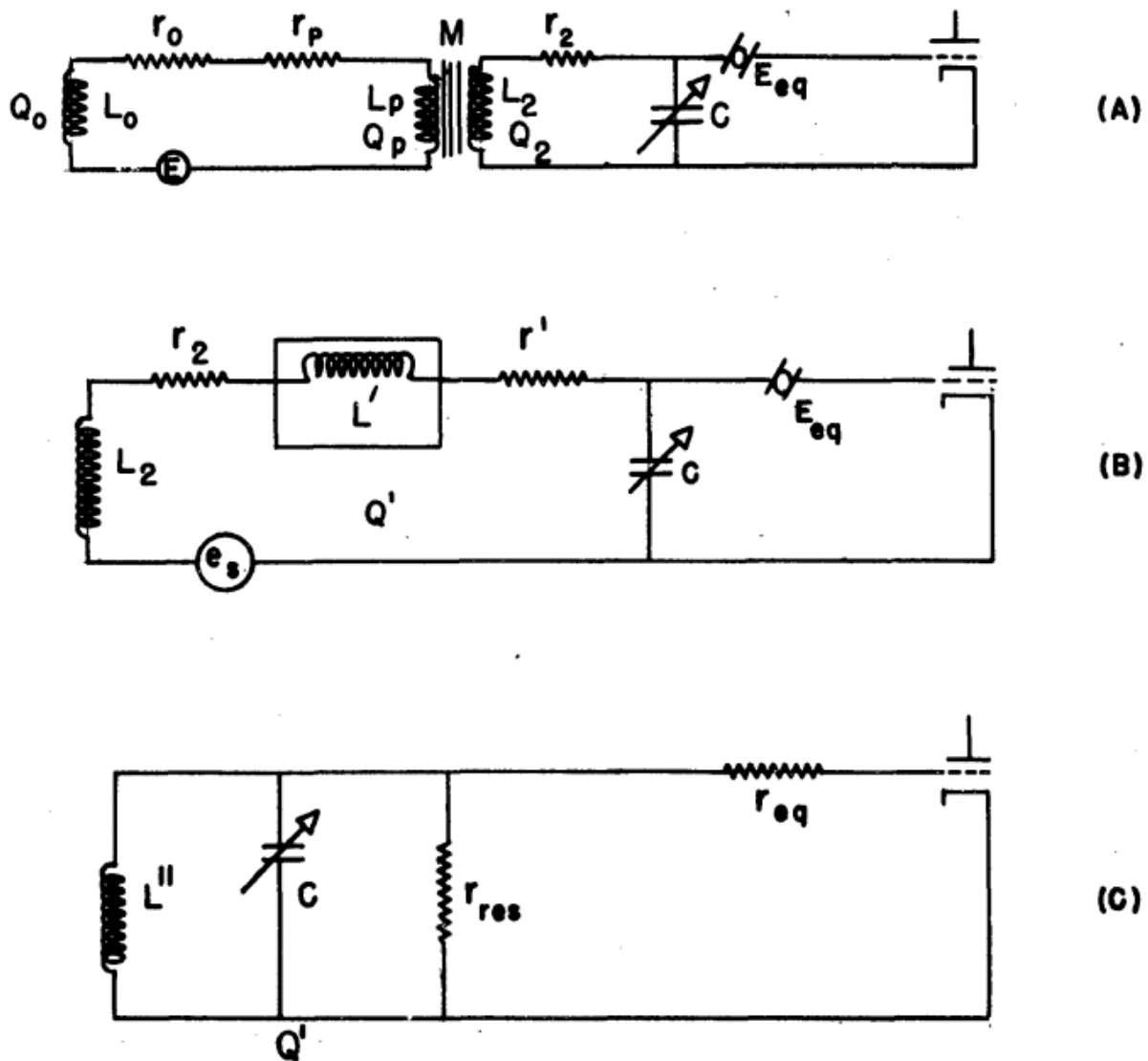


Fig. 3.5: : snr-transformer-coupled.

$$\psi = \frac{7.94 \times 10^9}{(\Delta f)^{1/2}} \text{EN} \left(\frac{Q}{X_L} \right)^{1/2}$$

Fig. 3.6: : ex18.

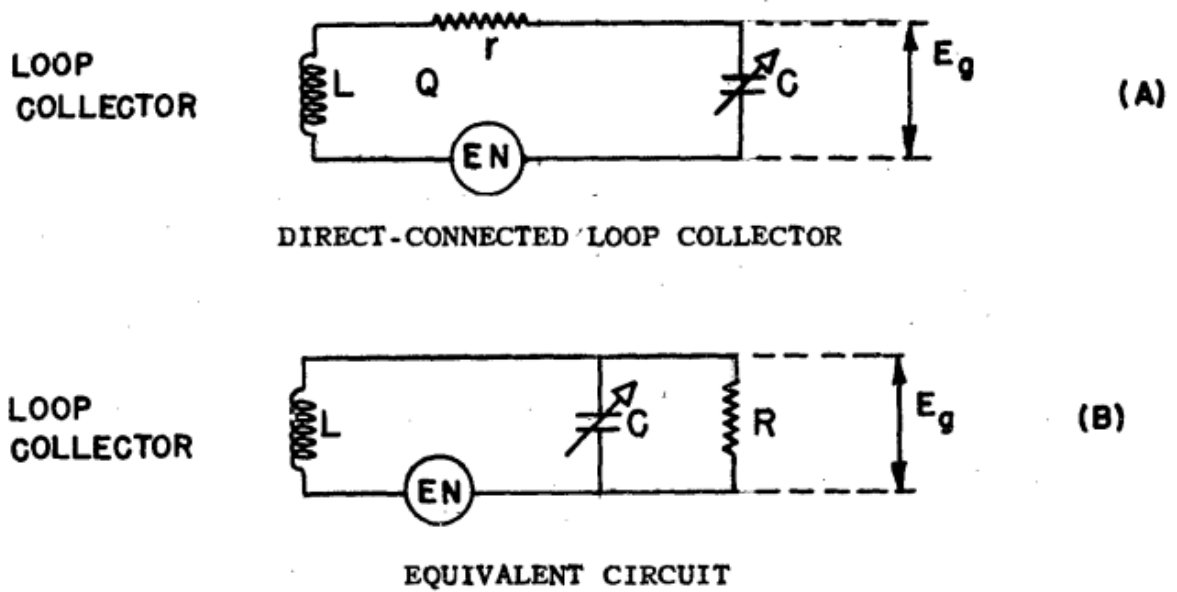


Fig. 3.7: : snr-direct-connected.

3.6.3 Direct Connected

- L_p : primary inductance
- L_o : loop inductance
- K_1 : coupling coefficient of transformer
- Q_0 : q value of loop
- Q_p : q value of primary
- Q_2 : q value of secondary
- Δf : the width in cps of the equivalent rectangle having the same area as the squared transmission characteristic of the input circuit
- XL_0 : reactance of loop
- E : loop induced voltage

4.1 Magnetic Dipole Moment

Magnetic dipole moment is a vector that point out of the plane of the loop and the magnitude of moment for a static field equals to the product of the flowing current in and cross-sectional area of the loop.

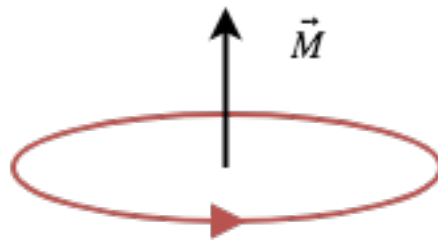


Fig. 4.1: : Magnetic dipole moment equivalent of a loop.

A comparison of magnetic and electric field components with those of the infinitesimal magnetic dipole indicates that they have similar forms. In fact, the electric and magnetic field components of an infinitesimal magnetic dipole of length l and constant “magnetic” spatial current I_m are given by

$$\begin{aligned} E_r &= 0 \\ E_\theta &= 0 \\ E_\phi &= -j \frac{k I_m l \sin \theta}{4\pi r} \left[1 + \frac{1}{jkr} \right] e^{-jkr} \end{aligned} \quad (4.1)$$

$$\begin{aligned} H_r &= \frac{I_m l \cos \theta}{2\pi \eta r^2} \left[1 + \frac{1}{jkr} \right] e^{-jkr} \\ H_\theta &= j \frac{k I_m l \sin \theta}{4\pi \eta r} \left[1 + \frac{1}{jkr} - \frac{1}{(kr)^2} \right] e^{-jkr} \\ H_\phi &= 0 \end{aligned} \quad (4.2)$$

These can be obtained, using duality, from the fields of an infinitesimal electric dipole. When (4.1) and (4.2) are compared with magnetic and electric field components, they indicate that a magnetic dipole of magnetic moment $I_m l$ is equivalent to a small electric loop of radius a and constant electric current I_0 provided that

$$I_m l = j S \omega \mu I_0 \quad (4.3)$$

where $S = \pi a^2$ (area of the loop). Thus, for analysis purposes, the small electric loop can be replaced by a small linear magnetic dipole of constant current. The magnetic dipole is directed along the z-axis which is also perpendicular to the plane of the loop.

Loop analysis based on magnetic dipole moment is given in Electromagnetic Waves & Antennas - S. J.Orfanidis – 2008 book CH 15.

4.1.1 Time-Varying, Cored and N-Turn Loop Antenna

Dunbar noted that in order to increase the effective area artificially through the use of a permeable core and a multi-turn coil. It is quite successful provided the flux density is kept well below the saturation level. Thus, the effective area becomes $N S \mu_{cer}$ and magnetic dipole moment becomes [Dunbar, 1972]. This magnetic moment can be also used in a conductive medium.

$$M = j \omega \mu_0 \mu_{cer} I S N \quad (4.4)$$

In order to quantify the magnetic moment for our rod antenna, we will compare its magnetic field to the magnetic field produced by an air core planar loop of current (i.e., $I S$, where S represents the loop area). Essentially, we will enforce the equivalence theorem to determine the necessary moment for an air core planar loop of current that will produce the same external magnetic field as our rod antenna. The magnetic moment will be determined by using the broadside magnetic field component [Jordan et.al., 2009].

The electromagnetic field of the ferrite-loaded transmitting loop is given by Eq 5-1 to 5-3 with the moment $m = \mu_r \odot d F_v I_o N A$. The ferrite-loaded loop, however, is seldom used as a transmitting antenna because of the problems associated with the nonlinearity and the dissipation in the ferrite at high magnetic field strengths [Antenna Engineering Handbook 3Ed - R.C.Johnson H.Jasik – 1993, p5-9].

4.1.2 Static, Cored and N-Turn Loop Antenna

Devore and Bohley noted that magnetic dipole moment of a ferrite loaded loop has two component that magnetic dipole moment of ferrite core and winding [Devore Bohley, 1977].

$$M = M_F + M_w \quad (4.5)$$

$$M_w = N I S \cong N I V / l \quad (4.6)$$

$$M_F = (\mu - 1) H_F V_F$$

where

$$\begin{aligned} H_F &= \frac{H_0}{1 + D_F (\mu - 1)} \\ H_0 \approx H_w &= \frac{n}{l_w} (1 - D_F) I \\ V_F &= l_F \pi a_F^2 \end{aligned} \quad (4.7)$$

4.1.3 Moment of Torquer

The definition of variables for the magnetic torquer is as shown in Fig. 4.3, where M represents the dipole moment of the torquer, θ is the angle with respect to the torquer axis, R is the distance from the center of the coil, and l is the

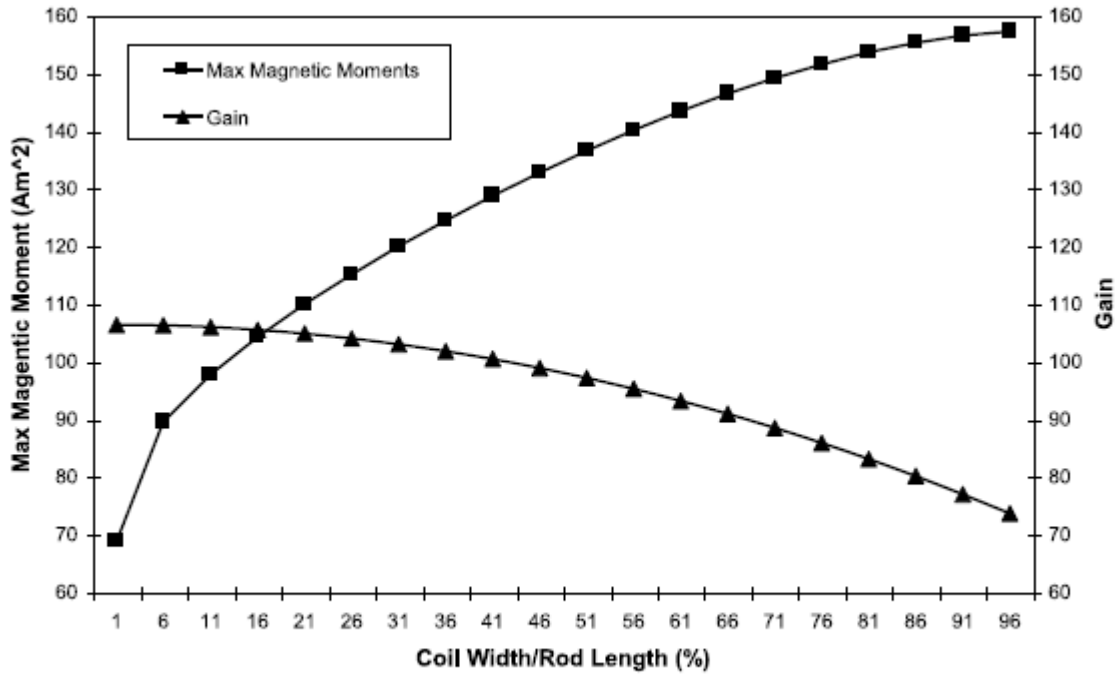


Figure 4. Maximum magnetic moment and gain versus the coil width/rod length percentage.

Fig. 4.2: : Maximum magnetic moment and gain versus the coil width/rod length percentage [Jordan et.al., 2009].

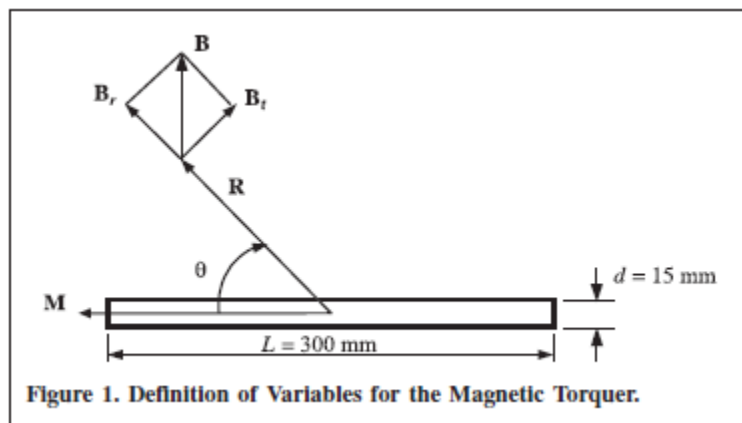


Fig. 4.3: : Torquer.

effective coil length. Also, B is the magnetic-flux density, B_r and B_t are the radial and tangential components of B , respectively [Lee et. al., 2002].

If $\theta = 90^\circ$,

$$M = \frac{4\pi}{\mu_0} \left(R^2 + \frac{L^2}{4} \right)^{3/2} B_t \quad (4.8)$$

If $\theta = 0^\circ$,

$$M = \frac{4\pi}{\mu_0} \frac{1}{\frac{\frac{R}{L} - \frac{1}{2}}{(R^2 - RL + \frac{L^2}{4})^{3/2}} - \frac{\frac{R}{L} + \frac{1}{2}}{(R^2 + RL + \frac{L^2}{4})^{3/2}}} B_r \quad (4.9)$$

Mehrjardi and Mirshams noted that an equation of magnetic dipole moment [Mehrjardi and Mirshams, 2010]

$$M = \mu_{cer} N S I \quad (4.10)$$

4.2 Effective Height (Length)

Effective height (or length) of an air core loop in meters is [Rohner, 2006]

$$h_{eff} = \frac{2\pi AN}{\lambda} = \frac{\pi^2 D^2 N}{2\lambda} \quad (4.11)$$

For transmitter antenna, it is a length that a dipole homogeneously carrying the feed point current I_0 would have to have in order to generate the same field strength in the main direction of radiation as

$$h_{eff} = \int_0^L \frac{I(z)}{I_0} dz \quad (4.12)$$

where $I(z)$ is the current distribution, I_0 is the feed point current (maximum). In the case of a half-wave dipole antenna ($I(z) = I_0 \cos 2\pi L/\lambda$), $h_{eff} = \lambda/\pi = 2L/\pi = 0.64L$. This is shown Fig. 4.4.

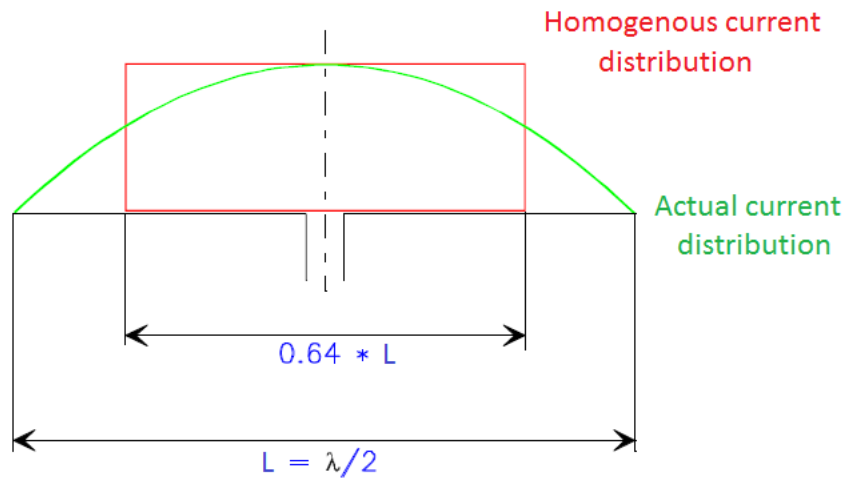


Fig. 4.4: : Explanation of the effective length concept.

For receiver antenna, the effective height of the dipole antenna is [Laurent and Carvalho, 1962]

$$h_{eff} = \frac{v_{ind}}{E} h_{eff} = \frac{\omega_0 N A_r}{C} \left[\mu_{cer} + \left(\frac{d_c^2}{d_r^2} - 1 \right) \right] \quad (4.13)$$

where ω_0 is resonance frequency, N is number of turns, A_r is area of the rod, μ_{cer} is effective relative permeability of the rod, d_c and d_r are diameters of the coil and rod respectively [Laurent and Carvalho, 1962].

Therefore, for an N turn ferrite rod antenna, [Snelling, 1969]

$$h_{eff} = \mu_{cer} \frac{\omega AN}{c_0} = \mu_{cer} \frac{2\pi AN}{\lambda_0} \quad (4.14)$$

Another effective height formula for ferrite loaded solenoid [Burhans, 1979]:

$$h_{eff} = \frac{2\pi AN \mu_{cer} F_a}{\lambda} \quad (4.15)$$

where F_a is averaging factor of coil and rod (typically 0.5 to 0.7).

4.3 Directivity and Efficiency

One very important quantitative description of an antenna is how much it concentrates energy in one direction in preference to radiation in other directions. This characteristic of an antenna is called directivity and is equal to its gain if the antenna is 100% efficient.

Directivity is defined as the ratio of the radiation intensity in a certain direction to the average radiation intensity [Stutzman and Thiele, 2012]. Directivity of any small antenna can be assumed approximately equal to $3/2$ [38].

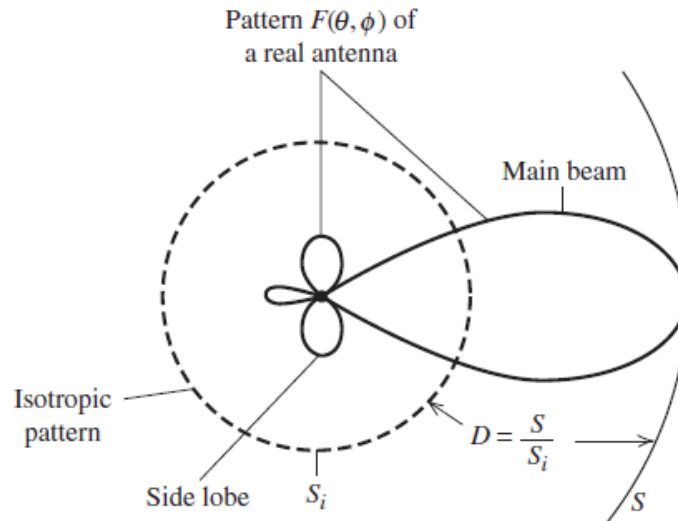


Figure 1-7 Illustration of radiation pattern $F(\theta, \phi)$ and directivity D . The power densities at the same distance are S and S_i for the isotropic and real antennas, respectively.

Fig. 4.5: : Illustration of radiation pattern and directivity.

Directivity can be tied more directly to the pattern function. First, we define beam solid angle, Ω_A :

$$\Omega_A = \iint_{sphere} |F(\theta, \phi)|^2 d\Omega \quad (4.16)$$

$$D = \frac{4\pi}{\Omega_A} \quad (4.17)$$

These results show that directivity is entirely determined by the pattern shape; it is independent of the details of the antenna hardware [Stutzman and Thiele, 2012].

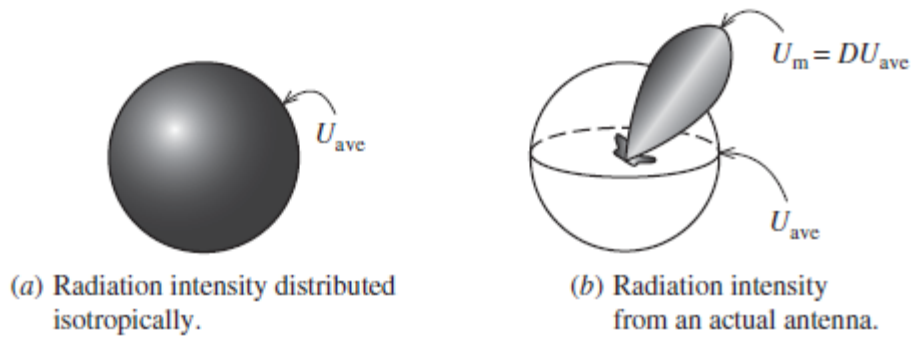


Figure 2-14 Illustration of directivity.

Fig. 4.6: : Illustration of directivity.

The concept of directivity is illustrated in Fig. 4.6 [Stutzman and Thiele, 2012].

The *radiation efficiency* of an antenna is defined as the portion of power that is not absorbed in the antenna structure as ohmic losses. This is characterized by the R_{rad} and the ohmic loss resistance, R_{loss} , with which the radiation efficiency, η_r , is [Koskimaa, 2016]

$$\eta_r = \frac{R_{rad}}{R_{rad} + R_{loss}} = \frac{P_{rad}}{P_{in}} = \frac{P_{rad}}{P_{rad} + P_{loss}} \quad (4.18)$$

where P_{rad} is the radiated power, P_{in} is the power accepted by the antenna and P_{loss} is the power loss in the antenna. The antenna has losses due to the impedance mismatch between the antenna output and feed input. The mismatch causes power reflection. The total efficiency of the antenna is defined as [Koskimaa, 2016]

$$\eta_t = (1 - |\Gamma|^2)\eta_r \quad (4.19)$$

A simple study about efficiency enhancement of transmitting loops was done. The study contains some investigation of previous works and analyse some parameters of antennas regarding to the previous works with a viewpoint of efficiency [33].

These are used to define antenna gain, G , and realized gain, G_{real} , respectively [Koskimaa, 2016]:

$$G = \eta_r G_{real} = \eta_t D \quad (4.20)$$

4.3.1 Omnidirectivity

The two loop antennas are positioned perpendicular to each other to make the receiver omnidirectional. If a 90 degree electrical phase shift is added to the loop antennas, a circular antenna pattern is formed as shown in Fig. 4.7 [59].

Electrical circuit of an omnidirectional loop antenna system is given by Fig. 4.8 [59].

In an application where omnidirectivity is required, two separate loop antennas located at right angles to each other can be used to give equal reception in all directions by introducing a 90 deg phase shift in one of the induced signals before they are combined [Laurent and Carvalho, 1962].

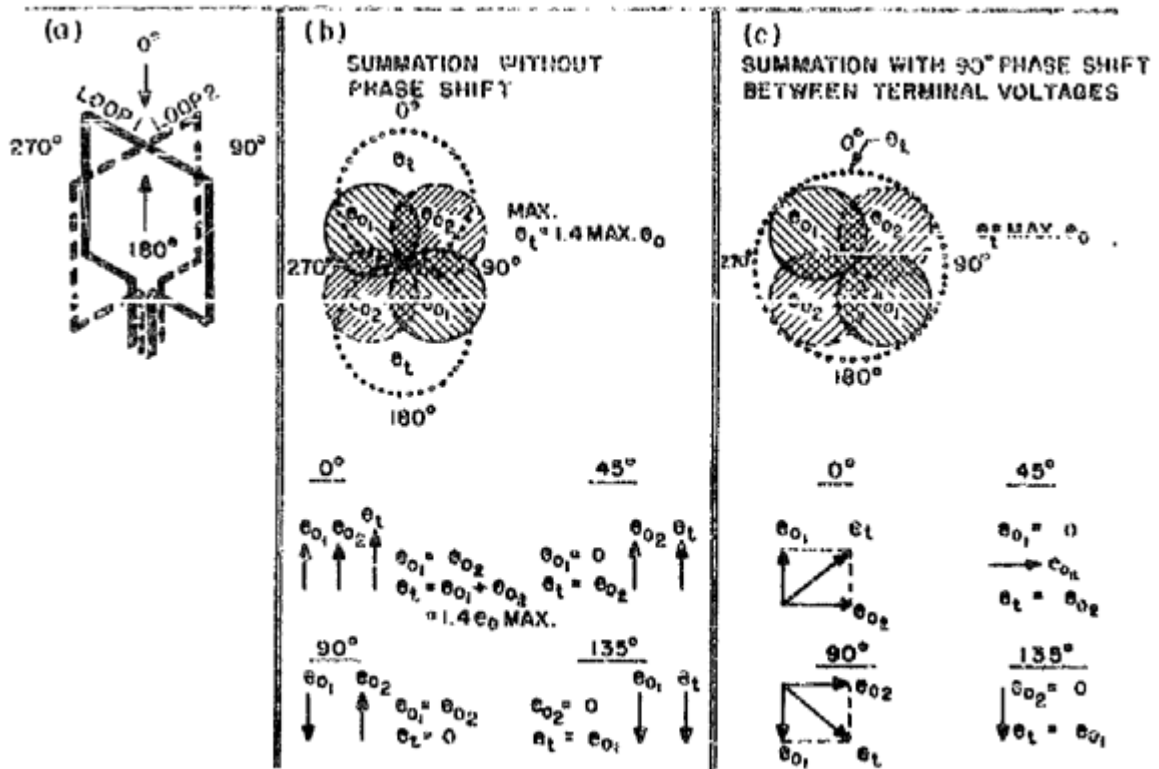
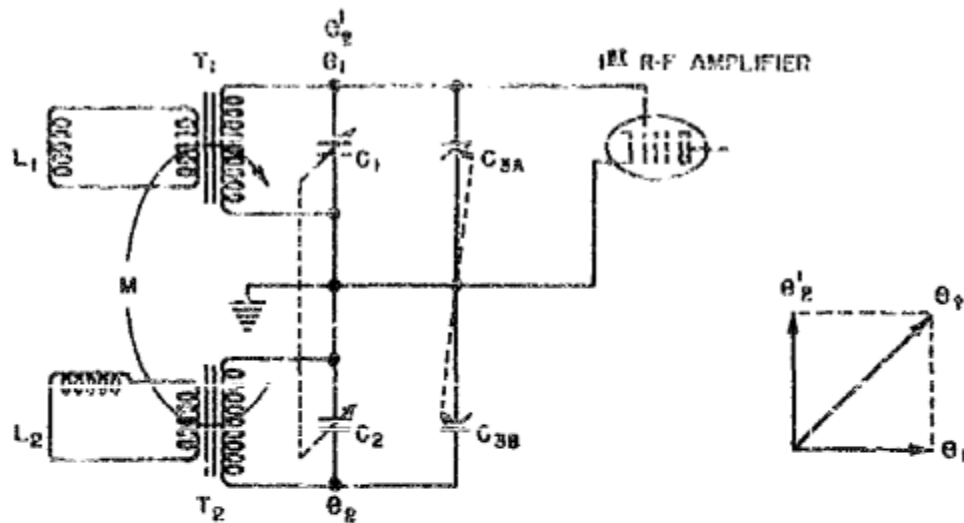


Figure 11 - field patterns of crossed loops

Fig. 4.7: : Field patterns of crossed loops.



L_1 AND L_2 = IDENTICAL LOOPS AT RIGHT ANGLES.
 T_1 AND T_2 = IDENTICAL COUPLING TRANSFORMERS.
 C_1 AND C_2 = GANGED SECONDARY TUNING CONDENSERS.
 C_{3A}, C_{3B} = DIFFERENTIAL TRIMMER CONDENSER.
 M = "CRITICAL" MUTUAL COUPLING BETWEEN LOOP SYSTEMS
 (MAY BE CAPACITIVE, INDUCTIVE, OR COMBINED).
 θ_1 AND θ_2 = SECONDARY VOLTAGES OF LOOP SYSTEMS 1 AND 2.
 θ_2' = SYSTEM 2 VOLTAGE APPEARING ACROSS
 SYSTEM 1 SECONDARY.
 θ_g = VOLTAGE APPLIED TO GRID OF AMPLIFIER TUBE.

Figure 12 - Omnidirectional loop system

Fig. 4.8: : Electrical circuit of an omnidirectional loop antenna system.

**THE LOOPSTICK
PATTERN**

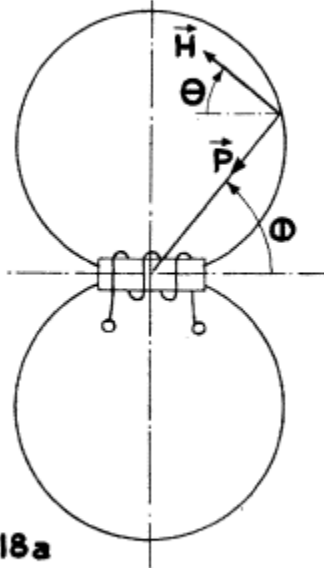


Fig. 18a

**OMNIDIRECTIONAL
ARRAY**

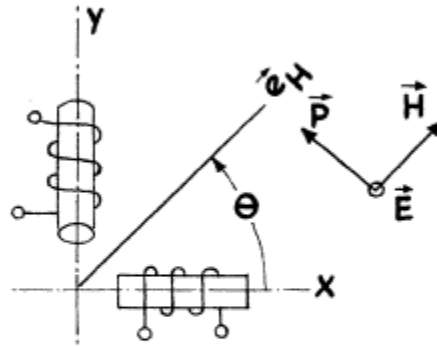


Fig. 18b

Figure 18—Loopstick Reception Pattern & Omnidirectional Array.

Fig. 4.9: : Loopstick Reception Pattern & Omnidirectional Array.

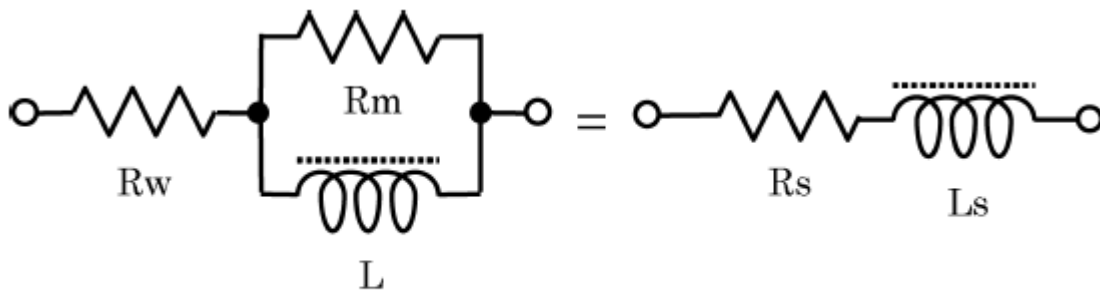


Fig. 2 The equivalent circuit of small MCLAs.

Fig. 4.10: : Equivalent circuit of small magnetic core loop antenna.

4.4 Quality Factor

Quality factor of the equivalent circuit can be approximated as follows where R_w is assumed [Abe and Takada, 2007].

$$Q = \frac{1}{\frac{R_w}{\omega L} + \frac{\omega L}{R_m}} \cong \frac{1}{\frac{R_w}{\omega L} + \left(\frac{\tan \delta}{\mu_i} \mu_{app}\right)} \quad (4.21)$$

where $\tan \delta / \mu_i$ is relative loss factor of the core (from datasheet), $\mu_{app} = L/L_0$ is ratio between the inductance of the coil attached to the core and the coil itself and R_w is winding resistance.

Quality factor of a resonator, Q , indicates its bandwidth relative to the center frequency:

$$Q = \frac{f}{\Delta f} \quad (4.22)$$

Alternatively, it can be defined as a ratio of average stored energy and energy loss:

$$Q = \omega \frac{W_m + W_e}{P_{loss}} \quad (4.23)$$

where W_m and W_e are the average magnetic and electric energy stored in the circuit and P_{loss} is the power loss. At resonance W_m and W_e are equal.

Higher Q indicates a lower rate of energy loss relative to the stored energy of the resonator; the oscillations die out more slowly [wiki: Q factor].

As the ferrite rod antenna is not a pure parallel resonator mainly due to the series resistance of the inductor, the quality factor is derived from the total quality factor of the individual quality factors of the inductor and the parallel capacitor:

$$Q_i = \frac{\omega L}{R_i} \quad (4.24)$$

$$Q_c = \frac{1}{\omega C R_c} \quad (4.25)$$

The resulting quality factor is

$$Q = \frac{\omega L}{\omega^2 L C R_c + R_i} \quad (4.26)$$

which at resonance becomes

$$Q = \frac{\omega L}{R_c + R_i} \quad (4.27)$$

Typically, capacitors have a much higher quality factor with a small resistance R_c compared to the coil resistances. The quality factor of the system is determined by the quality factor of the coil [Koskimaa, 2016].

4.5 Losses

There are three major losses related to an antenna: the structural losses of the antenna itself, near-field losses and the planar wave path losses (Fig. 4.11). The structural loss of an antenna is seen as ohmic and dielectric losses depending on the environment surrounding the antenna, such as free space, lossy or any other medium and the loss is converted into heat over the antenna. Reactive near-field losses are transformed into thermal energy by heating the environment around the antenna. The near-field losses are highly dependent on the antenna type as it is related to the current distribution on the antenna. Finally, the path losses are related to the planar waves due to the remote area and are independent of the antenna type [38].

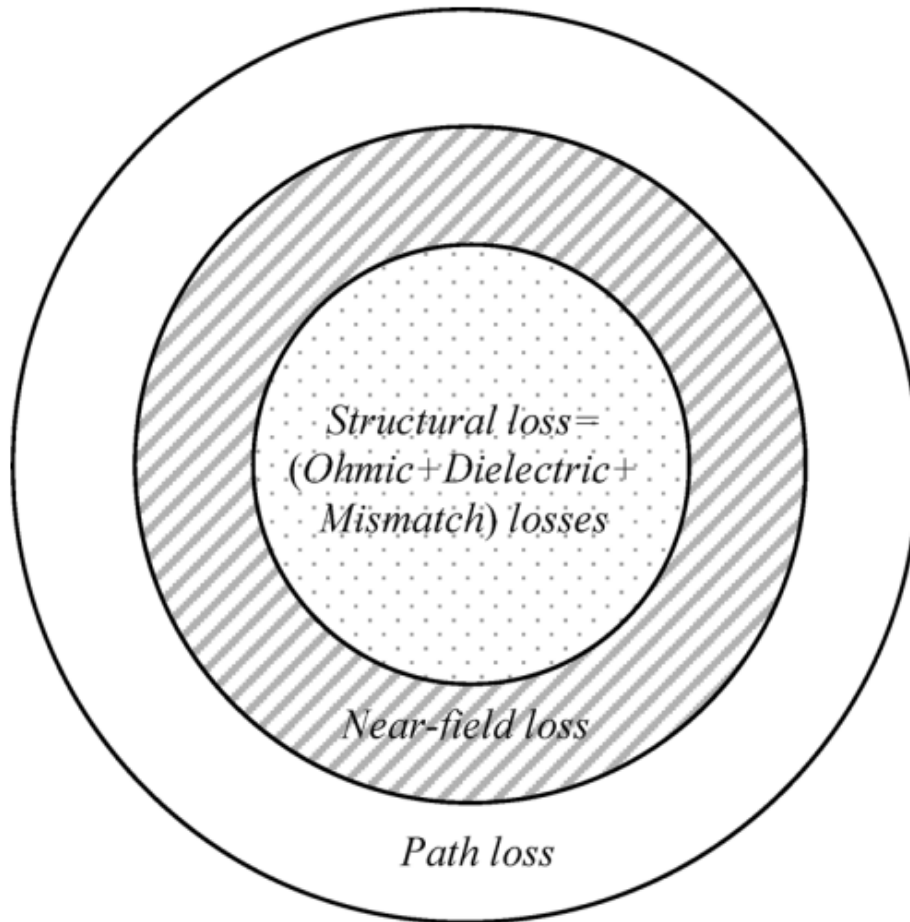


Fig. 4.11: : Antenna loss regimes.

4.6 Near field Propagation

4.6.1 Phase Behaviour

In the far field, the electric and the magnetic fields move with perfectly synchronized phase. In the near field, phases of the electric and the magnetic field diverge. These fields are 90 degree out of phase close to an electrically small antenna [52].

Schantz explained as follows: “A simple thought experiment involving electromagnetic energy flow establishes why the fields are in quadrature close to an electrically small antenna and in phase far away. The Poynting vector ($S = E \times H$) is the measure of the energy flux around the hypothetical small antenna. If the electric and magnetic fields are phase synchronous, then when one is positive, the other is positive and when one is negative the other is negative. In either case, the Poynting flux is always positive and there is always an outflow of energy. This is the radiation (or “real power”) case. If the electric and magnetic fields are in phase quadrature, then half the time the fields have the same sign and half the time the fields have opposite signs. Thus, half the time the Poynting vector is positive and represents outward energy flow and half the time the Poynting vector is negative and represents inward energy flow. This is the reactive (or “imaginary power”) case. Thus, fields in phase are associated with far field radiation and fields in quadrature are associated with near field quadrature.” [52]

Schantz investigated phase behaviour of an electric dipole regards to dipole moment and carried out numerical analysis and experimental tests. Analytical formulations of the electric and magnetic field phases in the near field region were given below. Numerical analysis of phases was good agreement with theoretical formulas. In addition, experiment results of phase difference of electric and magnetic field in the near field region have also good agreement with theory [52].

$$\Phi_H = -\frac{\omega r}{c} - \cot^{-1}\left(\frac{\omega r}{c}\right) - n\pi$$

$$\Phi_E = -\frac{\omega r}{c} - \cot^{-1}\left(\frac{\omega r}{c} - \frac{c}{\omega r}\right) - n\pi$$

There is a 90 degree phase difference between electric and magnetic components of the electromagnetic wave at close to a small antenna. These components converge to be in phase as far from the antenna. This near field behaviour of an antenna as shown in Fig. 4.12 The relation between distance and the phase difference is given by:

$$r = \frac{\lambda}{2\pi} \sqrt[3]{\cot \Delta_\phi}$$

Tip: MathCAD calculation file can be downloaded from [here](#).

where r is the distance from the antenna, λ is the wavelength and Δ_ϕ is the phase difference of electric and magnetic components [54][48].

4.6.2 Near Field Propagation based on Friis Law

Within the near-field, propagation relation for electric-electric or magnetic-magnetic antennas (like antennas) is

$$\frac{P_{rx}}{P_{tx}} = \frac{G_{rx}G_{tx}}{4} \left(\frac{1}{(kr)^6} - \frac{1}{(kr)^4} + \frac{1}{(kr)^2} \right)$$

in which the ratio of received power P_{rx} to transmitted power P_{tx} follows from the transmit antenna gain G_{tx} , the receive antenna gain G_{rx} , the distance r between antennas, and the wave number $k = 2\pi/\lambda$ and wavelength λ [48].

Note: All these works provides a basis to *Real-time Locating System*.

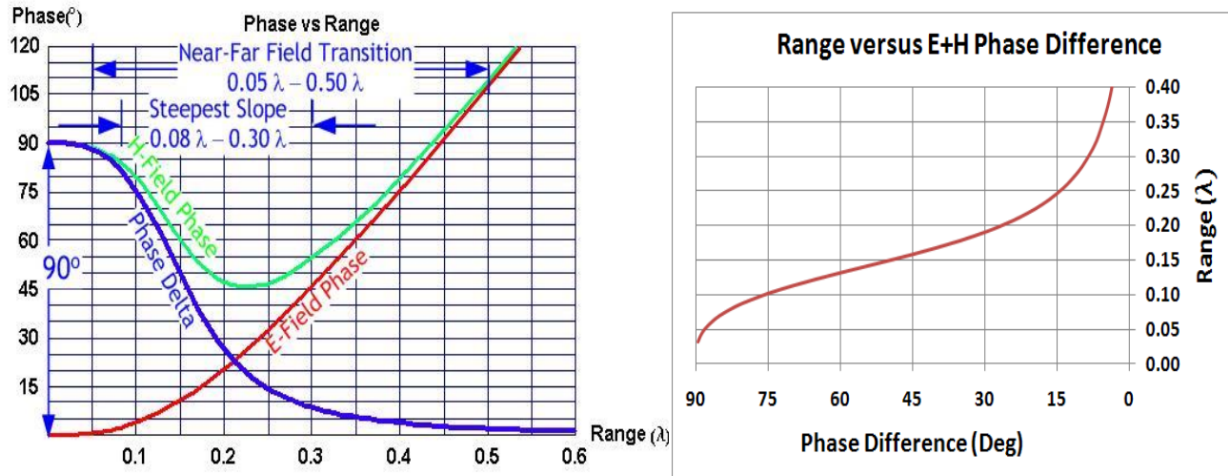


Fig. 4.12: : Phase relationships around an electrically small Hertzian dipole (left). Range versus electric-magnetic phase difference for a NFER signal (right).

4.7 Antenna Gain

An antenna’s gain is a key performance number which combines the antenna’s *directivity* and *electrical efficiency*. In a transmitting antenna, the gain describes how well the antenna converts input power into radio waves headed in a specified direction. In a receiving antenna, the gain describes how well the antenna converts radio waves arriving from a specified direction into electrical power. When no direction is specified, “gain” is understood to refer to the peak value of the gain, the gain in the direction of the antenna’s main lobe. A plot of the gain as a function of direction is called the radiation pattern [63].

Schantz investigated a fundamental limit to antenna gain versus size in 2005. The limit for antenna gain versus size was established for a matched pair of like antennas [53]. In 2008, Compston et al. improved the fundamental limit on antenna’s gain. First, a propagation formula derived similar to Friis’s formula. With this formula, the fundamental limit was shown, then a number of gain measurements taken from actual antennas were compared. There was an important assumption that not referenced: “For the special case where both antennas are at $\theta = 90^\circ$ relative to each other that the electric and magnetic fields have no radial components. Therefore, the near-field effective areas of the antennas are equivalent to their far-field effective areas.”. Near-field radial component directivity was calculated. Finally, they noted that the near-field gain might be greater than or equal to the far-field gain [13].

$$G_{ff} \leq G_{nf} \leq (4\pi R_\lambda)^3 \sqrt{\frac{2}{1 + (4\pi R_\lambda)^2}}$$

The operation of the antenna can be analyzed by using an equivalent circuit. The ferrite rod antenna consists of a coil which can be modeled as an inductor that has various resistances in series due to the antenna losses. Together with a parallel capacitance the antenna forms a parallel RLC circuit. The RLC resonance frequency can be tuned by adjusting the capacitance of the capacitor. The impedance seen from the antenna terminals is the antenna impedance [Koskimaa, 2016]:

$$Z_A = R_A + jX_A \quad (5.1)$$

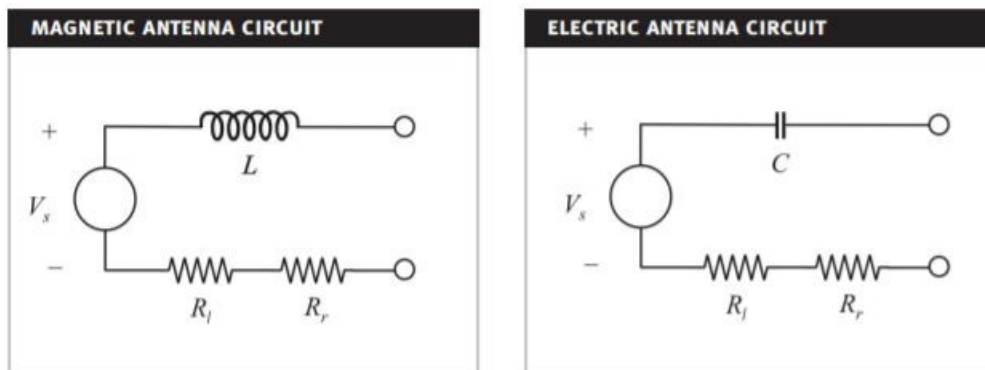


Fig. 5.1: : Circuit models of magnetic and electric antennas.

5.1 Complete Model

Some substantial papers about circuit model of electric dipole antennas in the literature. There is a special chapter in this document *Circuit Model of Dipole Antenna*.

5.1.1 Circuit Model of Solenoid Receiver

Cheng et. al. investigated optimization of a solenoid type receiver coil for biomedical implants in order to create a WPT link. Lumped RLC model was seen in Fig. 5.2. The model was valid at the frequency lower than the SRF of the coil [14].

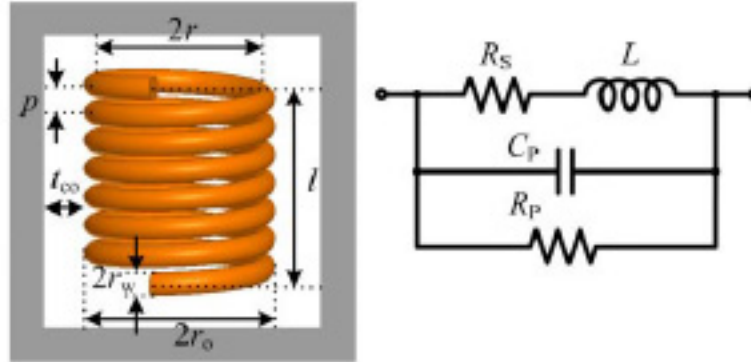


Fig. 5.2: : Lumped RLC model of a solenoid coil.

- L : self-inductance of coil
- R_S : the parasitic series resistance due to conductor's ohm loss
- C_P : parasitic capacitance
- R_P : parasitic parallel resistance due to dielectric loss in the coating and tissue

Series Resistance:

The parasitic series resistance was sum of the skin effect and proximity effect resistance. R_{sk} and R_{pr} were formed by Kelvin functions.

$$R_S = R_{sk} + R_{pr} \quad (5.2)$$

Inductance:

The self-inductance at high frequency was given (5.3) and the derivation was explained in paper.

$$L = \mu_{eff} \pi r^2 N^2 K_L K_P \quad (5.3)$$

Capacitance and Parallel Resistance:

The parasitic parallel capacitance C_P was proportional to the relative permittivity ϵ_r of the dielectric medium surrounding the solenoid. For a lossy dielectric medium, ϵ_r was a complex number. In other words, C_P could be considered as a complex capacitance. The complex capacitance was represented by a real capacitance and a parallel resistance. The model in the study had a multielectric medium and which was an extension of the uniform dielectric medium.

$$C_P = \text{Re} \left(C_{Pco1} + \frac{C_{Pco2} C_{Pti}}{C_{Pco2} + C_{Pti}} \right) \quad (5.4)$$

$$\frac{1}{R_P} = -\omega \cdot \text{Im} \left(C_{Pco1} + \frac{C_{Pco2} C_{Pti}}{C_{Pco2} + C_{Pti}} \right)$$

Coil Impedance:

$$Z = \frac{1}{1/(R_S + j\omega L) + j\omega C_P + 1/R_P}$$

Q-Factor:

$$Q = \text{Im}(Z)/\text{Re}(Z)$$

Self Resonance Frequency:

The SRF could be obtained by finding the frequency in which $\text{Im}(Z) = 0$.

5.2 Circuit Model of Loop Antennas

Cheng et. al. developed the circuit model of a solenoid coil as shown in Fig. 5.3 with ferrite tube that regards to their previous work. This work was based on the analytical effective permeability model of the ferrite tube. Formulation of components were given. Coils which one has a hollow cylinder ferrite core and the other one has ferrite rod were measured and compared. In addition, measurements of inductance and impedance of coils were compared with different works [15].

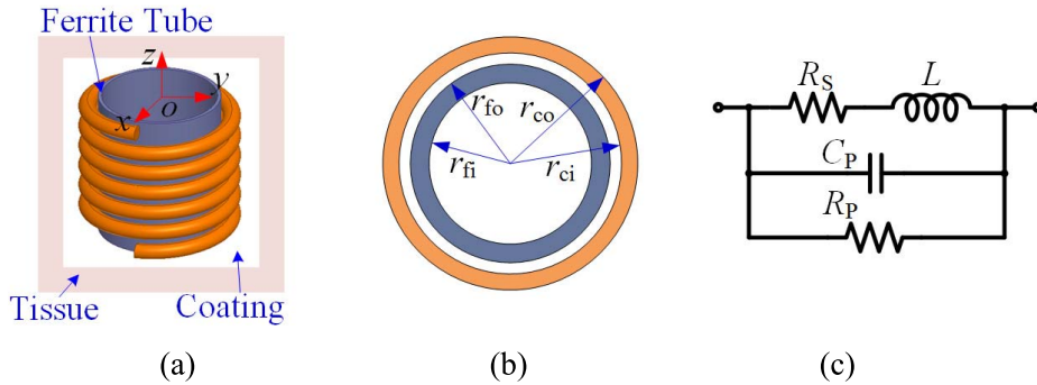


Fig. 5.3: : (a) Diagram of the solenoidal Rx coil which is wound around a ferrite tube, coated with the biocompatible material, and implanted into the tissue. (b) Top view of the Rx coil and the ferrite tube. (c) Equivalent lumped model.

5.2.1 Model 2

Simpson and Zhu investigated an analysis of the electrically small multi turn loop antenna with a spheroidal core and a full-wave analysis of a practical loop with a cylindrical core in 2005 and 2006 [Simpson, 2005, Simpson and Zhu, 2006].

$$\begin{aligned} R &= \frac{R_0}{6\pi} \left(\frac{S_{coil}}{l^2} \right)^2 [1 + (\mu_m - 1)F(\xi_0, \mu_m)]^2 \\ L &= \mu_0 \mu_m (N/2a) S_{coil} F(\xi_0, \mu_m) \\ C &= \frac{\pi \epsilon_0}{25} \frac{b^2}{\sqrt{a^2 - b^2}} [12K_1 + \frac{1}{7}K_3] \end{aligned} \quad (5.5)$$

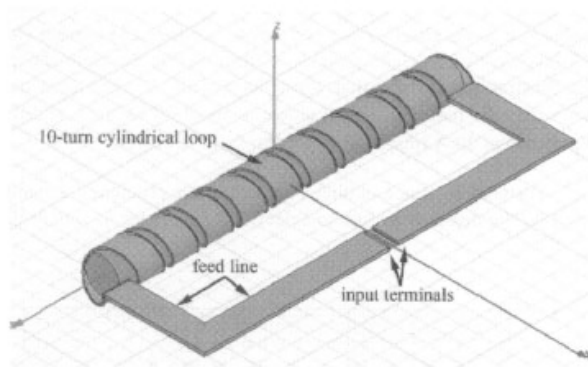


Figure 8a. The HFSS model of a 10-turn loop, wound on a cylindrical core with a length-to-diameter ratio of 10.

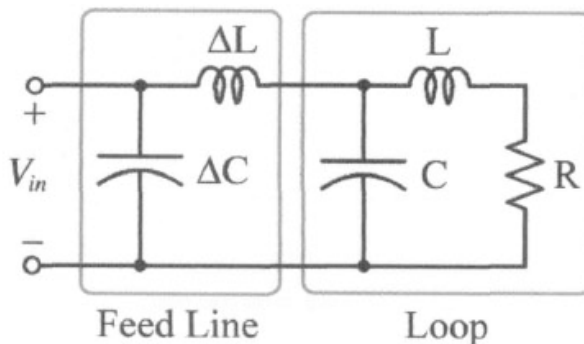


Figure 8b. An equivalent circuit for the feed line and loop of Figure 8a.

Fig. 5.4: : Circuit model 2.

Approximate values for the series inductance $\Delta L = 1.8 \mu H$, and shunt capacitance, $\Delta C = 25.1 pF$, were determined.

5.2.2 Model 3

Kazimierczuk et. al. investigated a circuit model of ferrite core inductors. The behavior of the model parameters vs frequency is considered [Kazimierczuk et. al., 1999].

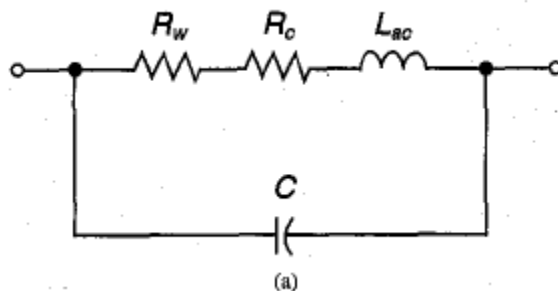


Fig. 5.5: : Circuit model 3.

As shown in figures above all parameters of circuit model are constant and independent from frequency below 1 kHz.

5.2.3 Model 4 - Air Core Solenoid

Fraga et. al. investigated the impedance of long solenoids. In the case of ac, their properties can be studied in terms of an equivalent circuit. When frequency is not too high so that the distributed capacitances have a negligible influence, this circuit is the series connection of a resistance R_s , and an inductance L_s , both parameters usually taking their dc values, and thus the impedance $Z_s = R_s - i\omega L_s$. They noted that corrections are needed for low and high frequencies [Fraga et. al., 1998].

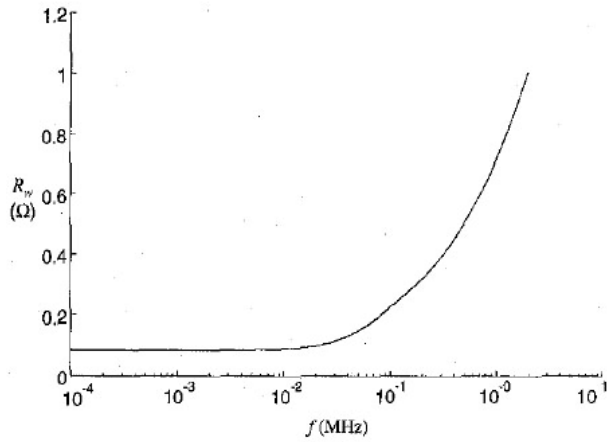


Fig. 5. Winding resistance R_w versus frequency.

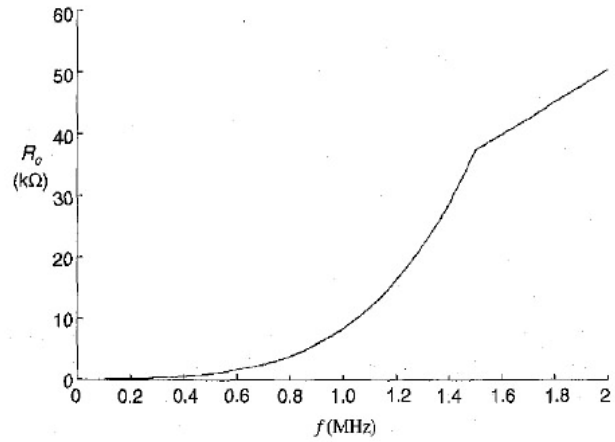


Fig. 6. Core equivalent series resistance R_c versus frequency.

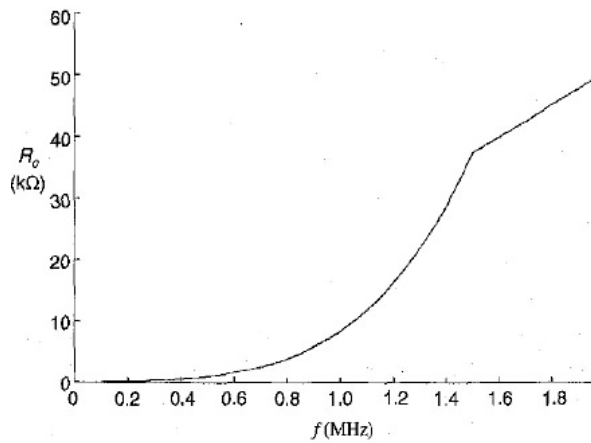


Fig. 6. Core equivalent series resistance R_c versus frequency.

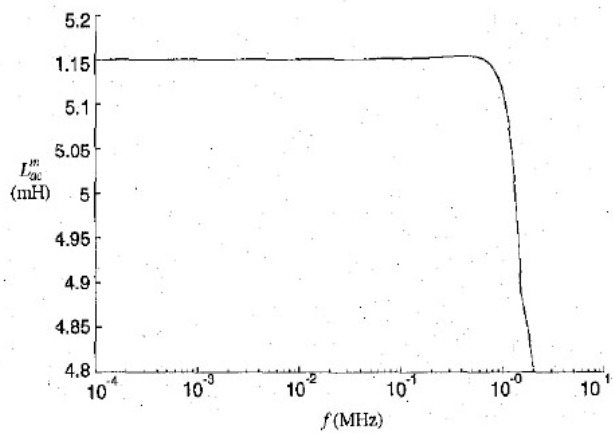


Fig. 7. Main inductance L_{ac}^m versus frequency.

Fig. 5.6: : Circuit model 3 graphics.

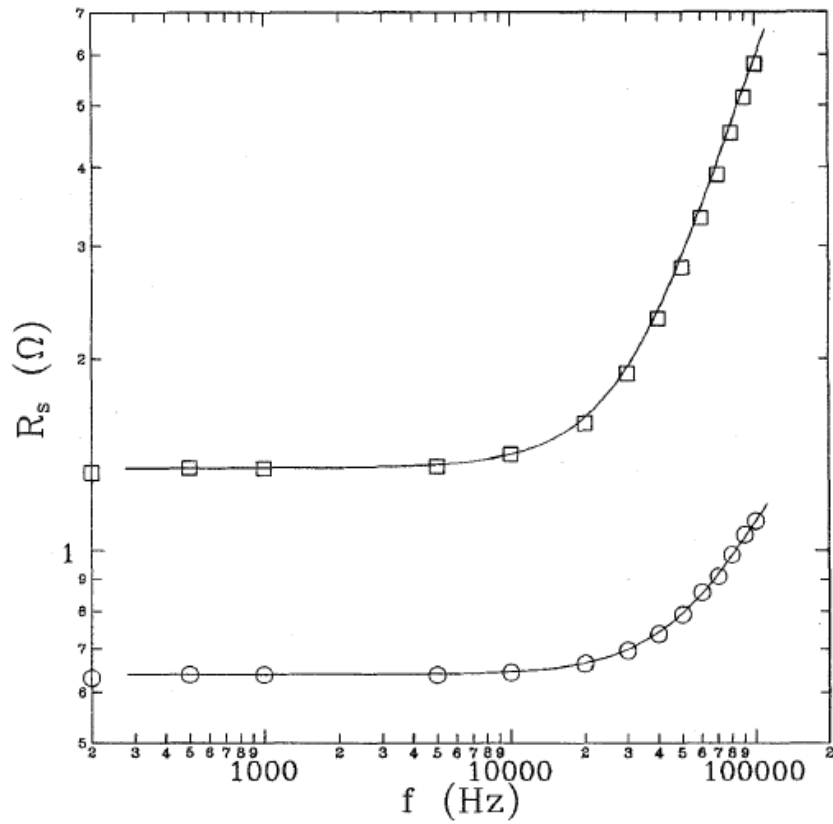


Fig. 2. The measured ac resistance R_s of the single (circles) and double-layer (open squares) solenoids as a function of frequency f . The lines are calculated using (35).

Fig. 5.7: : Circuit model 4 graphics.

5.2.4 Model 5

The ferrite rod antenna consists of a coil which can be modeled as an inductor that has various resistances in series due to the antenna losses. Together with a parallel capacitance the antenna forms a parallel RLC circuit as shown in figure 3 [Koskimaa, 2016].

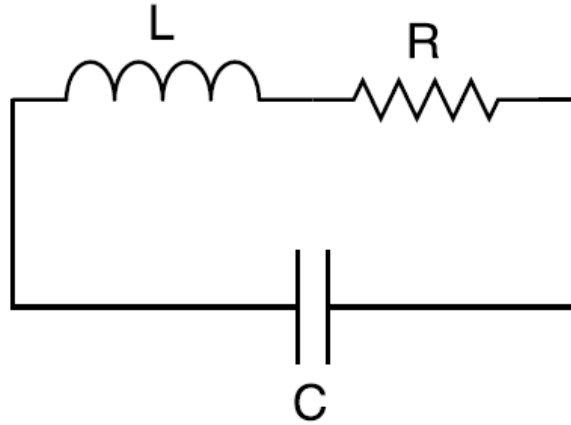


Figure 3: RLC circuit showing the coil inductance (L), resistances (R) including radiation resistance and ohmic losses and parallel capacitance (C).

Fig. 5.8: : Circuit model 5.

Inductance formula is [Koskimaa, 2016, Snelling, 1969]

$$L = \mu_0 \mu_{cer} N^2 \frac{A}{l_f} \quad (5.6)$$

Most of the capacitance in the circuit is due to the parallel capacitor. The coil itself has a small capacitance between individual turns and the total capacitance between all turns is

$$C = \frac{\pi^2 2r_c \epsilon_0 \epsilon_r}{\cosh^{-1} \left(\frac{2r_w + d_w}{2r_w} \right) (N - 1)} \quad (5.7)$$

where d_w is the distance or gap between individual wires and r relative permittivity of the medium which in a tightly wound coil is the coating on the metal wire. The resistances in the antenna are divided into ohmic losses and the radiation resistance. Ohmic losses in the antenna are caused by losses in the wire itself and losses in the ferrite core. Increased losses lead to the antenna being less sensitive at the resonant frequency. The half-power bandwidth also becomes wider [Koskimaa, 2016].

Ferrite Core loss

Ferrite core is a lossy material that absorbs power from the magnetic field flowing through the coil. The magnitude of the ferrite loss depends on the material of the rod and the dimensions of both the wire coil and the rod. The equation for the ferrite loss is

$$R_f = \omega \mu_0 \mu_{cer} \tan \delta_m N^2 \frac{A}{l_f} \quad (5.8)$$

5.2.5 Model 6 - Receiving Loaded Antenna

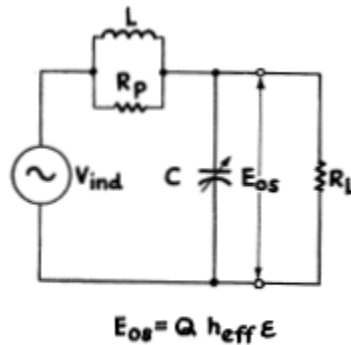


Figure 5—Ferrite Loopstick Antenna Circuit.

Fig. 5.9: : Circuit model 6 [Laurent and Carvalho, 1962].

5.3 Radiation Resistance

As the energy lost on the ohmic resistance transforms into heat, the energy that is lost in the radiation resistance turns into electromagnetic radiation.

The radiation resistance of receiving loop antennas is usually very small that in the milli- or micro-ohm range. The loops are typically extremely inefficient because losses due to wire resistance and core magnetic material (if exist) are literally hundreds of times larger than radiation resistance [57].

Radiation resistance of N-turn, air-cored loop is given by

- C : circumference of the loop [m]
- A : area of the loop [m]
- λ : wavelength [m]
- N : number of turns of the loop

The relation is about 2 % in error when the loop perimeter is $\lambda/3$. A circular loop of this perimeter has a diameter of about $\lambda/10$ [37].

5.4 Coil Resistance

The resistances in the antenna are divided into ohmic losses and the radiation resistance. Ohmic losses in the antenna are caused by losses in the wire itself and losses in the ferrite core. Increased losses lead to the antenna being less sensitive at the resonant frequency. The half-power bandwidth also becomes wider [Koskimaa, 2016].

Witzig investigated high-frequency resistance of coils [Witzig, 1947].

$$R_c = K_\tau R_0 (0.38d\sqrt{f} + 0.25) \tag{5.9}$$

K_τ is an empirical constant. When a coil is used at a frequency near its resonant frequency, its resistance is modified by its self-capacitance. This self-capacitance increases the circulating current flowing in the coil and hence gives rise

to a greater coil loss. Apparent coil resistance can be shown as [Witzig, 1947]

$$R_c^{resonance} = \frac{R_c}{(1-\omega^2 LC_0)^2} \quad (5.10)$$

$$C_0 = 4.55 \cdot 10^{-14} \frac{l_r}{\ln 0.72 l_r / d_r}$$

Wire Resistance with Skin and Proximity Effect

The **skin effect** is caused by eddy currents in the conductor. A current flowing in a conductor creates a magnetic field around it. Magnetic field induces circular eddy currents that oppose the change in the magnetic field. This leads to the eddy currents being in the opposite direction of the original current flow in the center of the conductor. Near the surface or skin of the conductor the eddy currents flow in the original current direction. Most of the current now flows near the conductor surface thus the effective conducting area is reduced.

The surface resistance of a conductor is

$$R_s = \sqrt{\frac{\omega\mu}{2\sigma}} \quad (5.11)$$

For a wire with length l_w and radius r_w the wire resistance is

$$R_w = \frac{l_w}{2\pi r_w} \sqrt{\frac{\omega\mu}{2\sigma}} \quad (5.12)$$

For a coil with radius r_c this becomes

$$R_w = N \frac{r_c}{r_w} \sqrt{\frac{\omega\mu}{2\sigma}} \quad (5.13)$$

The **proximity effect** loss is similarly to the skin effect caused by eddy currents. The magnetic field created by a conductor induces eddy currents in nearby conductors.

$$R_w = N \frac{r_c}{r_w} \sqrt{\frac{\omega\mu}{2\sigma}} \left(\frac{R_p}{R_0} + 1 \right) \quad (5.14)$$

where the ratio R_p/R_0 is a factor of how much the total wire resistance is increased due to the proximity effect [Smith, 1971]. By knowing the easily calculated skin effect resistance, the proximity effect can be determined with other means such as simulations and measurements [Koskimaa, 2016].

Skin Effect

Fig. 1 is a chart giving the surface resistivity R , and the depth of penetration d for various metals, over a wide range of frequency f [Wheeler, 1942].

5.4.1 Loaded Loop Resistance

Hill and Bostick investigated a sensor (*magnetometer*) that had laminated mumetal core. The length and resistance of the coil in the sensor had been studied in detail. Within the core, eddy current and hysteresis losses and Within the winding, losses caused by skin effect, proximity effect, distributed capacity, and wire resistance were considered [27].

5.4.2 Skin Effect Resistance

When the wire diameter is much smaller than the coil diameter, a circular coil can be approximated as a straight conductor for the calculation of the skin effect resistance [14][35]

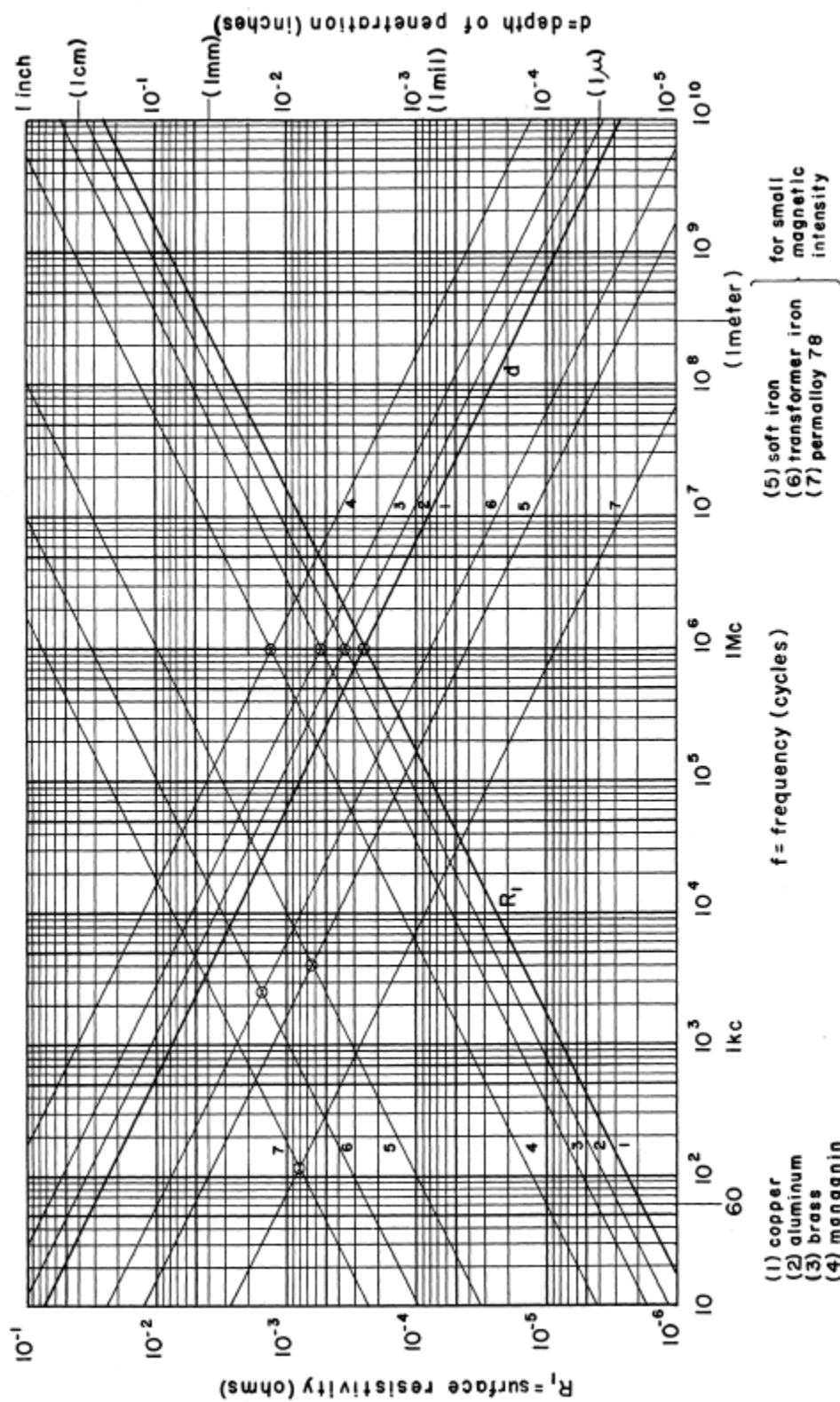


Fig. 1—Surface Resistivity and Depth of Penetration.

Fig. 5.10: : Surface resistivity and the depth of penetration over a wide range of frequency.

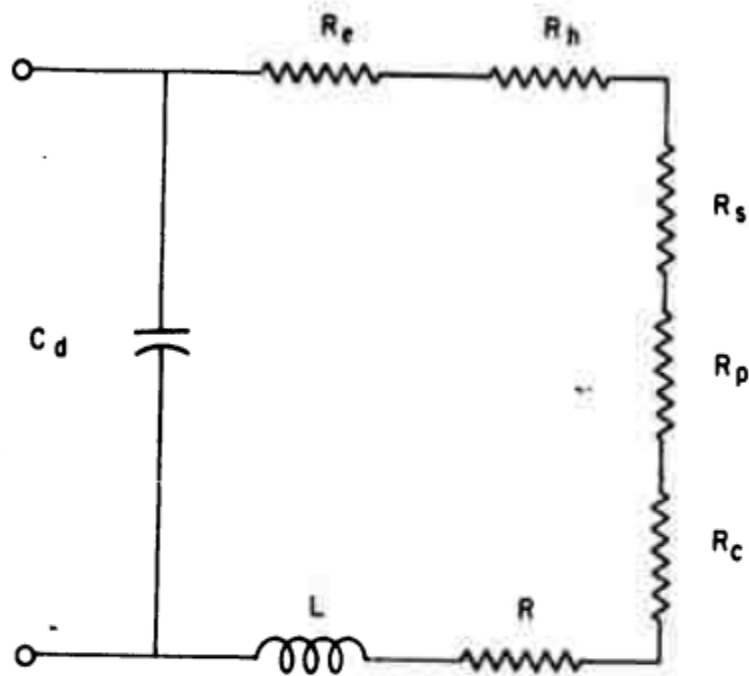


FIG. 1. EQUIVALENT CIRCUIT OF SENSOR
WITH MAGNETIC CORE

Fig. 5.11: : Equivalent circuit of sensor with magnetic core.

5.4.3 Proximity Effect Resistance

The proximity effect resistance R_{pr} induced by adjacent parallel conductors is a classic and yet difficult problem. Butterworth [38] considered R_{pr} as a part of R_{sk} by multiplying an empirical factor from a lookup table. This table was revised by Medhurst [39] for higher accuracy. However, both [38] and [39] are valid only when the number of turns is large [40] and not appropriate for general use because of the limited scope of its applications [41]. Smith [42] obtained an exact solution for the case of two parallel conductors. However, an approximation method using Fourier series expansion with cumbersome numerical calculations is needed when $N > 2$ [43]. Dwell [44] and Ferreira [45] considered these parallel turns as a foil and used a porosity factor to revise the error induced from omitting the gap between turns, which were improved further by weighting these two methods [46], [47]. The methods reported in [44]–[47] are suitable for traditional transformers with ferrite cores. On the other hand, eddy current in a cylindrical conductor and its corresponding resistance have analytical closed-form solutions [48]. Note that the formulas in [35] and [49] have typos [48]. The turns in solenoid coils can be considered as several parallel cylindrical conductors, changing the problem to how to calculate H_n for each turn. An iterative method has been proposed to solve this problem [49]. The successive approximations method starts by considering the wires as filaments to calculate the initial magnetic field and proceeds by using the new magnetic field to calculate the induced current and magnetic field. A simpler and more direct approximation method from [37] is selected and improved in this paper [14].

5.4.4 Resistance of Inductors

Reatti and Kazimierzczuk investigated the AC resistance of an inductor. Several expressions in the literature for high-frequency winding resistance of inductors were reviewed and compared. In addition, an expression was presented to predict accurately both the high-frequency resistance and the quality factor of inductor. Equivalent circuit models of inductors in the literature were given as well [47].

5.5 Coil Inductance

5.5.1 Air Core Loop

Wheeler gave simple inductance formulas for circular and square coils [Wheeler, 1982].

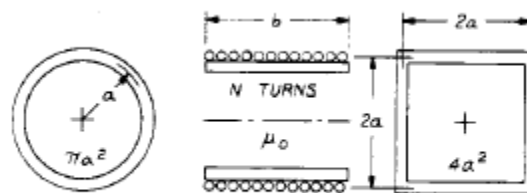


Fig. 1. A circular or square coil.

Fig. 5.12: : A circular or square coil.

	Circular Coil	Square Coil
Simple	$L = \mu_0 n^2 a [0.48 \ln (1 + \pi a/b) + 0.52 a \sinh \pi a/b]$	$= \mu_0 n^2 a [0.802 \ln (1 + \pi a/b) + 0.471 a \sinh \pi a/b]$
Short Coil	$L = \mu_0 n^2 a \left(\ln (1 + \pi a/b) + \frac{1}{2.3 + 1.6 b/a + 0.44 (b/a)^2} \right)$	$L = \mu_0 n^2 a (4/\pi) \left(\ln (1 + \pi a/b) + \frac{1}{3.64 + 2b/a + 0.51(b/a)^2} \right)$
Long Coil	$L = \mu_0 n^2 a \left(\frac{2.78}{b/a + 1.1} + \ln (1 + 0.39 a/b) \right)$	$L = \mu_0 n^2 a (4/\pi) \left(\frac{2.67}{b/a + 1.26} + \ln (1 + 0.5 a) \right)$

Lundin gave a formula for the inductance of a single-layer circular coil or solenoid. He noted that a single-layer circular coil can be idealized to a cylindrical current sheet. If $2a < b$ then [Lundin, 1985]:

$$L = \frac{\mu_0 n^2 \pi a^2}{b} \left\{ f_1 \left(\frac{4a^2}{b^2} \right) - \frac{4}{3\pi} \frac{2a}{b} \right\}$$

$$f_1(x) = \frac{1 + 0.383901x + 0.017108x^2}{1 + 0.258952x}, \quad 0 \leq x \leq 1$$

5.5.2 Air Core Solenoid

A simple chart as shown in Figure 1 presents the relation between inductance, over-all dimensions, and density of winding for a solenoid coil. Any one unknown may be determined if the other quantities are given. The chart is accurate for many turns of fine wire, close wound in a single layer. It is also accurate at low frequencies for one turn or many turns of thin ribbon, close-wound in a single layer [Wheeler, 1950].

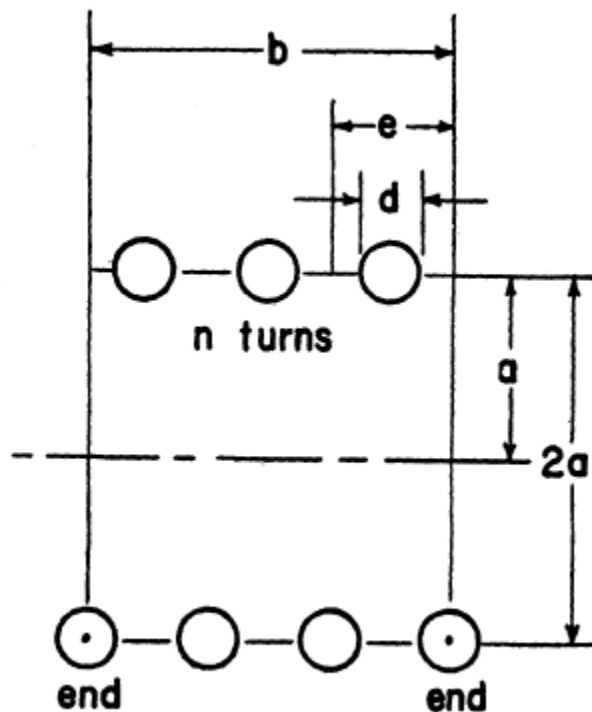


Fig. 1—Dimensions of solenoid coil.

Fig. 5.13: : Dimensions of solenoid coil.

Self-inductance of solenoid is given by [Smythe, 1989]

$$L = \mu_0 \pi a^2 N^2 \frac{1}{\sqrt{l_s^2 + a^2} - a} \tag{5.15}$$

where a is radius of the loop or solenoid in meters, l_s is length of solenoid in meters and N is number of turns of the loop.

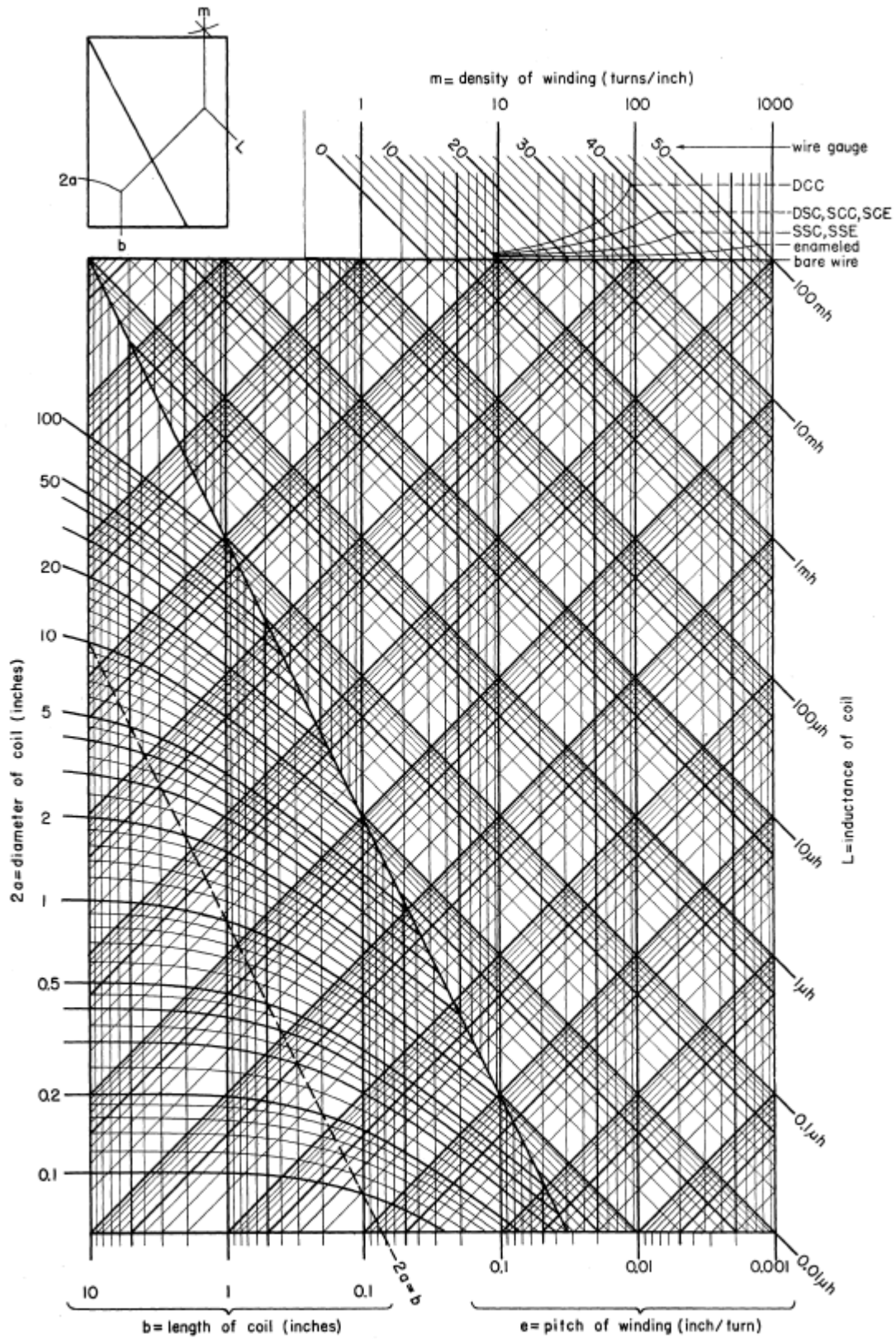


Fig. 2—Inductance chart.

Fig. 5.14: : Relation between inductance, over-all dimensions, and density of winding for a solenoid coil [Wheeler, 1950].

Inductance of solenoid air core for single layer [Burhans, 1979]:

$$L_h = \frac{0.2d^2 N^2}{3d + 9b} \tag{5.16}$$

where d is diameter and b is length in inches. Then, inductance of loop on core [Burhans, 1979]:

$$L_{cored} = \mu_{cer} L_h \tag{5.17}$$

5.5.3 Magnetic Core Loop

Devore and Bohley gave the inductance of coil formulation. They also noted that $\mu_r \ll \mu_r'$ which is reasonable assumptions for long solenoids with low loss cores. [Devore and Bohley, 1977].

$$L = \mu_0 \frac{n^2}{l} (\pi a^2)(1 - D) \left[1 + (1 - D_F) \frac{l_F}{l} \left(\frac{a_F}{a} \right)^2 \frac{\kappa' - 1}{1 + D_F(\kappa' - 1)} \right]$$

Jutty et. al. developed an equivalent model of inductors at high frequencies.

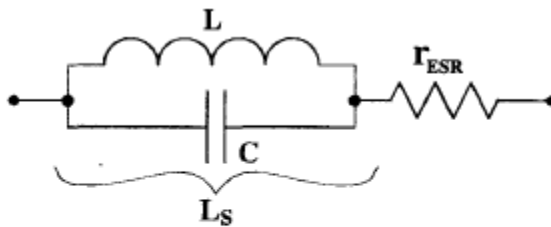


Figure 2: Equivalent circuit of an inductor composed of an inductor, a resonant capacitor, and an ESR.

Fig. 5.15: : Equivalent circuit of an inductor.

It is shown that an inductor behaves like a capacitor beyond its resonant frequency. The measured inductance L_S of an inductor with the effect of the capacitance included given by

$$L_s = \frac{L}{1 - \omega^2 LC} = \frac{L}{1 - (\omega/\omega_{res})^2} \tag{5.18}$$

Figure 1 shows the rod permeability as a function of the length to diameter ratio for the six materials available in rods. The inductance modifier is found in Figure 2. The ratio winding length divided by the rod length will give the inductance modifier. If the rod is totally wound the $K=1$. Shorter but centered winding will yield higher K values [Fair-Rite Rods Datasheet].

To calculate the inductances of a wound rod the following formula can be used,

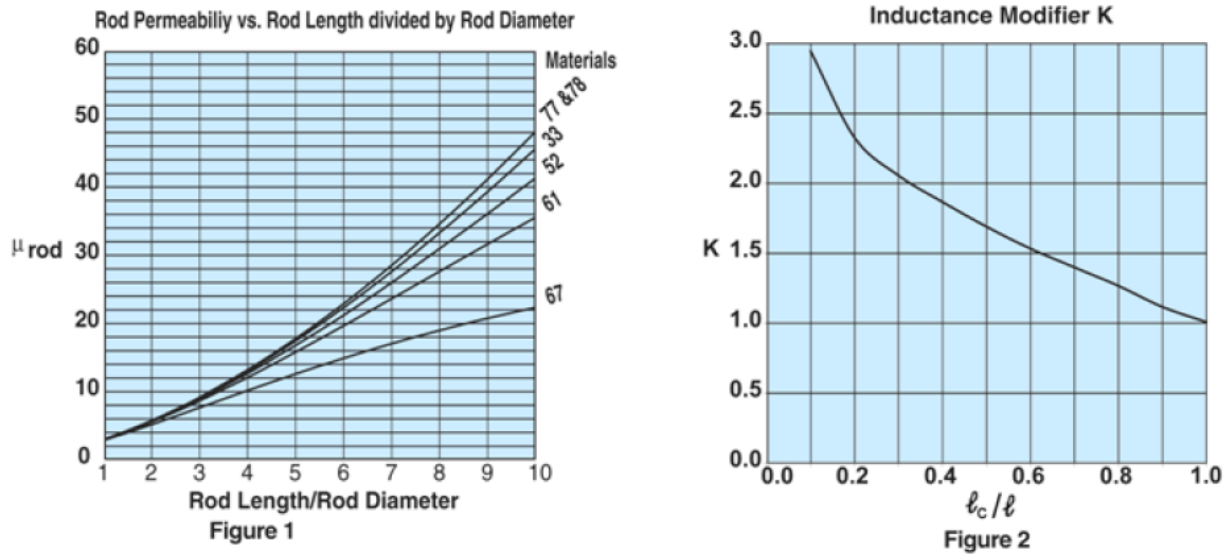


Fig. 5.16: : Rod permeability and inductance modifier.

$$L = K \mu_0 \mu_{rod} \frac{N^2 A_e}{l} 10^4 (\mu H)$$

- Where: **K = Inductance modifier**
 $\mu_0 = 4\pi 10^{-7}$
 μ_{rod} = rod permeability found in Figure 1.
N = Number of turns
Ae = Cross sectional area of the rod (cm²)
 l = Length of the rod (cm)
 l_c = Length of the winding (cm)

This formula was also given in Soft Ferrites book. [Snelling, 1969, Fair-Rite Rods Datasheet]

5.5.4 Effective Radius of Solenoid

Current distribution in the wire of a solenoid is not uniform at low frequency due to path-length variation and strain. Therefore, there can be an error in inductance calculations. Knight investigated effective radius of coils and gave formulas and numerical algorithms for the effective radius for solid rectangular and round wire [36].

5.6 Coil capacitance

Fraga et. al. noted that the capacitance effect of a solenoid is quite small regards to measurements at frequencies below 100 kHz [19].

5.7 Impedance Matching

The impedance in the antenna's main RLC circuit is not well matched to 50Ω . The induced voltage is highly reflected if connected directly to a 50Ω input. One way to improve the matching is to use a secondary coil or a so called pick-up coil next to the main coil [Koskimaa, 2016].

5.7.1 Pick-up Coil

The pick-up coil will act as an impedance transformer. The impedance transformer transforms the main coil impedance and voltage into the secondary coil according to the equation

$$\frac{N_2}{N_1} = \frac{U_2}{U_1} = \sqrt{\frac{Z_2}{Z_1}} \quad (5.19)$$

When the pick-up works as intended the output voltage from the decreased secondary coil voltage is still higher than the original main coil output voltage due to the improved matching.

When inductors are coupled a current change in one inductor induces a voltage in the second inductor. The mutual inductance between the inductors is defined as

$$M = k\sqrt{L_1L_2} \quad (5.20)$$

where k is the coupling coefficient. The equivalent circuit of two coupled inductors is a T-circuit shown in figure below.

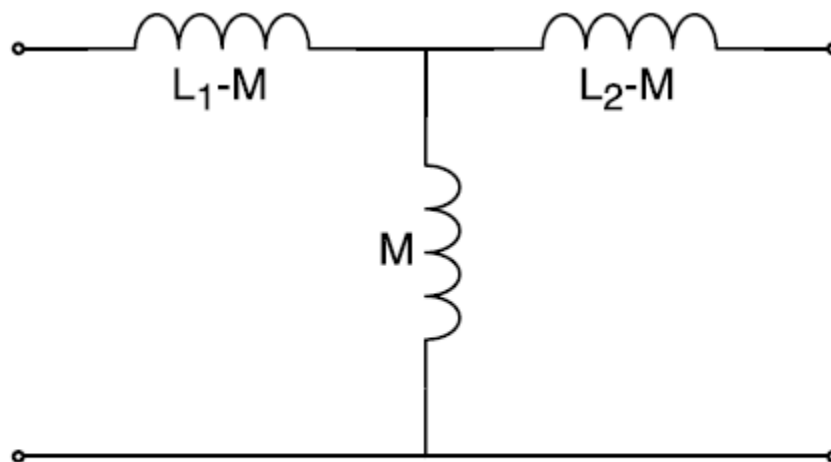


Figure 5: Equivalent circuit of two coupled inductors.

Fig. 5.17: : Equivalent circuit of two coupled inductors.

The voltage over the two coils can be expressed with the mutual inductance as the following:

$$\begin{aligned} U_1 &= j\omega(L_1 I_1 + M I_2) \\ U_2 &= j\omega(M I_1 + L_2 I_2) \end{aligned} \quad (5.21)$$

The coupling coefficient of the two coils can be measured by changing the secondary coil from open circuit to shorted and observing the change in the resonant frequency. When the second coil is shorted the voltage in the secondary coil becomes zero and the current will be

$$I_2 = -\frac{M I_1}{L_2} \quad (5.22)$$

By inserting this into the voltage equation of the primary coil in equation U1_U2

$$U_1 = j\omega L_s I_1 \quad (5.23)$$

where L_s is the apparent/measured inductance over the primary coil when the secondary coil is shorted. Now the mutual inductance squared can be written as

$$M^2 = L_2(L_1 - L_s) \quad (5.24)$$

Using this the coupling coefficient becomes

$$k = \frac{M}{\sqrt{L_1 L_2}} = \sqrt{1 - \frac{L_s}{L_1}} = \sqrt{1 - \left(\frac{f_0}{f_s}\right)^2} \quad (5.25)$$

where f_0 and f_s are the resonance frequencies related to the inductances L_1 and L_s according to resonance frequency of the RLC with the secondary coil open and shorted, respectively.

The impedance at the antenna output is Z_2 . A portion of the pick-up voltage U_2 is reflected at the antenna output according to equation

$$\Gamma = \frac{Z_L - Z_2}{Z_L + Z_2} \quad (5.26)$$

where the load impedance is 50Ω . The output voltage of the antenna is [Koskimaa, 2016]

$$U_{out} = (1 - \Gamma)U_2 \quad (5.27)$$

5.7.2 Transformer Coupling

Bachman investigated a low-impedance loop with coupling transformer and explained the transformer parameters in terms of the circuit and transformer coupling coefficients in 1945. The gain of the transformer coupled loop system was analysed. The low-impedance transformer-coupled loop and a high-impedance loop connected directly to the same tuning capacitor was compared. He concluded that an ideal transformer-coupled loop has 38.4% of the gain from a direct-connected loop of the same area, assuming the same Q in the transformer secondary as in the direct connected loop. In Fig. 5.18 the low-impedance loop coupling-transformer circuit was shown [6].

In 1948 Fratianni investigated methods of coupling loops to receivers that transformer-coupled and direct connected as shown in Fig. 5.19. Mathematical analysis and theoretical treatment of transformer-coupled was done. Coupling design for *maximum voltage amplification* and *optimum signal-to-noise ratio* was studied. In order to show the effects of parameters on circuit performance eight conditions were built. All direct coupled cases were better than transformer-coupled cases with regard to signal-to-noise ratio. Only two transformer-coupled sets better than direct coupled sets for voltage amplification basis. He also noted that if a long cable length was required, transformer-coupled circuits could be preferred [20].

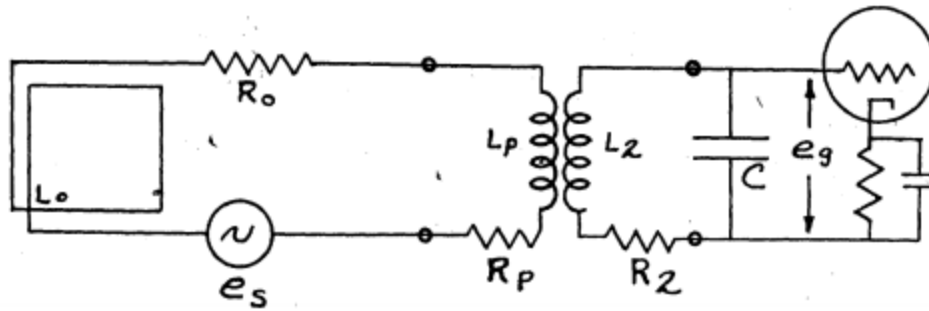
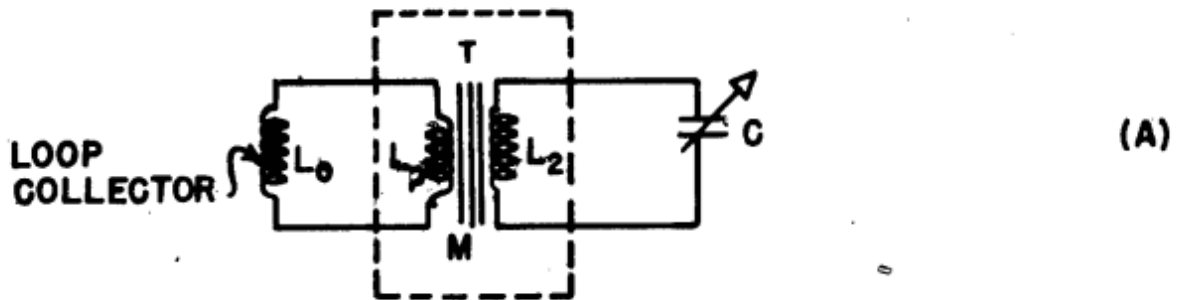


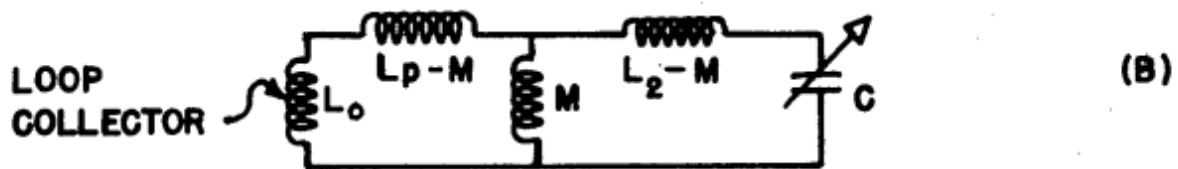
Fig. 5.18: : Low-impedance loop coupling-transformer circuit.

5.8 Self Resonance Frequency

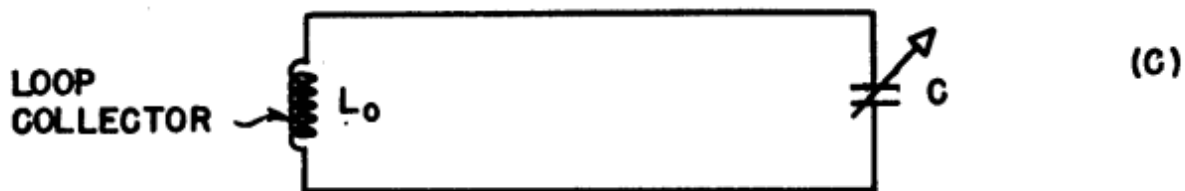
Payne investigated self resonance frequency of coils and relationship of inductance, resistance, and Q factor of the coils. Derived equations of resistance, inductance, and Q factor were given. In addition, discussion of self capacitance was presented [43].



TRANSFORMER-CONNECTED LOOP COLLECTOR



EQUIVALENT OF CIRCUIT (A)



EQUIVALENT DIRECT-CONNECTED LOOP CONNECTOR

Figure 1

Fig. 5.19: : Transformer-coupled and direct connected receiving loops.

6.1 Introduction

The insertion of a ferromagnetic core into a coil increases its self-inductance and effective resistance due to the increase of flux [11].

A ferrite core in the loop that tends to increase the magnetic flux, the magnetic field, the open-circuit voltage, and in turn the antenna efficiency of the loop.

Ferrite core electrically small loops are often used for receiving signals, such as in radios and pagers, where the signal to noise ratio is much important than efficiency.

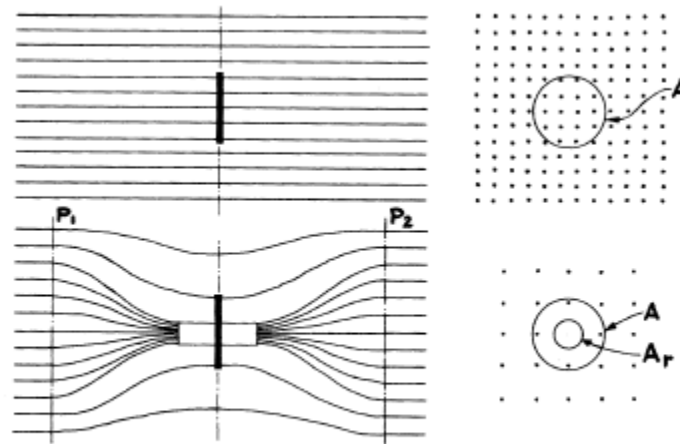


Figure 2—Effect of the Ferrite Rod.

Fig. 6.1: : Effect of the ferrite rod [Laurent and Carvalho, 1962].

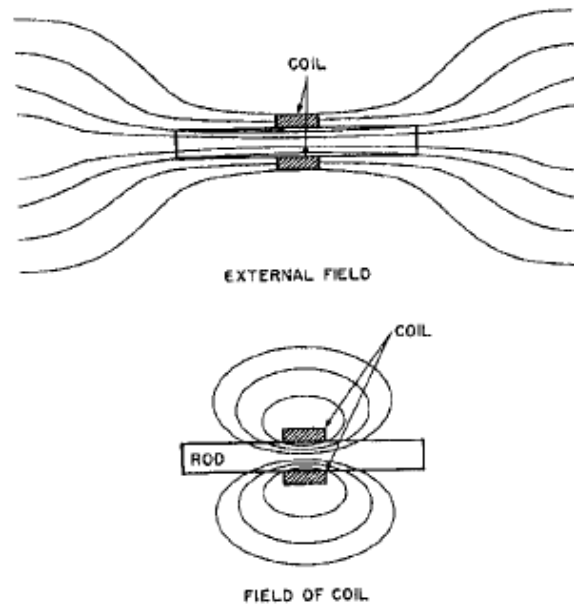


Figure 12.18- The influence of a ferrite rod in concentrating the flux in an antenna coil. From Philips.

Fig. 6.2: : Influence of a ferrite rod [Alex Goldman-Modern Ferrite Technology-Springer (2010) p305].

Eshraghian et al. (1982), Ranasinghe (2007), and Cole et al. (2003) show that without the magnetic core the coupling volume of a long solenoid is just the physical volume, but when a magnetic core is inserted, the coupling volume increases by a factor equal to the effective permeability of the magnetic core [Serkan Aksoy, Mail, 10.08.2017].

The loops are rarely used as transmitting antennas above low levels of power due to their poor radiation efficiency (low radiation resistance). As transmitting antennas, they become less significant below 30 MHz. If the efficiency is not an issue and power levels are very low, they are used as a transmitter. Because they would soon become very hot when any reasonable levels of power are fed into them, they must be cooled (for example by water as in torpedo transmitter).

As an exception, a tuned transmitting loop, can be equipped with a remotely controlled capacitor to make a resonant circuit, is used to transmit waves. However, such loops have to be retuned whenever the frequency is changed (even in the same operating band) because they are extremely narrowband. Nonetheless, they are sometimes the only practicable option for transmission when space is restricted [Serkan Aksoy, Mail, 01.06.2017].

6.1.1 Dimensions

For magnetic core antennas, the length of the magnetic core should be equal to the diameter of the equivalent air-core loop antenna in order to achieve an comparable performance over the air-core antennas. The two dimensions of the air-core antenna are large, whereas the magnetic core antenna is only one dimension large. Thus, the magnetic core antenna has the advantage of packaging. Electrostatic immunity is better and electrostatic protection can be applied more easily [57].

Cylindrical cores longer than a solenoid winding are used to increase L for a given physical size. Cylindrical cores shorter than the solenoid winding and moved along the winding axis are used for L tuning with the greatest L occurring with the core centered [Serkan Aksoy, Mail, 04.04.2017].

6.1.2 Measurement

Stewart investigated measurement of a ferrite core loop antenna. A general discussion was given about applications of small loops with air core and ferrite core. The data received by static measurement (below audio frequency) are largely valid and can be collected very quickly so that the tests of the magnetic core antennas with many parameters are obtained on a reasonable budget. Losses of the magnetic core increase above 20 MHz frequency and the magnetic core antennas are no longer as good as air-cored loops. RF measurements of the magnetic dipole antenna usually require that the antenna is electrically shielded; otherwise, it is impossible to separate radiation into electric and magnetic components [57].

6.1.3 Permeability (Influence of High-Frequency Magnetic Fields)

The reaction of the magnetic induction B (and thus also of the magnetization) on an external alternating magnetic field H with a time dependence can be expressed as:

$$\begin{aligned} B &= B_0 e^{i(\omega t - \delta)} \\ H &= H_0 e^{i\omega t} \end{aligned} \quad (6.1)$$

As a consequence the permeability μ becomes complex:

$$\mu = \frac{B}{H} = \frac{B_0 e^{i(\omega t - \delta)}}{H_0 e^{i\omega t}} = \frac{B_0}{H_0} e^{-i\delta} \quad (6.2)$$

Using $e^{-i\delta} = \cos \delta - i \sin \delta$ we get:

$$\mu = \frac{B_0}{H_0} \cos \delta - i \frac{B_0}{H_0} \sin \delta \quad (6.3)$$

Characterizing the real and negative imaginary part of the permeability by:

$$\begin{aligned} \mu' &= \frac{B_0}{H_0} \cos \delta \\ \mu'' &= \frac{B_0}{H_0} \sin \delta \end{aligned} \quad (6.4)$$

we obtain [Fundamentals of magnetism - M.Getzlaff – 2008, p.139]:

$$\mu = \mu' - i\mu'' \quad (6.5)$$

Due to the finite size of the ferrite rods, the effective permeability of the rod decreases near the ends of the solenoid. As a consequence of this, the inductance of the solenoid does not always grow as the square of the number of turns, as would be expected [Serkan Aksoy, Mail, 15.03.2017].

Figure 1 shows the rod permeability as a function of the length to diameter ratio for the six materials available in rods [Fair-Rite Rods Datasheet].

6.1.4 Two Winding Solenoid

Loopstick antenna from an AM radio having two windings, one for long wave and one for medium wave (AM broadcast) reception. Typically, 10 cm long, these loop antennas are usually hidden inside the radio receiver [Serkan Aksoy, Mail, 03.04.2017].

In the contra-wound configuration, introduced by the US Army Signal Corp many years ago and described in publications by Burhans and by Cornell, the coil wound on the ferrite rod is split into two equal parts wound with opposite sense. If the “outside” ends of these coils are grounded, a single-ended signal can be taken from the midpoint of the coil resulting in much simplified preamp design. Also, since the total coil inductance is halved (the half-coils would be in parallel), for a given required total inductance the number of turns can be increased providing increased sensitivity. (The total self-capacity of the windings is increased but ordinarily such would not be of principal concern.) [Serkan Aksoy, Mail, 29.07.2017]

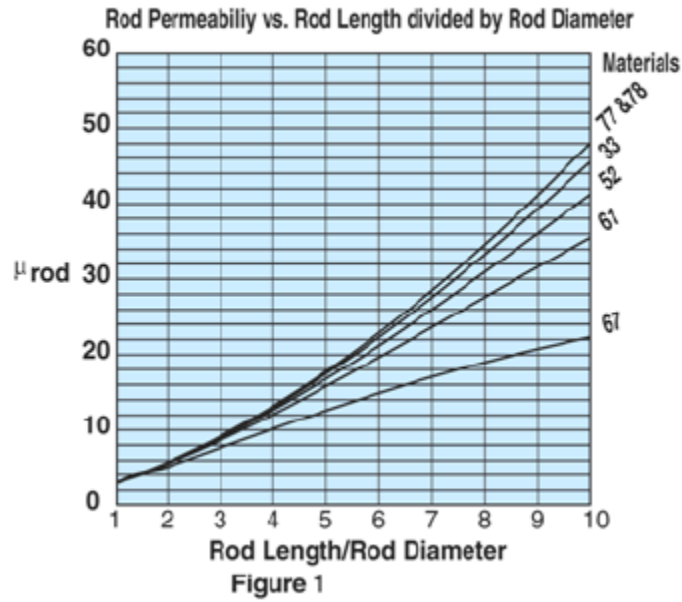


Fig. 6.3: : Rod permeability [fair-rite-datasheet].

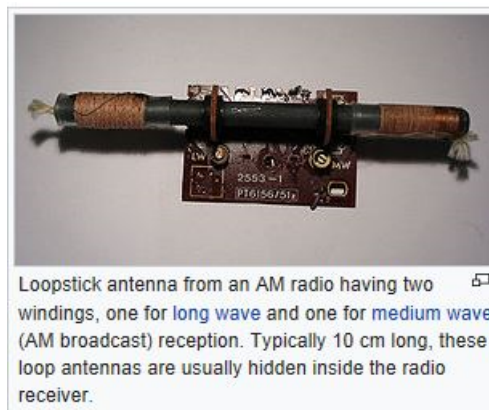


Fig. 6.4: : Two winding solenoid.

6.1.5 Notes

Mark 48 torpedo

Unconfirmed reports indicate that the torpedo's sensors can monitor surrounding electrical and magnetic fields. This may refer to the electromagnetic coils on the warhead (at least from 1977 to 1981), used to sense the metallic mass of the ship's hull and detonate at the proper stand-off distance [Serkan Aksoy, Mail, 08.04.2017].

A magnetic fuze reacts to the variable magnetic field of a ship is necessary for the most successful position of detonation under the keel of the ship. Work on this aspect of the bomb was found to be far from complete. The susceptibility to disturbances and the reaction capacity of such fuzes had not been investigated thoroughly either. A magnetic proximity fuze, however, is necessary for greater release ranges and for curved underwater trajectories.

Good detonation positions can be achieved with straight underwater travel if the fuze is set to go off after a specific distance through the water. The angle of entry must naturally not be altered as the underwater travel depends on the angle of entry. The time delay set on the fuze can be determined most simply by assuming a constant time for underwater travel.

In designing the fuze system, the following points must be borne in mind. Further, the speed and range of release must be functioned very accurately for a pre-set time as the tolerance of plus or minus 0.1 second can only be achieved with a clockwork fuze. Finally, the tail section must be jettisoned by explosive bolts or by some other adequate method on impact with the water [Serkan Aksoy, Mail, 11.04.2017].

The (modern) German navy uses submarines whose hulls are made entirely out of some classified non-magnetic alloy. This protects them from setting off static magnetic fuses and submarine detection systems [Serkan Aksoy, Mail, 11.04.2017].

Analytical calculations of magnetic cored loops could not be calculated except for the special case of an ellipsoidal core, and even then calculations were approximate [57].

6.2 History

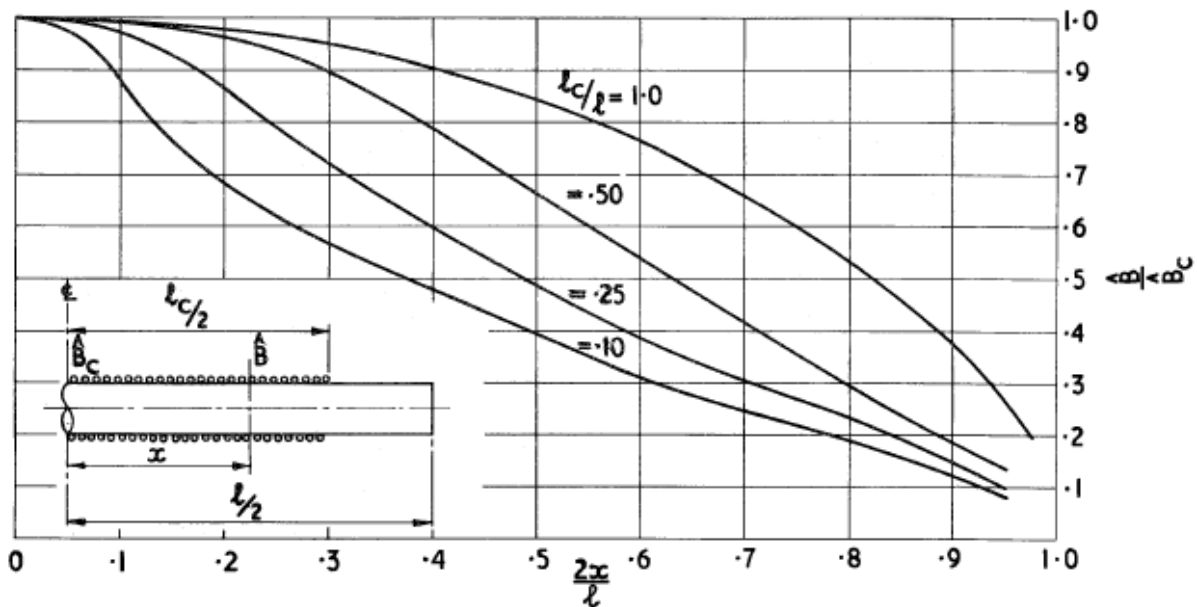
Fратиани investigated the effect of iron cores on the receiving efficiency of VLF loop antennas, in air and underwater [Fратиани, 1950].

Rumsey and Weeks investigated electrically small, ferrite loaded loop antennas. Approximate formulas have been developed for the impedance, efficiency, and Q of electrically small, ferrite-loaded loop antennas. The formulas are based on an assumed knowledge of these parameters for the antenna without ferrite loading. Radiation resistance formulation is also given [Rumsey and Weeks, 1956].

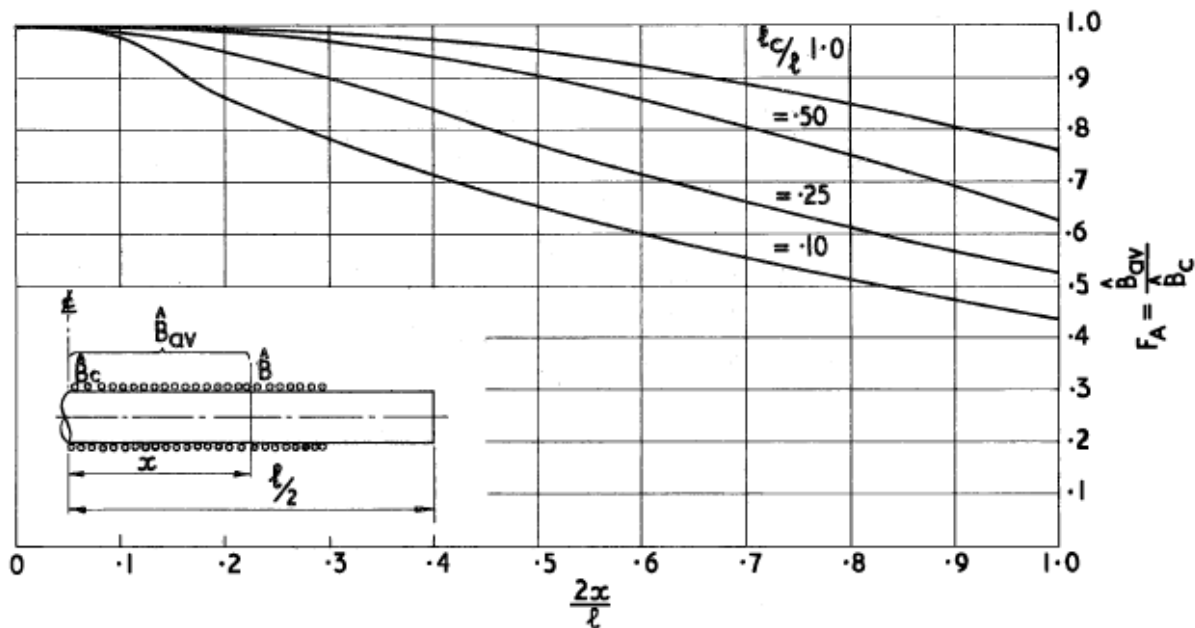
Devore and Bohley investigated an analytical model of a class of electrically small multiturn loop antennas has been formulated and compared with experimental measurements over a frequency range of 3 to 86 MHz. Both air core and magnetically loaded cases were examined. The analytical model described in this paper should prove an effective design aid for a volumetrically constrained antenna of the class [Devore and Bohley, 1977].

Burton et. al. investigated the electromagnetic field of an electrically small loop antenna with a cylindrical core. The infinitely long cylinder may be conducting or insulating. With the help of the principle of similitude, measurements made with a small loop at a high frequency with cylinders of water with widely different conductivities are applied to a very large loop around a mountain at a very low frequency. An approximate equivalent circuit for the loop with a core is described and tested [Burton et. al., 1983].

The goal of this research is to develop and validate a low-frequency modeling code for high-moment transmitter rod antennas to aid in the design of future low-frequency TX antennas with high magnetic moments. modeling code can predict the TX antenna's gain, maximum magnetic moment, saturation current, series inductance, and core series loss resistance, provided the user enters the corresponding complex permeability for the desired core magnetic flux density [Jordan et. al., 2009].



(a) Flux distribution as a function of fractional distance from centre



(b) E.m.f. averaging factor, F_A , as a function of the averaging length, centrally heated

Fig. 4.11. Distribution of flux density measured along a ferrite cylinder energized by a central solenoid, the parameter being the fraction of the cylinder covered by the solenoid. The result is almost independent of μ_{rod}

6.3 Radiated Fields

Islam introduced a solution for retarded vector potential of a permeable *infinitely-long cylinder* loaded circular loop that is derived from Maxwell's equations. Islam also noted that vector potential of a loop antenna that wrapped around the finite cylinder core is very difficult due to the complexity at the end of the cylinder. Resulting vector potential consisted of two parts: first part of potential was from loop alone and the other part was from the permeable core [31].

Islam then investigated methods of obtaining the electromagnetic field quantities (magnetic vector potential) due to a circular loop of current surrounding a *prolate spheroidal core*. First, static case was handled and then time-varying case was discussed [32].

#The field generated by J in the presence of core is the same as the superposition of the fields generated in the absence of the core by J and the volume density of magnetic dipoles (or currents) $j\omega(\mu-\mu_0)H$, where H is the magnetic field generated by J in the presence of the core and mu and mu0 are the permeabilities of the core and free space respectively [Rumsey and Weeks, 1956].

#Harmon investigated electric and magnetic fields of an empty solenoid at frequency up to 100 MHz. Inside and outside the solenoid are separated. The expressions for the field components are simplified if the frequency is less than 100 Mhz [Harmon, 1991].

$$B_{zi} \approx \mu_0 N I_0 \exp(-i\omega t), \quad (43)$$

$$E_{\phi i} \approx \mu_0 N I_0 \omega r / 2 \exp[-i(\omega t - \pi/2)], \quad (44)$$

$$E_{zi} \approx \frac{\mu_0 \omega I_0}{4 \cos \delta_2} \exp[-i(\omega t - \delta_2)], \quad (45)$$

$$B_{\delta i} \approx \frac{\mu_0 \omega I_0}{4 \cos \delta_2} \left(\frac{k_i}{\omega}\right) \left(\frac{k_i r}{2}\right) \exp[-i(\omega t - \delta_2 + \pi/2)]. \quad (46)$$

6.4 Magnetic Cores

A magnetic core is a piece of magnetic material with a high magnetic permeability, high electrical resistivity, low coercive field strength, and low core loss used to confine and guide magnetic fields in electrical devices. It is made of ferromagnetic metal such as iron or soft magnetic alloys, or ferrimagnetic compounds such as ferrites. The high permeability, relative to the surrounding air, causes the magnetic field lines to be concentrated in the core material [65][2].

By using a magnetic core, the magnetic field strength inside the coil can be increased by a hundred times. However, magnetic cores have some side effects to consider. In alternating current applications such as transformers and inductors, they cause core losses due to hysteresis and eddy currents. Usually, soft magnetic materials with low coercivity and hysteresis such as silicon steel or ferrite are used [65].

#The great sensitivity of Induction coils is due to the high magnetic permeability of the material used to build the core. This material can be very expensive (try to search for mu-metal or permalloy on internet and you'll see!). But first of all we must consider the propriety of this coils in order to correctly dimension our project and get the best performances from our expensive metal.

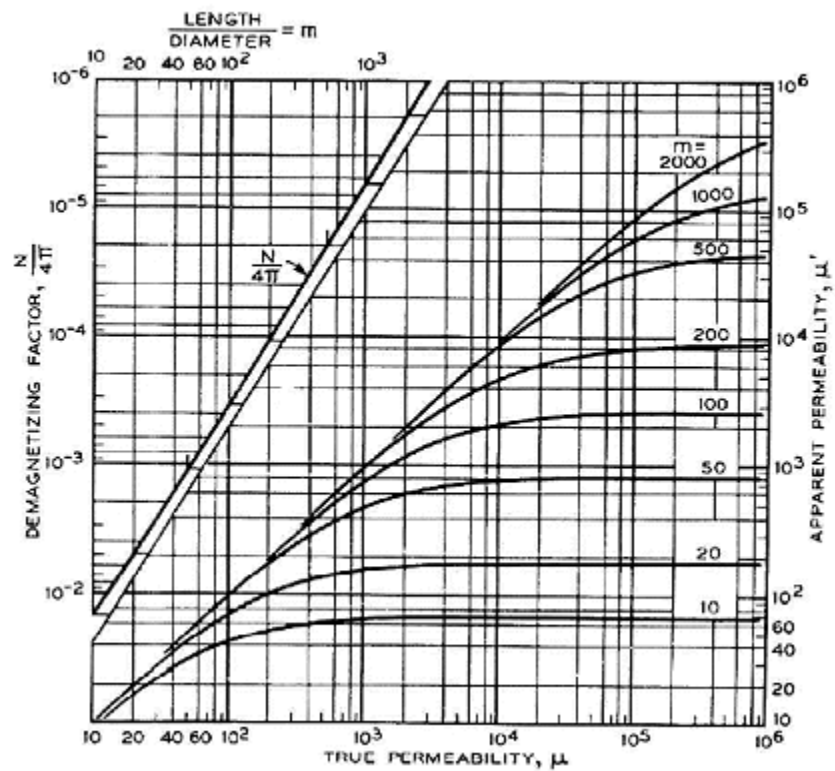


Fig. 6.6: : Permeability of core [http://www.vlf.it/matteobruna/ULF_Induction-Coil.htm].

#When we construct coils like these we must consider that they haven't an ideal behavior. The graph on the left shows that the apparent magnetic permeability of a cylindrical core can be different from the magnetic permeability of the metal of which is made. In fact the apparent permeability depends on the geometric dimensions of the core, in particular on the length-to-diameter ratio. So before buying the metal for the core we must ensure that we can make the core with the right length-to-diameter ratio to get from it all the permeability that can give.

#The metal I choose for my coil's core is magnetic steel used for the construction of electrical transformers. It has a permeability around 1000, so I built the core with a length-to-diameter ratio around 50.

#A variable magnetic field in a conductor material makes currents to flow. These are called Foucault's currents and will surely flow also in our core absorbing part of the signal we want to receive. There is no possibility to eliminate this phenomenon, but it can be limited. The only way is to "cut" this currents by using materials with a high internal resistance (composite alloys) or to build the core with many little pieces of metal (bars or laminations) insulated from each other. The magnetic steel I used is sell in insulated foils, so, to build my core, I simply put many of these together trying to obtain a cylindrical shape to completely fill the free space inside the coil. The procedure is also well shown by Hans Michlmair in his article .

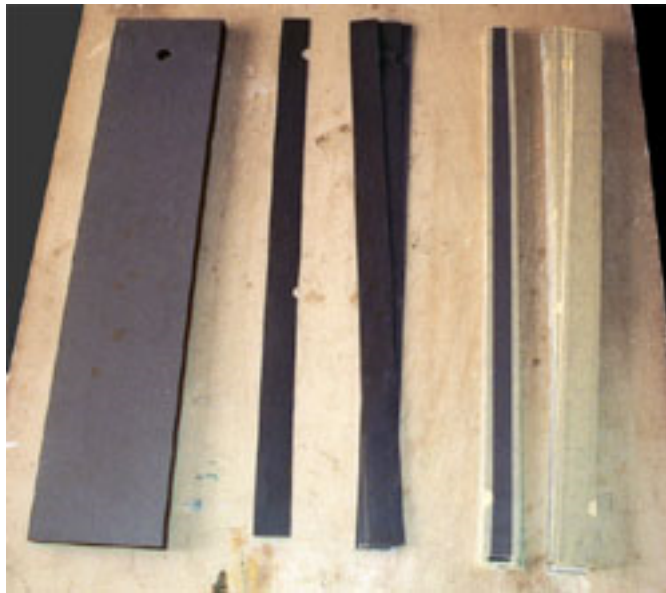


Fig. 6.7: : core-lamination-sheets [http://www.vlf.it/matteobruna/ULF_Induction-Coil.htm].

#To save money I got the magnetic steel from the discards of a transformers factory. Naturally it wasn't already in the right shape so I had to cut it in order to get foils narrow enough to fill the core's volume. At the end were composed four bars with a diameter of 4.5 cm and 70 cm long, that linked together forms a core of about 280 cm, so, with a length-to-diameter ratio of about 56 [http://www.vlf.it/matteobruna/ULF_Induction-Coil.htm].

#For the purpose of expressing material properties and design relations it is convenient to consider only sinusoidal wave forms. Ferrite cores are often used at quite low amplitudes. At these low amplitudes the non-linearity between B and H is small so that, to a first order, the waveform distortion may usually be neglected. Under these conditions, if the field strength is sinusoidal then the flux density and the e.m.f. (proportional to dB/dt) may be taken as sinusoidal. Thus simple a.c. theory may be used to describe the influence of a magnetic material on an electric circuit [snelling].

#The inductance of a circuit may be defined as the flux linkage per unit current, i.e. for an alternating current of peak amplitude I ,

$$L = \frac{N\phi}{I} \quad (6.6)$$

#For a winding of N turns on an ideal toroid of magnetic length l and cross-sectional area A

$$\begin{aligned}
 L &= \frac{NBA}{I} & (6.7) \\
 &= \frac{NA}{I} \mu_0 \mu \left(\frac{NI}{l} \right) \\
 &= \frac{\mu_0 \mu N^2 A}{l} \\
 &= \mu_0 \mu \left(\frac{N^2 A}{l} \right) \\
 L_0 &= \frac{\mu_0 N^2 A}{l} & (6.7)
 \end{aligned}$$

6.4.1 Modeling of B-H Curves

Mirzaei and Ripka investigated modeling of very high permeability B–H curves with combination of rational function and power function. The unknowns of the analytical function could be calculated with the simple curve fitting function. Also, they noted that [40]:

- Closed-form formulas gives maximum magnetic relative permeability and magnetic saturation without B–H data table.
- Standard rational function has the disadvantage of probable zeros in denominator and discontinuities in the curve.
- Exponential functions for B–H curve modeling are not as precise as rational functions.
- Power functions can precisely model a fraction part of B–H curve but not the whole B–H curve.

Note: Free B-H curve data can be found [here](#).

6.4.2 Nickel-Iron Soft Magnetic Materials

Nickel-Iron (Ni-Fe) alloys are a special class of magnetic materials based on the face-centered cubic crystal structure. Usually they contain 40% - 90% Ni, contains a few percent of other alloying elements such as Cu, Mo, Cr, Co, Mn, and the remainder is balanced with Fe. The Ni-Fe alloys or permalloys that contains nickels over 76-80% have been widely used in various applications since 1920. The magnetic properties of 80% Nickel alloy material were investigated under different conditions of *annealing temperature*, *cooling rates* and *holding time*. Magnetic properties of material such as induction, remanence, core loss, coercivity and peak permeability were evaluated at 300 Hz and 1 kHz by changing the magnetic field [24].

There is a standard about Nickel-Iron (Ni-Fe) soft magnetic materials that includes permeability and coercive field strength values for different shapes and four different alloy types [2].

6.4.3 Magneto-mechanical Effect

Magneto-mechanical effect (i.e., mechanical stress) causes characteristics deterioration that decrease of permeability of electrical steel sheets used in electric machines [46]. Aydin et al., investigated magneto-mechanical modeling of electrical steel sheets and compared two models based on simplified multiscale and Helmholtz free energy approach [4]. A testing device of magneto-mechanical effects in steel sheets was designed [5] and then equivalent strain and stress approach was proposed for modeling permeability change in ferromagnetic materials due to mechanical loadings [46].

6.4.4 Dust Core (Mass Core)

The powder cores (dust core or mass core) produced by compressing the insulated magnetic powder are easy to form and are expected to be useful for the reduction of components with cores; however, there are energy loss or core loss issues. Pure iron powder, the raw material of powder cores, has more compressibility and higher saturated magnetic flux density than alloy powders [28].

The effective magnetic permeability of an iron powder core consisting of uniformly spherical iron particles with magnetic permeability μ_r and conductivity σ (CGS) was given by [11]

- V_c : Fractional volume of the iron [m^3]

For a cubical arrangement of the spheres in contact, the value of V_c is $\pi/6 = 0.52$, while the closest packaged formation is $\sqrt{2}\pi/6 = 0.74$. Therefore, in cores having a V_c value greater than 0.74, the particles cannot be spherical and generally have irregularities distributed randomly, so that the core is still magnetically isotropic.

This equation was only valid for magnetostatic fields. In alternating fields, eddy currents are set up in the particles which introduce a power loss depending upon the particle size and frequency, and therefore the effective permeability of the core would be a complex value that $\mu_e = \mu'_e - j\mu''_e$. So, imaginary part of the effective permeability was given by [11]

$$\mu''_e = \frac{18\pi}{5} \frac{V_c \mu^2 \omega r^2 \sigma}{[(\mu + 2) - V_c(\mu - 1)]^2}$$

6.5 Demagnetization Factor

Demagnetization factor has been found experimentally for different core geometries, as shown in Fig. 6.8. In general, demagnetization factor is a function of the geometry of the ferrite core [8].

The demagnetizing factor can be calculated precisely only for ellipsoids of revolution, which have uniform magnetization. For a sphere, $D_F = 1/3$, for a very thin plate, $D_F = 1$; and for an infinitely long cylinder in a transverse field, $D_F = 1/2$. For some specimens of simple shape, the demagnetizing factor is calculated by empirical formulas, but in most cases, it is determined experimentally [Dictionary, 2003].

The literature distinguishes between “magnetometric” and “fluxmetric” (or “ballistic”) demagnetizing factors D_m and D_f . If the sample is in a uniform applied field H_a along its axis, the fluxmetric (or ballistic) demagnetizing factor D_f is defined as the ratio of the average demagnetizing field to the average magnetization at the midplane perpendicular to the axis. The magnetometric demagnetizing factor D_m , is defined as the ratio of the average demagnetizing field to the average magnetization of the entire sample [Chen et al., 1991].

6.5.1 Demagnetization Factor from Charts

Bozorth and Chapin investigated D_F of rods. A chart is constructed for converting the μ_{ce} to μ of cylinders of any given ratio of l_r/d_r . The demagnetizing factors for oblate and prolate ellipsoids of revolution, and for rods having finite permeabilities, are plotted in Fig. 6.9 [Bozorth and Chapin, 1942].

Osborn investigated demagnetizing factors of the general ellipsoid. This article presents charts and tables which make possible easy determination of the demagnetizing factor for any principal axis of an ellipsoid of any shape. Formulas for the demagnetizing factors of the general ellipsoid are included together with supplementary formulas which cover many special cases [Osborn, 1945].

Rumsey and Weeks noted that the value of D_F is known from the static solution; it depends on the shape of the ellipsoid and is independent of μ [Rumsey and Weeks, 1956].

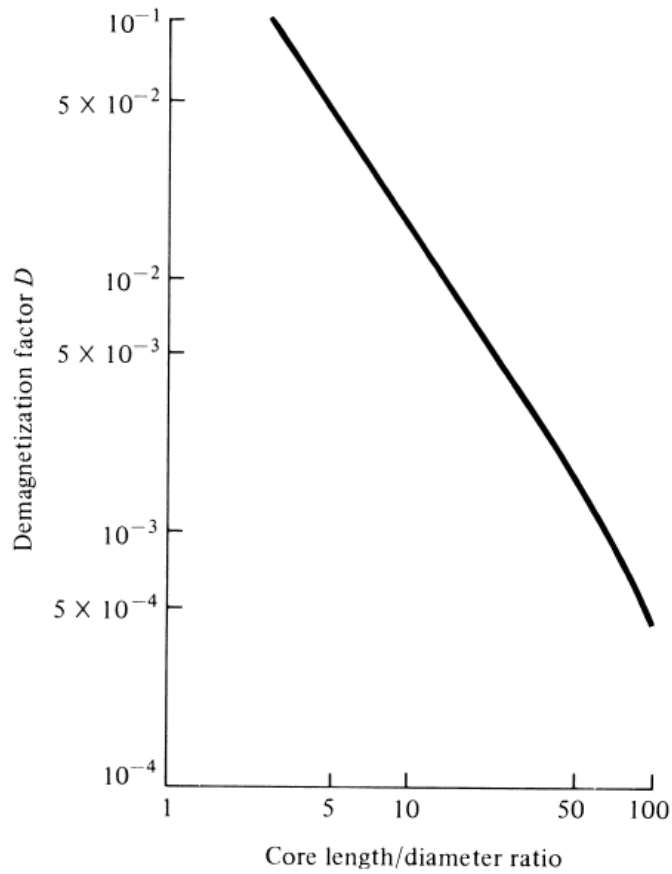


Figure 5.19 Demagnetization factor as a function of core length/diameter ratio. (SOURCE: E. A. Wolff, *Antenna Analysis*, Wiley, New York, 1966).

Fig. 6.8: : Demagnetization factor as a function of core length/diameter ratio.

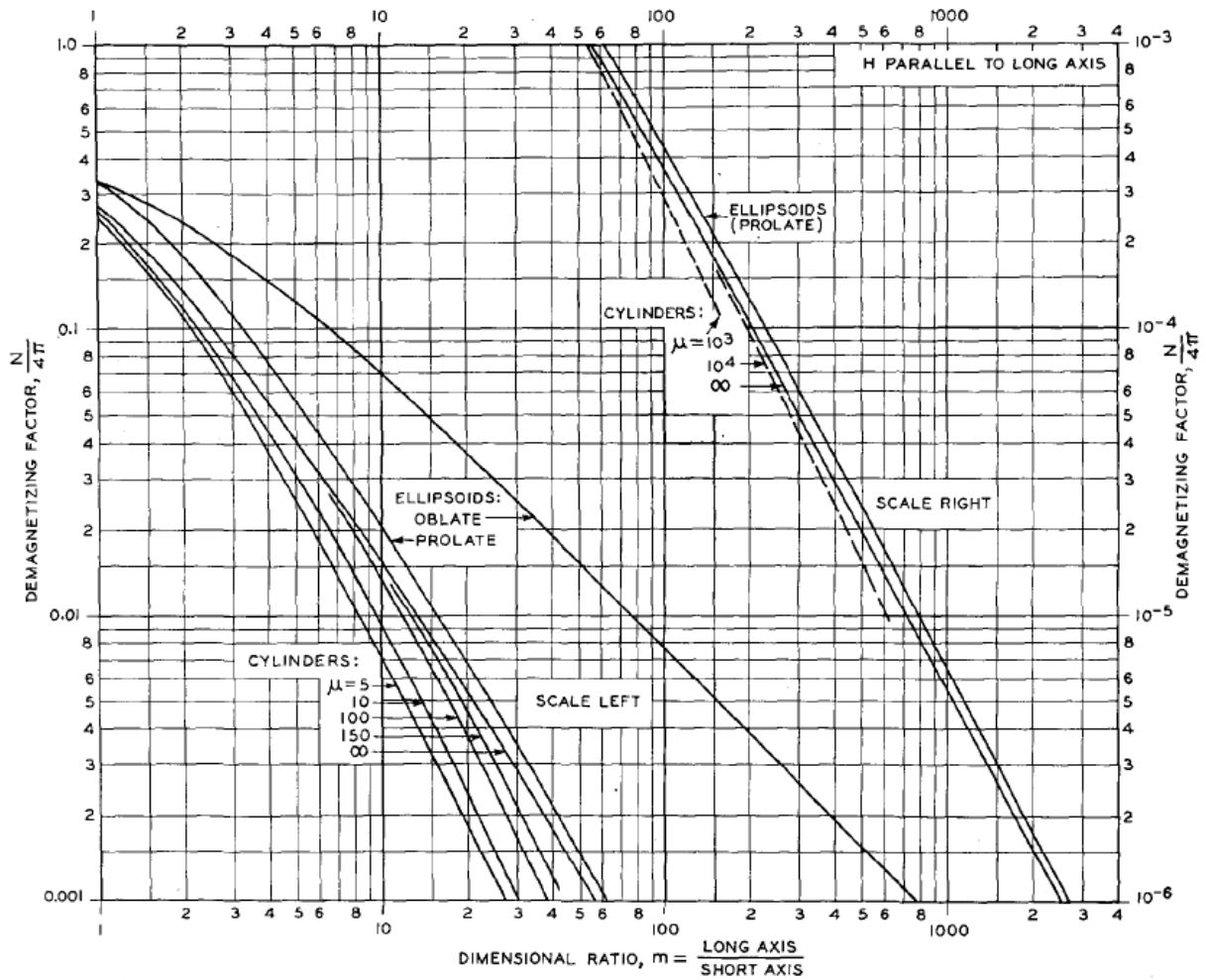


FIG. 2. Demagnetizing factors of ellipsoids and cylinders (see the equations and reference 1).

Fig. 6.9: : Demagnetization factors of ellipsoids and cylinders.

Moskowitz et. al. investigated magnetometric demagnetization factors for regular polygonal cylinders. Longitudinal magnetometric demagnetization factors for several equilateral polygonal cylinders have been determined by inductance analogy from available tables of inductance. These values are listed in Table at Fig. 6.10 as a function of the equivalent-area aspect ratio l_r/d_r [Moskowitz et. al., 1966].

TABLE I

LONGITUDINAL MAGNETOMETRIC DEMAGNETIZATION FACTORS
FOR EQUILATERAL POLYGONAL CYLINDERS

Aspect Ratio m_A	Triangle	Square	Hexagon	Octagon	Dodecagon	Circle
0.01	0.9706	0.9674	0.9658	0.9654	0.9652	0.9650
0.02	0.9449	0.9415	0.9398	0.9393	0.9390	0.9389
0.03	0.9233	0.9192	0.9171	0.9166	0.9163	0.9161
0.04	0.9036	0.8989	0.8966	0.8960	0.8956	0.8954
0.05	0.8853	0.8801	0.8776	0.8769	0.8766	0.8764
0.06	0.8681	0.8626	0.8599	0.8592	0.8588	0.8586
0.07	0.8518	0.8460	0.8432	0.8424	0.8421	0.8419
0.08	0.8363	0.8302	0.8273	0.8266	0.8263	0.8261
0.09	0.8216	0.8153	0.8123	0.8116	0.8112	0.8110
0.10	0.8074	0.8010	0.7979	0.7972	0.7969	0.7967
0.15	0.7443	0.7375	0.7345	0.7337	0.7334	0.7333
0.20	0.6909	0.6842	0.6813	0.6806	0.6803	0.6802
0.30	0.6041	0.5981	0.5956	0.5950	0.5948	0.5947
0.40	0.5360	0.5309	0.5288	0.5284	0.5282	0.5281
0.50	0.4811	0.4767	0.4750	0.4747	0.4745	0.4745
0.60	0.4358	0.4321	0.4308	0.4305	0.4304	0.4303
0.70	0.3978	0.3948	0.3937	0.3935	0.3934	0.3933
0.80	0.3657	0.3631	0.3622	0.3620	0.3619	0.3619
0.90	0.3382	0.3360	0.3352	0.3350	0.3350	0.3349
1.00	0.3144	0.3124	0.3118	0.3117	0.3116	0.3116
2.00	0.1828	0.1821	0.1819	0.1819	0.1819	0.1819
5.00	0.0801	0.0799	0.0799	0.0799	0.0799	0.0799
8.00	0.0512	0.0511	0.0511	0.0511	0.0511	0.0511
10.00	0.0412	0.0412	0.0412	0.0412	0.0412	0.0412

Fig. 6.10: : Demagnetization factors of polygonal cylinders.

6.5.2 Demagnetization Factor from Formulas

D_F is the demagnetizing factor of an ellipsoid with the dimensional ratio l_r/d_r [Mager, 1968].

$$D_F = \frac{1}{(l_r/d_r)^2 - 1} \left[\frac{l_r/d_r}{\sqrt{(l_r/d_r)^2 - 1} \ln \left(l_r/d_r + \sqrt{(l_r/d_r)^2 - 1} \right)} - 1 \right] \quad (6.8)$$

A formula for can be constructed by fitting data given in the book [Snelling, 1969] as

$$D = \frac{0.28}{l_r/d_r} - 0.0158 - \frac{0.0915}{\mu_r} + \frac{0.00063 l_r/d_r}{\log(\mu_r)}$$

where l_r/d_r is the length to diameter ratio of the core, not the winding. The validity ranges are $1 < l_r/d_r < 100$ and $1 < \mu_r < 1000$ [Rhea, 1994].

Over a practical range of interest ($2 < l_r/d_r < 20$) D can be modeled as [Pettengill et.al., 1977, Burhans, 1979]

$$D = 0.37 \left(\frac{l_r}{d_r} \right)^{-1.44}$$

Demagnetizing factors of the rectangular rod

$$D = \frac{1}{2(l_r/d_r) + 1}$$

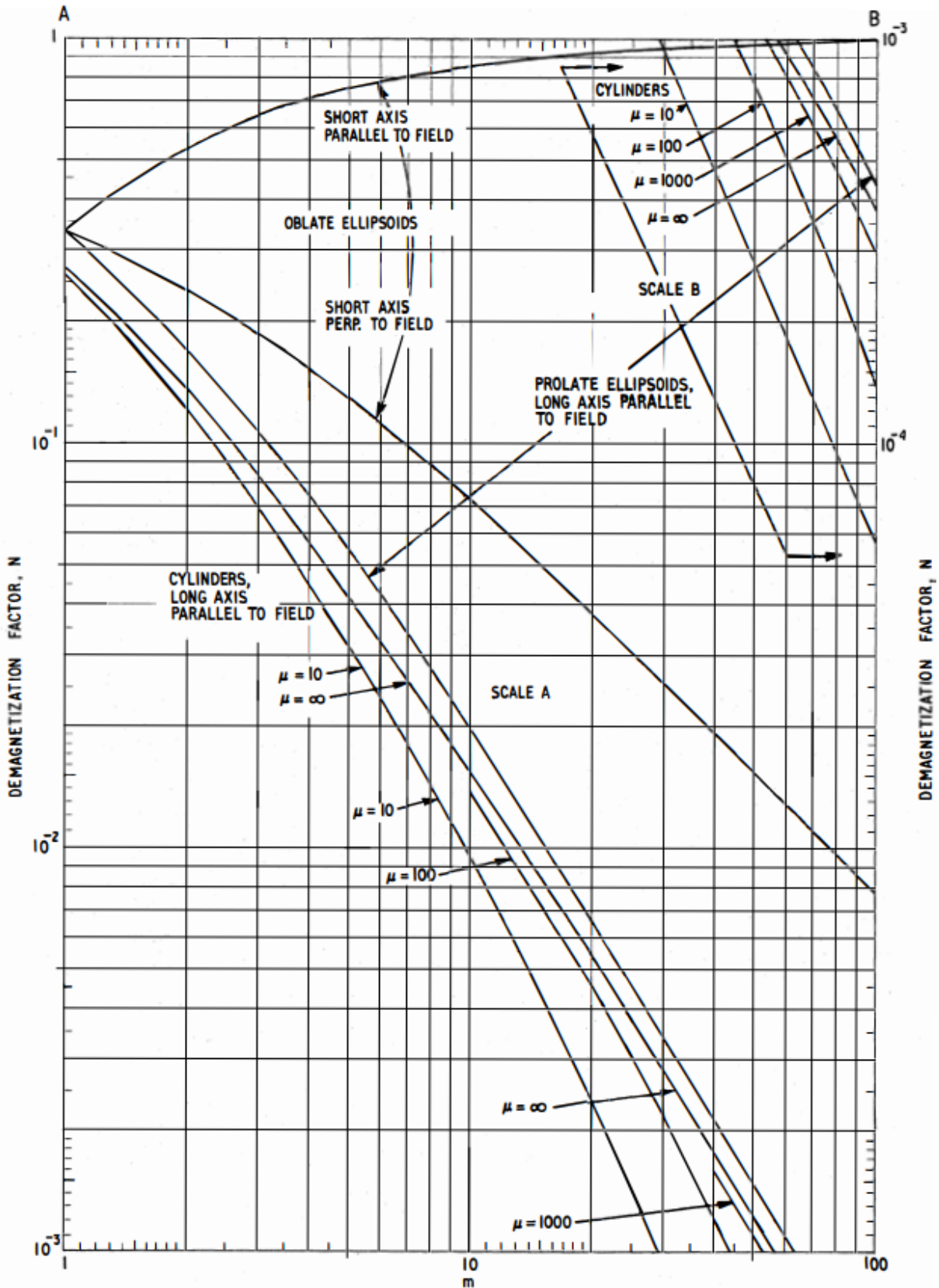


Fig. 4.8. Demagnetizing factors for ellipsoids and cylinders as functions of m (= long axis/short axis for ellipsoids and length/diameter for cylinders) (After Bozorth et al.⁶) Note: The values of N are appropriate to S.I. units; $(N)_{SI} = 1/4\pi(N)_{CGS}$

6.5. Demagnetization Factor

Fig. 6.11: : Demagnetizing factors for ellipsoids and cylinders as functions of m (= long axis/short axis for ellipsoids and length/diameter for cylinders) [Snelling, 1969, p184].

and cylinder

$$D = \frac{1}{2 \left(\frac{2(l_r/d_r)}{\sqrt{\pi}} \right) + 1}$$

magnetized uniformly along the long axis are found to be expressed by the simple and approximate expressions [Sato and Ishii, 1989].

TABLE I. Demagnetizing factor in a uniformly magnetized rectangular rod N_z . a is evaluated from Eq. (1b) and b is evaluated from the exact expression given by Rodes and Rowlands (Ref. 2). The percentage difference is $[(a - b)/b] \times 100$.

Dimensional ratio n	N_z		Percentage difference
	a	b	
0.1	0.833333	0.805078	3.51
0.2	0.714286	0.694194	2.89
0.3	0.625000	0.612439	2.05
0.5	0.500000	0.495922	0.82
0.7	0.416667	0.415742	0.22
1	0.333333	0.333333	0.00
2	0.200000	0.198316	0.85
3	0.142857	0.140363	1.78
5	0.090909	0.088316	2.94
7	0.066667	0.064363	3.58
10	0.047619	0.045731	4.13
12	0.040000	0.038330	4.36
15	0.032258	0.030839	4.60
20	0.024390	0.023262	4.85
30	0.016393	0.015595	5.12
50	0.009901	0.009398	5.35
70	0.007092	0.006724	5.48
100	0.004975	0.004684	6.21

TABLE II. Demagnetizing factor in a uniformly magnetized cylinder N_z . a' is evaluated from Eq. (2b) and b' is evaluated from the exact expression given by Arrott *et al.* (Ref. 4). The percentage difference is $[(a' - b')/b'] \times 100$.

Dimensional ratio n	N_z		Percentage difference
	a'	b'	
0.1	0.815876	0.796677	2.41
0.2	0.689013	0.680175	1.30
0.3	0.596293	0.594731	0.26
0.5	0.469841	0.474490	-0.98
0.7	0.387637	0.393310	-1.44
1	0.307054	0.311577	-1.45
2	0.181372	0.181864	-0.27
3	0.128696	0.127769	0.73
5	0.081408	0.079907	1.88
7	0.059533	0.058086	2.49
10	0.042431	0.041193	3.01
12	0.035611	0.034501	3.22
15	0.028693	0.027739	3.44
20	0.021675	0.020908	3.67
30	0.014555	0.014008	3.91
50	0.008784	0.008438	4.10
70	0.006290	0.006038	4.19
100	0.004412	0.004232	4.25

Fig. 6.12: : demagnetizing-factor-sato-ishii-1989.

It is found in Tables I and II that the results obtained by the simple and approximate expressions given by two equations above (ref!) well agree with the results obtained by the exact of the demagnetizing factors [Sato and Ishii, 1989].

Aharoni gave an analytic expression for the magnetometric demagnetizing factors of the general rectangular prism [Aharoni, 1998, Magpar, 2017].

$$\begin{aligned} \pi D_z = & \frac{b^2 - c^2}{2bc} \ln \left(\frac{\sqrt{a^2 + b^2 + c^2} - a}{\sqrt{a^2 + b^2 + c^2} + a} \right) + \frac{a^2 - c^2}{2ac} \ln \left(\frac{\sqrt{a^2 + b^2 + c^2} - b}{\sqrt{a^2 + b^2 + c^2} + b} \right) + \frac{b}{2c} \ln \left(\frac{\sqrt{a^2 + b^2} + a}{\sqrt{a^2 + b^2} - a} \right) + \frac{a}{2c} \ln \left(\frac{\sqrt{a^2 + b^2} + b}{\sqrt{a^2 + b^2} - b} \right) \\ & + \frac{c}{2a} \ln \left(\frac{\sqrt{b^2 + c^2} - b}{\sqrt{b^2 + c^2} + b} \right) + \frac{c}{2b} \ln \left(\frac{\sqrt{a^2 + c^2} - a}{\sqrt{a^2 + c^2} + a} \right) + 2 \arctan \left(\frac{ab}{c\sqrt{a^2 + b^2 + c^2}} \right) + \frac{a^3 + b^3 - 2c^3}{3abc} \\ & + \frac{a^2 + b^2 - 2c^2}{3abc} \sqrt{a^2 + b^2 + c^2} + \frac{c}{ab} (\sqrt{a^2 + c^2} + \sqrt{b^2 + c^2}) - \frac{(a^2 + b^2)^{3/2} + (b^2 + c^2)^{3/2} + (c^2 + a^2)^{3/2}}{3abc} \end{aligned}$$

Fig. 6.13: : ex14.

6.5.3 Demagnetization Factor from Formulas with Inductance

Moskowitz and Della Torre investigated a magnetometric demagnetization tensor for uniformly-magnetized samples of arbitrary geometry. The axial demagnetizing factor can be obtained from existing tables designed for calculating the inductance of solenoids. This is due to the analogous fields of the solenoid and the uniformly-magnetized cylinder. The analogy between the single-layer solenoid and the uniformly-magnetized cylinder

$$D_m = 1 - \left(\frac{L}{\mu_0 n^2 l_r A_r} \right)$$

where L is the inductance, A_r is the cross-section of the cylinder.

It is of interest to consider samples of uniform equilateral-polygonal cross-section. For such samples the aspect ratio l_r/d_r is the ratio of length to the diameter of the right circular cylinder of equal cross-sectional area. Thus, in general,

$$\frac{l_r}{d_r} = \frac{1}{2} \sqrt{\frac{\pi}{A_r}}$$

where l is the length of the particle and d is the diameter of the circular cylinder of equal cross-sectional area A_r .

The demagnetization factor curves in Figure 4 are based on inductance values from [Grover, 1962, 1973], for coils of polygonal geometry. For any of the shapes given, there is less than 1% deviation between demagnetization factors of polygonal and circular cylinders for aspect ratios l_r/d_r above unity. For acicular particles ($l_r/d_r \sim 6.0$) this deviation is less than 0.25% even for the most radical shape, the triangular cross-section [Moskowitz and Della Torre, 1966].

Values of D_f have been calculated for the right circular cylinder by direct integration and by the inductance analogy. Both results agree with tables published by Brown [Brown, 1962] and will not be repeated here. From Figure 4 note that the square cylinder has a demagnetization factor of 1/3 when it becomes a cube [Moskowitz and Della Torre, 1966].

Chen et. al. evaluated fluxmetric (ballistic) and magnetometric demagnetizing factors D_f and D_m , for cylinders as functions of susceptibility χ and the ratio m_A of length to diameter. D_f and D_m were computed exactly using inductance formulas [Chen et. al., 1991].

Chen et al. evaluated, using exact general formulas, the fluxmetric D_f and magnetometric D_m demagnetizing factors of a rectangular prism of dimensions $2a \times 2b \times 2c$ with susceptibility $\chi=0$ and the demagnetizing factor, D , of an ellipsoid of semiaxes a, b , and c along the c axis [Chen et al., 2002].

Chen et. al. calculated numerically fluxmetric and magnetometric demagnetizing factors, D_f and D_m , for cylinders along the axial direction as functions of material susceptibility χ and the ratio l_r/d_r of length to diameter. The results have an accuracy better than 0.1% [Chen et. al., 2006].

Note: Sintered magnet demagnetization curves and demagnetization force for magnets are given by Tokyoferrite Corporation [Tokyo Ferrite, 2017].

Demagnetization factor of a prolate spheroid was given by [11]

- $e_1 = \sqrt{1 - l_r/d_r}$

6.6 Induced Voltage and Power

A small air core loop of N turns with a cross sectional area A is placed in a uniform alternating magnetic field with the axis of the loop parallel to the field strength vector H , then the induced emf will be:

$$e_{ind_air} = \mu_0 \omega H A N$$

If the aperture of the winding is filled with a long ferrite cylinder parallel to the loop, then the flux density of the loaded-loop will be increased by the factor of permeability of core μ_r . Therefore, induced voltage is given by

$$e_{ind_fer} = \mu_0 \mu_r \omega H A N$$

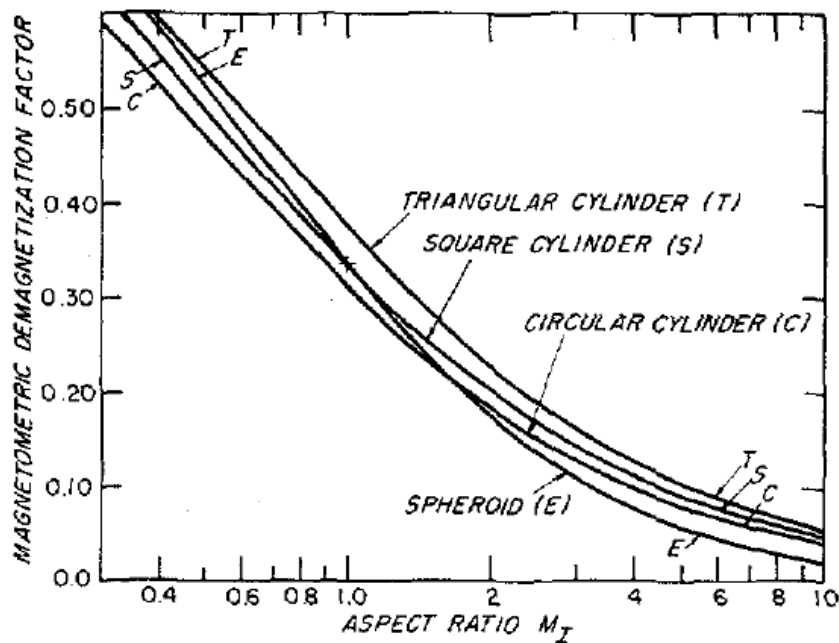


Fig. 1. Axial magnetometric demagnetization factors of equilateral-polygonal cylinders. The square cylinder has $D_{\text{square}} = \frac{1}{3}$ when it becomes a cube ($m_I = 1.0$). From Theorem I, transverse demagnetization factor can be obtained from above axial one by $D_{\text{trans}} = \frac{1}{2} (1 - D_{\text{axial}})$.

Fig. 6.14: : demagnetization-magnetometric-moskowitz-1966.

The strength of an electromagnetic field is usually expressed in terms of the electric field strength E . Using the fundamental relation:

$$H = \sqrt{\frac{\epsilon_0}{\mu_0}} E$$

$$\mu_0 H = \frac{E}{c}$$

where H is in A/m, E is in V/m, and c velocity of electromagnetic waves in free space approximately 3×10^8 m/s. Then, induced voltage can be written in terms of electric field strength [55]:

$$e_{ind_fer} = \mu_r \omega E A N / c$$

#Dunbar gave the formulation of induced voltage in the ferrite loaded receiving loop in free space

$$e_{max} = \frac{-j\omega\mu_0 I_0 (N_1\mu_{r1}S_1) (N_2\mu_{r2}S_2) e^{j(\omega t - \beta r)}}{4\pi} \left\{ -\frac{\beta_0^2}{r} + j\frac{\beta_0}{r^2} + \frac{1}{r^3} \right\}$$

#In addition, an expression may be obtained for the induced voltage in a similar ferrite-cored receiving loop at a distance r from the transmitting loop, the loops being in the same plane to maximize the H_θ component.

$$e_{max} = \frac{\omega^2 \mu_0^2 \mu_{r1} \mu_{r2} N_1 N_2 S_1 S_2 I e^{-j(\omega \gamma r)}}{4\pi} \left\{ \frac{j\omega\epsilon}{r} + \frac{1}{\eta r^2} + \frac{1}{j\omega\mu r^3} \right\}$$

[Dunbar, 1972]

#Laurent and Carvalho gave an induced voltage formula of the ferrite loaded loop antennas [Laurent and Carvalho, 1962].

$$e_{ind} = \omega N \frac{E}{c} A_r \left[\mu_r + \left(\frac{d_c^2}{d_r^2} - 1 \right) \right]$$

where

- E : electric field intensity vector
- c : speed of light
- A : cross section area of coil and rod
- d : diameter of coil and rod
- μ_r : effective relative permeability of the rod

#An expression for the available power from the antenna is obtained [Pettengill, 1977]:

$$P_A = \frac{1}{4\mu_0 c_0^2} \frac{0,69Q\mu_r V \omega E^2}{1 + D(\mu_r - 1)}$$

6.7 Core Loss

6.7.1 Spheroidal Core

The core loss may be computed if the loss tangent of the core material is known or is available from published data. The loss tangent is defined in terms of a complex effective relative permeability, $\mu_r = \mu_r' - j\mu_r''$, as $\tan \delta = \mu_r'' / \mu_r'$ [Simpson and Zhu, 2007].

$$R_{core} = \omega \mu_0 \mu_r'' \left| H_{1z} / I \right|^2 V$$

$$= \omega \mu_0 \mu_r'' \left(\frac{2\pi N b^2}{3} \right) \left(\frac{N}{2a} \right) \left| \frac{\xi_0 Q_1'(\xi_0)}{\xi_0 Q_1'(\xi_0) - \mu_1 Q_1(\xi_0)} \right|^2$$

Fig. 6.15: : ex15.

$$R_F = \omega \mu_0 \frac{n^2}{l} (\pi a^2) (1 - D)(1 - D_F) \frac{l_F}{l} \left(\frac{a_F}{a} \right)^2 \frac{\kappa''}{(\kappa')^2} \left[\frac{\kappa'}{1 + D_F(\kappa' - 1)} \right]^2 f_{\text{MHz}}.$$

Fig. 6.16: : ex16.

6.7.2 Cylindrical Core

Devore and Bohley gave the core loss formulation which is dependent complex permeability of core below [Devore and Bohley, 1977].

Another core loss formulation for ferrite loaded FM receiver antennas was given [Lindberg and Kaikkonen, 2007]

$$R_f = 2\pi f \mu_0 \mu_{cer} \frac{\mu''}{\mu'} n^2 \frac{A}{l}$$

6.7.3 Core Data

Example catalog data of complex permeability as a function of frequency is shown below [Data Handbook of Soft Ferrites and Accessories, 2004].

Another catalog data of Siemens EC52 ferrite core is given below [Kazimierczuk et. al., 1999].

6.8 Radiation Resistance

The radiation resistance of the magnetic-cored loop is obtained by multiplying *radiation resistance of the air-cored loop* and relative effective permeability of magnetic core [8][50].

- R_{rad}^{air} : *Radiation resistance of the air-cored loop*
- μ_{cer} : Relative effective magnetic permeability of the core

So, radiation resistance of the N-turn, magnetic-cored loop is given by

- C : Circumference of the loop [m]

3S1 SPECIFICATIONS

A low frequency EMI-suppression material specified on impedance and optimized for frequencies up to 30 MHz.

SYMBOL	CONDITIONS	VALUE	UNIT
μ_i	25 °C; ≤ 10 kHz; 0.25 mT	≈ 4000	
B	25 °C; 10 kHz; 1200 A/m 100 °C; 10 kHz; 1200 A/m	≈ 400 ≈ 230	mT
$ Z ^{(1)}$	25 °C; 1 MHz 25 °C; 10 MHz	≥ 30 ≥ 60	Ω
ρ	DC; 25 °C	≈ 1	Ωm
T_C		≥ 125	$^{\circ}\text{C}$
density		≈ 4900	kg/m^3

Note

1. Measured on a bead $\varnothing 5 \times \varnothing 2 \times 10$ mm.

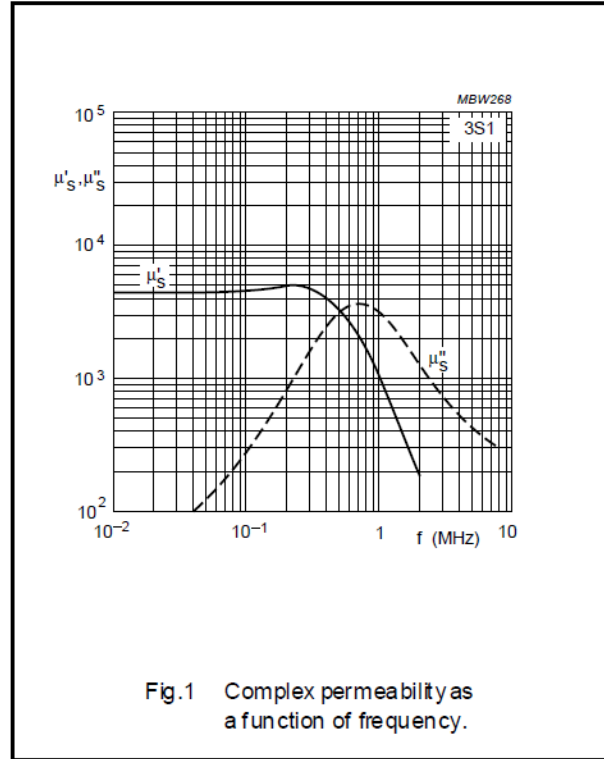


Fig.1 Complex permeability as a function of frequency.

Fig. 6.17: : core-data.

- A : Area of the loop [m]
- λ : Wavelength [m]
- N : Number of turns of the loop

In order to determine the radiation resistance of a ferrite core, it is necessary to find the *relative effective magnetic permeability* of the ferrite core (μ_{cer}). Other variables are known geometrical and electrical properties.

6.9 Relative Effective Permeability

A simple model of the relative effective permeability of the ferrite core μ_{cer} is related to the relative permeability of the unbounded ferrite material $\mu_r = \mu/\mu_0$ by [8]. This was explained as a step-up in flux and hence of emf due to the core by Burgess in 1946 [11].

- D_F : Demagnetization factor of ferrite core
- μ_r Relative permeability of the unbounded ferrite material

For most ferrite material, μ_r is very large ($\mu_r \gg 1$) so that μ_{cer} is approximately inversely proportional to the demagnetization factor:

$$\mu_{cer} \cong D_F^{-1}$$

Devore and Bohley mentioned that a improved model of relative effective permeability in the equation of radiation resistance [16].

- D_w is demagnetization factor of winding

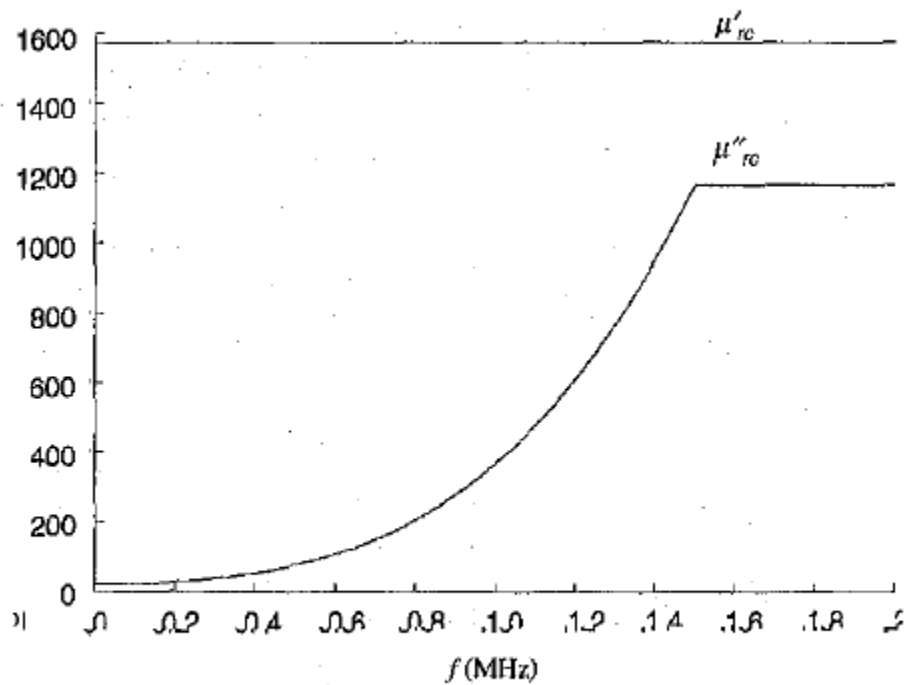


Fig. 3. Real part μ'_{rc} and imaginary part μ''_{rc} of the relative permeability of the Siemens N27 core material versus frequency.

Fig. 6.18: : core-data-siemens.

- l_F is length of ferrite core
- l_w is length of winding
- A_F is cross section area of ferrite core
- A_w is cross section area of winding

7.1 Biomedical Implant

The environment in which biomedical implant devices are located is characterized by a *high dielectric permeability* and a *high loss factor* to disrupt the electromagnetic signal [60].

Cheng et. al. investigated optimization of a solenoid type receiver coil for biomedical implants in order to create a WPT link. Analytical model of solenoid coil that includes the impact of tissue and coating around the coil was done. A four-turn coil had better results with 0.233 mm pitch at 700 MHz after a pitch optimization. An accurate formulation for the RLC model of implanted solenoid coil. The formulation was valid below self-resonance frequency of Rx coil [14].

2015	Electrically small loop antennas for RFID applications
2017	Analytical modeling and optimization of small solenoid coils for millimeter-sized biomedical implants

7.2 Magnetometer

A magnetometer or magnetic sensor is an instrument that measures magnetism either the magnetization of a magnetic material like a ferromagnet, or the direction, strength, or relative change of a magnetic field at a particular location [66].

In 1962, Hill and Bostick presented a report about a magnetometer (with their own words micropulsation sensor) that had laminated mumetal core based on the resistance of winding and the character of the output signal. Aim of the design was a sensor with a lower impedance than the 1000 ohm source impedance. Therefore, the length and resistance of the coil in the sensor had been studied in detail. Within the core, eddy current and hysteresis losses and Within the winding, losses caused by skin effect, proximity effect, distributed capacity, and wire resistance were considered [27].

In 1977 an induction coil magnetometer that contains mumetal rod core, several partial coils, and a preamplifier circuit was patented. Critical dimensions of magnetometer that coil width to core width ratio, coil diameter to core diameter ratio, and core diameter to core length ratio were given. In addition, manufacturing of magnetometer was described in details. The invention was that increasing the resolution of the magnetometer [42].

Patents:

Year	Name	Patent Number
1977	Magnetometer	DE2625964A1
1985	Magnetisches Sondentripel	EP0154129B1

7.2.1 Magnetotelluric

Magnetotelluric is a device that measure the electric and magnetic fields arising from natural sources (electromagnetic sounding of the Earth) at the surface of the earth over broad frequency bands and is based upon the skin depth effect in conductive media. Stanley and Tinkler investigated a practical, low-noise coil system for magnetotellurics. Aim of the work was implementation of the magnetometer with low-cost, light weight, broad bandwidth, ease of construction and reliability. Manufacturing steps were given in detail. A chopper amplifier had been improved according to existing systems [56].

7.3 Marker Beacon

Patents

Year	Name	Patent Number
1998	Ferrite core marker	US5767816

7.4 Radio Direction Finder

A radio direction finder (RDF) is a device for finding the direction, or bearing, to a radio source. Using two or more measurements from different locations, the location of an unknown transmitter can be determined; alternately, using two or more measurements of known transmitters, the location of a vehicle can be determined. RDF is widely used as a radio navigation system, especially with boats and aircraft [67].

In 1955, Hemphill investigated a magnetic radio compass antenna that the magnetic energy was picked up by the collector bars and conducted as magnetic energy to the small pickup coil in the center. Since the antenna was placed on the surface of the aircraft, it did not cause any additional drag [26].

7.5 Radio Receiver Antenna

Patents

Year	Name	Patent Number
2003	Twin coil antenna	US6529169

7.6 Real-time Locating System

Real-time locating systems (RTLS) are used to automatically identify and track the location of objects or people in real time, usually within a building or other contained area. Wireless RTLS tags are attached to objects or worn by people, and in most RTLS, fixed reference points receive wireless signals from tags to determine their location. Examples of real-time locating systems include tracking automobiles through an assembly line, locating pallets of merchandise in a warehouse, or finding medical equipment in a hospital [69].

Schantz investigated an application of real-time locating system that operate at AM broadcast band (530-1710 kHz). Performance of QT-400 system of Q-Track company was discussed [54].

Richards et al. investigated omnidirectional transmitting loopstick antennas with ferrite core that operates low frequency band for RTLS. Simulations run under various parameters which were type of ferrite, form factor, coil covering factor, number of turns, wire gauge, wire spacing, and gap between coil and ferrite. Comparative results were not given in details. They noted that resistive losses in the coil of the loopstick antenna dominate over in the ferrite core like 5% was core and 95% was solenoid [48].

Near field channel model document is to provide IEEE P802.15 for evaluating near field location aware wireless systems [51].

Patents

Year	Name	Patent Number
2004	System and method for near-field electromagnetic ranging	US20040032363A1
2005	System and method for near-field electromagnetic ranging	US6963301
2014	Method of near-field electromagnetic ranging and location	US20140062792A1

7.7 RFID

Turalchuk et al. investigated electrically small loop antennas for RFID applications. Two different condition were analyzed. Firstly, a receiving antenna was in the biological medium to link an implanted sensor and a transmitting (reader) antenna was outside of the medium. In this case, loops were operated in near-field zone in order to minimize effects of the dielectric properties of the biological medium. Secondly, a loop as a reader antenna for the identification of conventional tags in the far-field zone [60].

7.8 Underwater Loop Antenna

In the first world war, some submarines were equipped with radio signal receivers called “French” coils. An American submarine underwater at Long Island Sound received long-wave signals from Nauen, Germany in 1919 [59].

In 1941, Naval Research Laboratory presented a report which contains an investigation of a test that feasibility of receiving low frequency transmission signals while the receiving antennas completely submerged to the seawater. In order to determine this, it was necessary to make the following tests [30]:

- The signal strength and signal to noise ratio received by various types of antennas at various depths and for various frequencies.
- The best type of coupling device (input transformer and tuning unit) to transfer the received signals from the antennas to the receiver equipment.

Other tests to obtain other relevant information are as follows [30]:

- Underwater bearing of transmitter by null method.
- Q of loops.
- Effect of sea bottom on signals.
- Noise survey of ship.

In the report, some important results were highlighted [30]:

- The depth of the sea bottom seems to have practically no effect of the strength of the signals.
- Theoretical considerations of the design of a loop for underwater reception that a narrow loop with its long side parallel to the water surface is best.
- Signals of 1000 microvolts per meter in air should be readable to a depth of 10 meters (34 feet)(above loop) in ocean water and 11.5 meters (38 feet)(above loop) in water of less salinity.

In 1950, Toth and Fratianni investigated underwater loop reception and concluded that these results: a) Long-distance underwater radio receivers should be used in the range of 15-30 kHz and about maximum of 6 m (20 ft). b) A convenient underwater receiver system should be omnidirectional and at a certain distance from the water surface [59].

Induced voltage at the terminals of the antenna in the air is a function of the time of the frontwave that comes to the opposite edge of the coil that parallel to the electric vector. A similar induced voltage occurs at a loop antenna under water. However, since the wavelength of underwater wave propagation is much slower (1000 times slower than air) and the attenuation is too high, the phase differences of the induced voltages at the coil edges are high as shown in Fig. 7.1 [59].

The operation of the loop antenna under water significantly increases the efficiency of receiving. For example, in a 20 kHz system, the output voltage increased by 1650 times or 64 dB. However, there are losses in the field strength of about 66 dB. The loss of the output voltage is only about 2 dB in the transmissions from above the water surface to just below the water surface. Fig. 7.2 shows the amount of loss per foot under water [59].

In 1955, Fratianni investigated three experimental iron-cored omnidirectional loop antennas in regards to VLF signal reception. The aim of the investigation was to achieve greater receiving efficiency with no increase in physical size, and weight, as compared to the Model AT-317 antenna which was employed on submarines at that time. They also noted that the interference effects of undesired radio signals were not changed by the presence of the Faraday shield. The experimental antennas were superior in pickup efficiency than the Model AT-317 antenna because of the greater winding areas and core lengths [21].

In 2011, Waheed-uz-Zaman and Yousufzai presented a study about a VLF transmitting antennas for submerged submarines [61].

7.9 Wireless Power Transfer

Zhang et al. investigated a quadrature-shaped receiver (pickup) coil for omnidirectional wireless power transfer (WPT) as shown in Fig. 7.3. A cross-shaped core is placed inside the receiver and the windings are wrapped around the core. Receiver is simulated for different geometric dimensions of the core and the results are presented in terms of both power and efficiency [70].

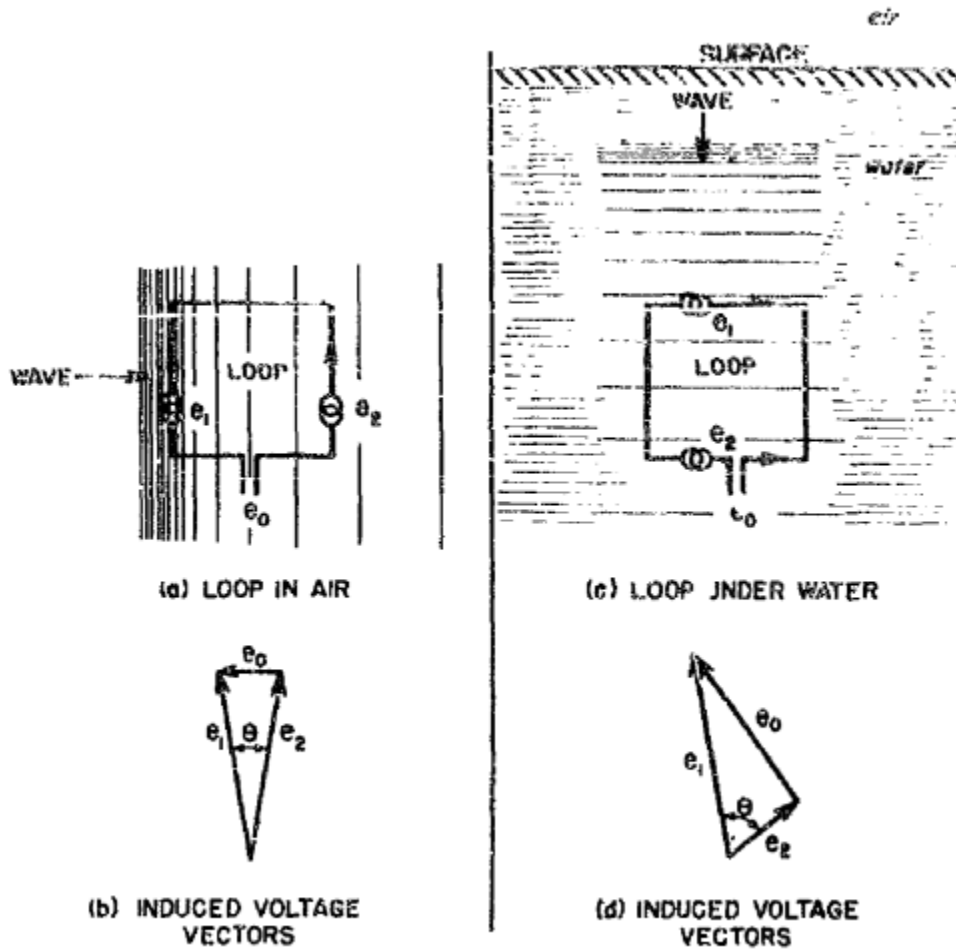


Figure 4 - Induced voltages in air and underwater loops

Fig. 7.1: : Induced voltages in air and underwater loops.

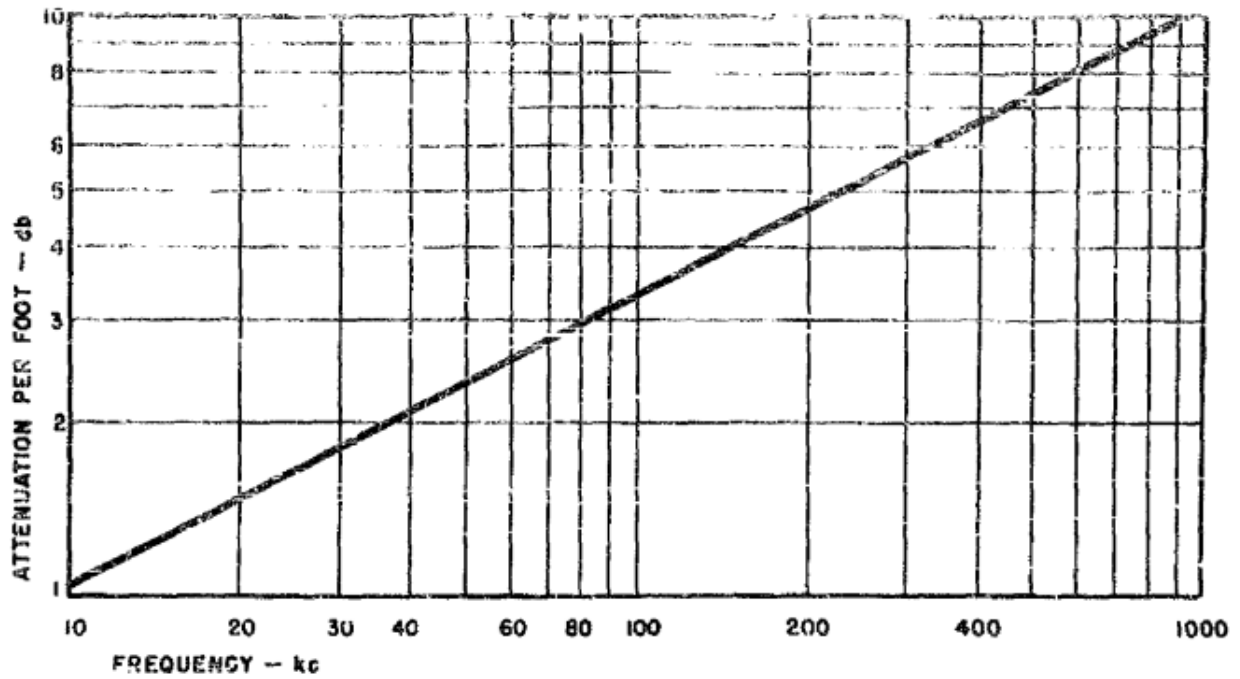


Figure 3 - Computed attenuation of underwater radio field per foot of submergence

Fig. 7.2: : Computed attenuation of underwater radio field per foot of submergence.

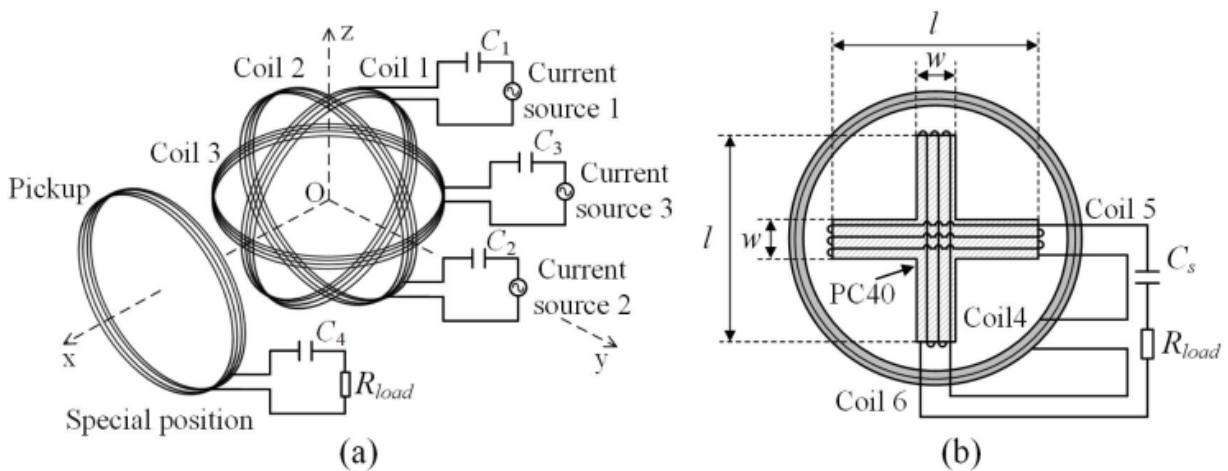


Fig. 7.3: : Schematics of (a) omnidirectional WPT system and (b) quadrature-shaped pickup.

#According to electromagnetic induction principle, alternate current produces alternate magnetic field. The metal produces alternate eddy current when it is in alternate magnetic field. The eddy current then produces secondary magnetic field and react to original alternate magnetic field by changing its amplitude and phase [c].

8.1 Multifield Eddy Current Effect

Rabinovici and Kaplan investigated an eddy current effect which occurs in nonlinear magnetic conductors excited by multiple alternating fields in 1983. The field penetrating into the material contains new magnetic fields whose frequencies is much lower than the frequencies of the excitation fields. They noted that this is due to the relative cancellation (filtering) of the originally high frequency fields by the screening of eddy currents [45].

In 1985, Kaplan and Rabinovici investigated an **eddy current sensor** for DC and low-frequency magnetic fields as shown in Fig. 8.1. This new sensor based on multifield eddy current effects could measure fields with intensities about 10^{-5} Oe or Gauss [34].

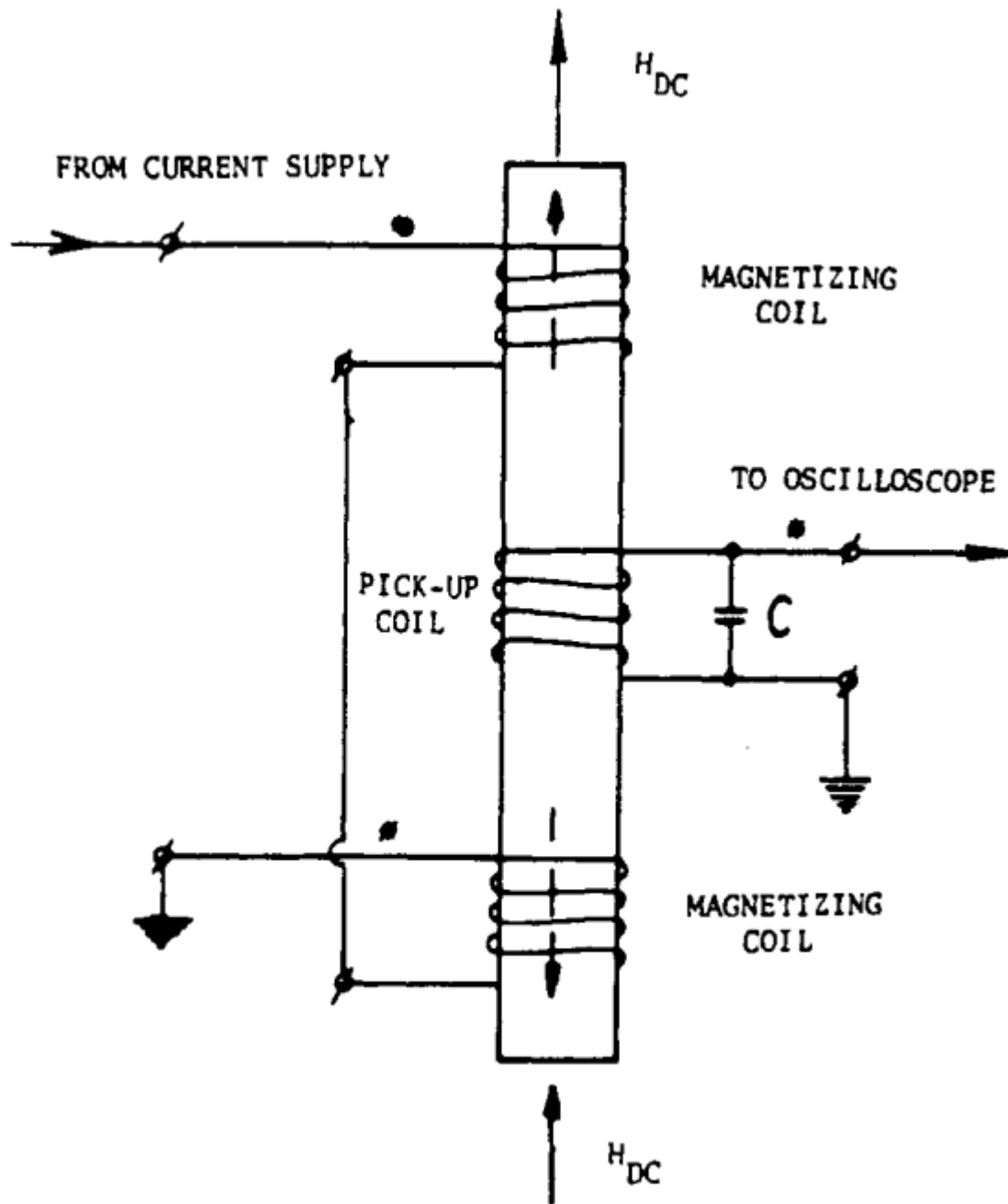


Fig. 1. A practical configuration of the eddy-current sensor.
 ←--: direction of the high-frequency magnetizing fields; ←—: direction of the measured magnetic fields.

Fig. 8.1: : Eddy current sensor.

9.1 Circuit Model of Dipole Antenna

Tang et al investigated a lumped equivalent circuit model as shown in Fig. 9.1 to represent the impedance of a electrically small dipole antenna that electrical half-length up to 0.3 wavelength. The elements were related to the physical dimensions of the antenna and independent of the operation frequency. The equivalent circuit comprises the first resonance and all frequencies below the resonance. The proposed model was shown that the radiation resistance had less than 1% error and the reactance had less than 6% error [58].

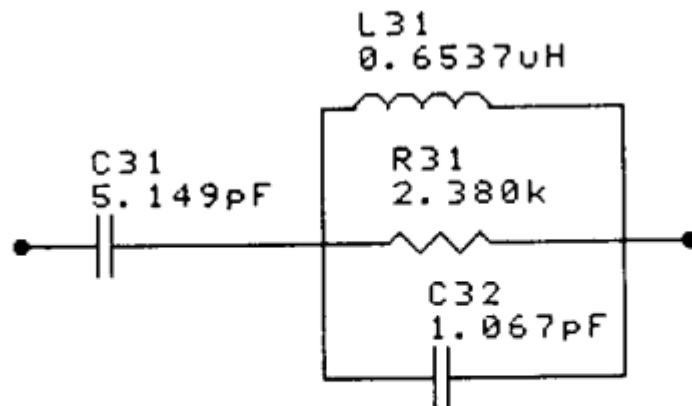


Fig. 3. New four-element equivalent circuit of a dipole ($h = 0.9$ m; $a = 0.00264$ m; $h/a = 341$).

Fig. 9.1: : Four-element equivalent circuit of a dipole.

$$C_{31} = \frac{12.0674h}{\log(2h/a) - 0.7245}$$

$$C_{32} = 2h \left\{ \frac{0.89075}{[\log(2h/a)]^{0.8006} - 0.861} - 0.02541 \right\}$$

$$L_{31} = 0.2h \{ [1.4813 \log(2h/a)]^{1.012} - 0.6188 \}$$

$$R_{31} = 0.41288[\log(2h/a)]^2 + 7.40754(2h/a)^{-0.02389} - 7.27408$$

CHAPTER 10

Fundamental Limit

11.1 Power Loss

Manteghi and Ibraheem investigated power loss of an electric and a magnetic dipole in a lossy medium. Near-field loss formulation was given and radiated power of antennas were also given. They concluded that magnetic antennas like loop antennas had *significant advantage* over electric field antennas such as dipoles regards to power loss in a lossy medium [38].

2014	On the study of the near-fields of electric and magnetic small antennas in lossy media
2017	Analytical modeling and optimization of small solenoid coils for millimeter-sized biomedical implants

Magnetically Shielded Wire

A magnetically shielded wire (MSW), in other words magnetoplated wire (MPW), is generally a copper wire which has magnetic-conductive thin layers on the surface of the wire. Main advantage of this type of wire is that reduced eddy current losses due to the proximity effect. Thus, the AC resistance of the MSW coil is lower than standard wire coil [41][22].

In order to calculate the eddy current losses in MSWs by the traditional finite element method (FEM), mesh must be generated sufficiently small elements from surface to center i.e. mesh elements must be smaller than the skin depth. This requires a high computing power. Fujita and Igarashi investigated finite-element analysis of MSW coils using homogenization method [22].

CHAPTER 13

Mutual Inductance

When two circuits are so placed that a current in one causes magnetic flux to link the other, a change of current in one necessarily induces an E.M.F. in the other, and the magnitude of this induced E.M.F. when the current is changing at unit rate is called the coefficient of mutual induction, or more briefly, the mutual inductance, between the two circuits [17].

By simply moving one circuit relatively to the other it is possible to change the direction of the induced E.M.F., so that the mutual inductance reverses its sign, and it becomes necessary in writing down the circuit equations to adopt some convention as to what is to be called a positive and what a negative mutual inductance [17].

CHAPTER 14

Nomenclature

- a : Radius of the loop [m]
- A : Cross section area of the loop [m²]
- A_F : Cross section area of ferrite core [m²]
- A_w : Cross section area of winding [m²]
- $c = 3 \cdot 10^8$: Speed of light [m/s]
- C : Circumference of the loop [m]
- D : Diameter of the loop antenna [m]
- D_F : Demagnetization factor of ferrite core
- D_w : Demagnetization factor of winding
- f : Frequency [Hz]
- l_F : Length of ferrite core [m]
- L_i : Self-inductance of the i th coil [H]
- l_w : Length of winding [m]
- M_{ij} : Mutual inductance between the i th coils
- N : Number of turns of the loop
- R_i : Internal resistance of the i th coil [Ω]
- R_{rad}^{air} : Radiation resistance of N-turn, air-cored loop [Ω]
- R_{rad}^{mc} : Radiation resistance of N-turn, magnetic-cored loop [Ω]
- v : Velocity of the EM wave [m/s]
- V_c : Fractional volume of the iron [m:sup:3]
- κ_{ij} : Coupling coefficient between the i th coils
- λ : Wavelength ($\lambda = v/f$) [m]

- μ : Magnetic permeability
- μ_0 : Magnetic permeability of air [$\approx 4\pi \times 10^{-7}$ H/m]
- μ_{cer} : Relative effective magnetic permeability of the core
- μ_e : Effective magnetic permeability of the core
- μ'_e : Real part of effective magnetic permeability of the core
- μ''_e : Imaginary part of effective magnetic permeability of the core
- μ_r : Relative magnetic permeability of air
- σ : Conductivity [S/m]

14.1 Derivations from other quantities

- $H = \text{kg.m}^2.\text{s}^{-2}.\text{A}^{-2}$
- $\text{Wb} = \text{V.s} = \text{kg.m}^2.\text{s}^{-2}.\text{A}$
- $S = 1/\Omega$

CHAPTER 15

Abbreviations

- EM: ElectroMagnetic
- FEM: Finite Element Method
- MPW: Magnetoplated Wire
- MSW: Magnetically Shielded Wire
- RLC: Resistance, Inductance, Capacitance
- Rx: Receiver
- SRF: Self-Resonance Frequency
- WPT: Wireless Power Transfer

CHAPTER 16

References

CHAPTER 17

Fingerprints of Papers

1929	Positive and negative mutual inductance	mutual inductance
2004	Low-frequency transient (time domain) electromagnetic fields propagating in a marine environment	seawater lossy medium

Note: Dictionary style definitions of terms are good organized and some important notes clarify complicated issues about magnetic testing [3]. See *Magnetic Testing* chapter.

18.1 Aperture (of an antenna)

#A surface, near or on an antenna, on which it is convenient to make assumptions regarding the field values for the purpose of computing fields at external points. **Note:** The aperture is often taken as that portion of a plane surface near the antenna, perpendicular to the direction of maximum radiation, through which the major part of the radiation passes [29].

#The power received by an antenna can be described in terms of a collecting area known as the effective aperture. This may be associated with a physical aperture but even a linear wire antenna can be described in terms of a notional collecting area. If the electromagnetic field has a power density of P_d , and the receiving antenna has an effective aperture of A_e then it will capture a power of $P_d A_e$. The effective area depends only on the wavelength of the radiation and the directivity or gain [23].

18.2 Balanced Line

A balanced line or balanced signal pair is a transmission line consisting of two conductors of the same type, each of which have equal impedances along their lengths and equal impedances to ground and to other circuits. They are to be contrasted to *unbalanced lines*, such as coaxial cable, which is designed to have its return conductor connected to ground, or circuits whose return conductor actually is ground. Balanced and unbalanced circuits can be interconnected using a transformer called a balun. [Read more from Wikipedia](#)

18.3 Balun

A balun (for balanced to unbalanced) is an electrical device that converts between a *balanced line* (or signal) and an *unbalanced line* (or signal). Transformer baluns can also be used to connect lines of differing impedance. [Read more from Wikipedia](#)

18.4 Chu Limit

#In electrical engineering and telecommunications the Chu–Harrington limit or Chu limit sets a lower limit on the Q factor for a small radio antenna. The theorem was developed in several papers between 1948 and 1960 by Lan Jen Chu, Harold Wheeler, and later by Roger Harrington. The definition of a small antenna is one that can fit inside a sphere of radius k^{-1} , where $k = 2\pi/\lambda$ is the wavenumber. For a small antenna the Q is proportional to the reciprocal of the volume of a sphere that encloses it. In practice this means that there is a limit to the bandwidth of data that can be sent to and received from small antennas such as are used in mobile phones.

More specifically, Chu established the limit on Q for a lossless and linear polarized antenna as

$$Q \geq \frac{1}{k^3 a^3} + \frac{1}{ka}$$

where a is the radius of the smallest sphere containing the antenna and its current distribution. A circular polarized antenna can be half the size. (an extension of the theory of Chu by Harrington). As antennas are made smaller, the bandwidth shrinks and radiation resistance becomes smaller compared to loss resistances that may be present, thus reducing the radiation efficiency. For users this decreases the bitrate, limits range, and shortens battery life. [http://en.turkcewiki.org/wiki/Chu–Harrington_limit]

18.5 Coupling Coefficient

The coupling coefficient between the transmitting and the receiving coils as [71]

$$\kappa_{12} = \frac{M_{12}}{\sqrt{L_1 L_2}}$$

18.6 Like and Unlike Antennas

In a two antennas system, if both antennas are electric or magnetic, it is called *like antennas* or if one antenna is electric and the other one is magnetic, it is called *unlike antennas*.

18.7 Magnetic susceptibility

#Magnetic susceptibility is a dimensionless proportionality constant that indicates the degree of magnetization of a material in response to an applied magnetic field. A related term is magnetizability, the proportion between magnetic moment and magnetic flux density. A closely related parameter is the permeability, which expresses the total magnetization of material and volume.

#The volume magnetic susceptibility, represented by the symbol χ_v (often simply χ , sometimes χ_m magnetic, to distinguish from the electric susceptibility), is defined in the SI units by the following relationship:

$$M = \chi H$$

Here

- M is the magnetization of the material (the magnetic dipole moment per unit volume), measured in amperes per meter,
- H is the magnetic field strength, also measured in amperes per meter.
- χ is therefore a dimensionless quantity.

18.8 Modal Analysis

Modal analysis is the study of the dynamic properties of systems in the frequency domain. [http://en.turkcewiki.org/wiki/Modal_analysis]

18.9 Orthogonal Signals

The orthogonality in signals means that the receiver can detect any one of them separately, and that is the meaning of non interference.

18.10 Torquer

Magnetic torquer rods (also known as torquers, torque rods, torque bars, torqrods, or magnetorquers) are widely used as attitude control system (ACS) actuators for geostationary satellites, small satellites, and microsatellites. A magnetic torquer rod is essentially a long copper wire wound around a core. The core material could be special alloys or simply air. With a metal core, the magnetic torquer rod can generate a larger magnetic dipole moment at the expense of a larger residual moment as compared with the air-core type. Magnetic torquer rods are designed to generate controllable magnetic dipole moments that interact with the Earth's magnetic field and generate torques for active attitude control purposes for spacecraft (Sidi, 1997;Wertz, 1978). Torque T_{mag} of a magnetic torquer is given by the cross product of its magnetic dipole moment M and the Earth's magnetic-field vector B , i.e., $T_{mag} = M \times B$. Magnetic control systems have the characteristics of relatively light weight and require no moving parts, expendables, or complex hardware.

18.11 Unbalanced Line

An unbalanced line is a transmission line, often coaxial cable, whose conductors have unequal impedances with respect to ground; as opposed to a *balanced line*. Microstrip and single-wire lines are also unbalanced lines. [Read more from Wikipedia](#)

CHAPTER 19

Useful Links

- Magnetic Field Shielding - <https://www.lessemf.com/mag-shld.html>

CHAPTER 20

Journals

Physics

- Canadian Journal of Physics
- Journal of Applied Physics (AIP)

Note: Loop antennas that operate low frequency (LF) or below are taken part in for the most part of this book. Medium frequency (MF) or above antennas are taken part in only if necessary.

Note: This book is a kind of Loop Antennas book by Prof. Serkan Aksoy. For further information, please visit the page of the book: .

Bibliography

- [1] American Radio Relay League. *The ARRL Antenna Book: The Ultimate Reference for Amateur Radio Antennas, Transmission Lines And Propagation 21*. Ed. Amer Radio Relay League, may 2007. ISBN 0872599876.
- [2] Specification for wrought nickel-iron soft magnetic alloys (UNS k94490, k94840, n14076, n14080). URL: <https://doi.org/10.1520/a0753-08r13>, doi:10.1520/a0753-08r13.
- [3] ASTM Committee A06. Standard terminology of symbols and definitions relating to magnetic testing. ASTM International, 7 2018.
- [4] Ugur Aydin, Paavo Rasilo, Florian Martin, Deepak Singh, Laurent Daniel, Anouar Belahcen, Mahmoud Rekik, Olivier Hubert, Reijo Kouhia, and Antero Arkkio. Magneto-mechanical modeling of electrical steel sheets. *Journal of Magnetism and Magnetic Materials*, 439:82–90, 2017.
- [5] U Aydin, F Martin, P Rasilo, A Belahcen, A Haavisto, D Singh, L Daniel, and A Arkkio. Rotational single sheet tester for multiaxial magneto-mechanical effects in steel sheets. *IEEE Transactions on Magnetics*, 55(3):1–10, 2019.
- [6] WS Bachman. Loop-antenna coupling-transformer design. *Proceedings of the IRE*, 33(12):865–867, 1945.
- [7] Shuzhong Bai and Yuhua Bai. High precision algorithm of metal detector based on balance coil. In *2018 21st International Conference on Electrical Machines and Systems (ICEMS)*, 684–687. IEEE, 2018.
- [8] Constantine A. Balanis. *Antenna Theory: Analysis and Design*. Wiley-Interscience, New York, NY, USA, 2005. ISBN 0471714623.
- [9] Gary Breed. Basic principles of electrically small antennas. *High Frequency Electronics*, 6(2):50–53, 2007.
- [10] Harold B Buie. An optimized ultra low frequency shielded-loop antenna. Technical Report, Radiation Branch, Electromagnetics Laboratory, Directorate of Research and Development, U.S. Army Missile Command, Redstone Arsenal, Alabama, 1963.
- [11] RE Burgess. Iron cored loop receiving aerial. *Wireless Engineer*, 23:172–178, 1946.
- [12] Charles Capps. Near field or far field. *EDN Magazine*, pages 95–102, August 2001.
- [13] Andrew J Compston, James D Fluhler, and Hans G Schantz. A fundamental limit on antenna gain for electrically small antennas. In *2008 IEEE Sarnoff Symposium*, 1–5. IEEE, 2008.
- [14] Yuhua Cheng, Gaofeng Wang, and Maysam Ghovanloo. Analytical modeling and optimization of small solenoid coils for millimeter-sized biomedical implants. *IEEE Transactions on Microwave Theory and Techniques*, 65(3):1024–1035, 3 2017.

- [15] Yuhua Cheng, Guoxiong Chen, Dongdong Xuan, Gaorong Qian, Maysam Ghovanloo, and Gaofeng Wang. Analytical modeling of small, solenoidal, and implantable coils with ferrite tube core. *IEEE Microwave and Wireless Components Letters*, 2019.
- [16] R DeVore and P Bohley. The electrically small magnetically loaded multiturn loop antenna. *IEEE Transactions on Antennas and Propagation*, 25(4):496–505, 1977.
- [17] Editorial. Positive and negative mutual inductance. *Experimental Wireless & The Wireless Engineer*, 6(68):233–234, 5 1929.
- [18] Evren Ekmekci. Vlf antennas. University Lecture, 2004.
- [19] E Fraga, C Prados, and D-X Chen. Practical model and calculation of ac resistance of long solenoids. *IEEE Transactions on Magnetics*, 34(1):205–212, 1998.
- [20] SV Fratianni. Theory and design of resonant transformer-coupled loop-antenna input systems for vlf reception. Technical Report, NAVAL RESEARCH LAB WASHINGTON DC, 1948.
- [21] SV Fratianni. Vlf signal reception capability of three experimental crossed-loop antennas. Technical Report, NAVAL RESEARCH LAB WASHINGTON DC, 1955.
- [22] S. Fujita and H. Igarashi. Finite-element analysis of magnetically shielded wire coils using homogenization method. *IEEE Transactions on Magnetics*, 54(3):1–4, March 2018. doi:10.1109/TMAG.2017.2758445.
- [23] David Gibson. *Channel characterisation and system design for sub-surface communications*. Lulu.com, 2010.
- [24] Kiran Gupta, KK Raina, and SK Sinha. Effect of annealing temperature on the magnetic behaviour of ni-rich permalloy magnetic materials. *Indian Journal of Engineering & Materials Sciences*, 12:577–585, 2005.
- [25] Pekka Heinonen, Markku Tuomola, Jukka Lekkala, and Jaakko Malmivuo. Properties of a thick-walled conducting enclosure in low-frequency magnetic shielding. *Journal of Physics E: Scientific Instruments*, 13(5):569, 1980.
- [26] AA Hemphill. A magnetic radio compass antenna having zero drag. *IRE Transactions on Aeronautical and Navigational Electronics*, pages 17–22, 1955.
- [27] Lorimer K Hill, Jr Francis X Bostick, and others. Micropulsation sensors with laminated mumetal cores. Technical Report, TEXAS UNIV AT AUSTIN ELECTRICAL ENGINEERING RESEARCH LAB, 1962.
- [28] Hojo, Hirofumi, Tomotsuna KAMIJO, Yuji TANIGUCHI, Nobuaki AKAGI, and Hiroyuki MITANI. Dust core with low core-loss for high-frequency applications. *Kobelco Technology Review*, pages 23–27, 2017.
- [29] IEEE Standards Board. Ieee standard definitions of terms for antennas. *IEEE Std 145-1993*, pages 1–32, 1993. doi:10.1109/IEEESTD.1993.119664.
- [30] FC Isely. Test of underwater reception of low frequency radio signals. Technical Report, NAVAL RESEARCH LAB WASHINGTON DC, 1941.
- [31] M. Islam. A theoretical treatment of low-frequency loop antennas with permeable cores. *IEEE Transactions on Antennas and Propagation*, 11(2):162–169, March 1963. doi:10.1109/TAP.1963.1138007.
- [32] Mohammed Azizul Islam. Mathematical analysis on the effect of a prolate spheroidal core in a magnetic dipole field. *Journal of Mathematical Physics*, 4(9):1206–1212, 1963.
- [33] Alhussain Jabbar S. Hussein Ahmed A. Aouda. Transmitting loop antenna for efficiency enhancement. *Journal of Babylon University Engineering Sciences*, 21(3):987–994, 2013.
- [34] BZ Kaplan and R Rabinovici. Eddy-current sensor for dc and low-frequency magnetic fields. *Proceedings of the IEEE*, 73(6):1147–1148, 1985.
- [35] Jinwook Kim and Young-Jin Park. Approximate closed-form formula for calculating ohmic resistance in coils of parallel round wires with unequal pitches. *IEEE transactions on Industrial Electronics*, 62(6):3482–3489, 2014.
- [36] David Knight. Low-frequency effective radius of a single-layer solenoid. Personal web page, 2000.

- [37] J.D. Kraus. *ANTENNAS, 2D ED*. Electrical Engineering Series. McGraw-Hill, 1988. ISBN 9780070354227. URL: <https://archive.org/details/Antennas2ndbyJohnD.Kraus1988>.
- [38] Majid Manteghi and Ali Ahmed Younis Ibraheem. On the study of the near-fields of electric and magnetic small antennas in lossy media. *IEEE Transactions on antennas and propagation*, 62(12):6491–6495, 2014.
- [39] Richard Q. Marris. Ultima loopstick vlf antenna. *Elector Electronics*, pages 108–111, 1998.
- [40] M. Mirzaei and P. Ripka. Analytical functions of magnetization curves for high magnetic permeability materials. *IEEE Transactions on Magnetics*, 54(11):1–5, Nov 2018. doi:10.1109/TMAG.2018.2827932.
- [41] T. Mizuno, S. Enoki, T. Asahina, T. Suzuki, M. Noda, and H. Shinagawa. Reduction of proximity effect in coil using magnetoplated wire. *IEEE Transactions on Magnetics*, 43(6):2654–2656, June 2007. doi:10.1109/TMAG.2007.893716.
- [42] Ruediger Dr Karmann. Magnetometer. Patent no: DE2625964A1, 12 1977.
- [43] Alan Payne. Self resonance in single layer coils. Personal web page, 2014.
- [44] R Pettengill, H Garland, and J Meindl. Receiving antenna design for miniature receivers. *IEEE Transactions on Antennas and Propagation*, 25(4):528–530, 1977.
- [45] R Rabinovici and BZ Kaplan. New multifold eddy-current effects. *Proceedings of the IEEE*, 71(5):682–683, 1983.
- [46] Paavo Rasilo, Ugur Aydin, Floran Martin, Anouar Belahcen, Reijo Kouhia, and Laurent Daniel. Equivalent strain and stress models for the effect of mechanical loading on the permeability of ferromagnetic materials. *IEEE Transactions on Magnetics*, 55(6):1–4, 2019.
- [47] Alberto Reatti and Marian K Kazimierczuk. Comparison of various methods for calculating the ac resistance of inductors. *IEEE Transactions on Magnetics*, 38(3):1512–1518, 2002.
- [48] Eric A Richards, Hans G Schantz, John A Uden, Kurt A von Laven, Drew Compston, and Christian Weil. Electrically small antenna design for low frequency systems. *NOTICE AND SIGNATURE PAGE*, pages 315, 2010.
- [49] Christof Rohner. Antenna basics. *Rohde & Schwarz White Paper*, pages 24–25, 2006.
- [50] V Rumsey and W Weeks. Electrically small, ferrite-loaded loop antennas. In *1958 IRE International Convention Record*, volume 4, 165–170. IEEE, 1966.
- [51] Hans Schantz. Near field channel model, ieeep802.15-04/0417r2. *IEEE P802*, 15(04):1–8, 2004.
- [52] Hans Gregory Schantz. Near field phase behavior. In *2005 IEEE antennas and propagation society international symposium*, volume 3, 134–137. IEEE, 2005.
- [53] Hans Gregory Schantz. Near field propagation law & a novel fundamental limit to antenna gain versus size. In *2005 IEEE Antennas and Propagation Society International Symposium*, volume 3, 237–240. IEEE, 2005.
- [54] Hans G Schantz. A real-time location system using near-field electromagnetic ranging. In *2007 IEEE Antennas and Propagation Society International Symposium*, 3792–3795. IEEE, 2007.
- [55] Eric Charles Snelling and others. *Soft ferrites: properties and applications*. Iliffe Books London, 1969.
- [56] William D Stanley and Richard D Tinkler. A practical, low-noise coil system for magnetotellurics. Technical Report, US Geological Survey, 1983.
- [57] J Stewart. On ferrite loop antenna measurements. In *1958 IRE International Convention Record*, volume 5, 42–48. IEEE, 1966.
- [58] Tee G Tang, Quang M Tieng, and Moms W Gunn. Equivalent circuit of a dipole antenna using frequency-independent lumped elements. *IEEE Transactions on Antennas and Propagation*, 41(1):100–103, 1993.
- [59] Emerick Toth and SV Fratianni. Underwater loop reception phenomena and techniques-and appendix. Technical Report, NAVAL RESEARCH LAB WASHINGTON DC, 1950.

- [60] Pavel Turalchuk, Irina Munina, Michail Derkach, Orest Vendik, and Irina Vendik. Electrically small loop antennas for rfid applications. *IEEE antennas and wireless propagation letters*, 14:1786–1789, 2015.
- [61] Yousufzai M.A.K. Waheed-uz-Zaman, M. Design and construction of very low frequency antenna. *Journal of Basic & Applied Sciences*, 2011.
- [62] JR Wait and KP Spies. Low-frequency impedance of a circular loop over a conducting ground. *Electronics Letters*, 9(15):346–348, 1973.
- [63] Wikipedia contributors. Antenna gain — Wikipedia, the free encyclopedia. 2019. [Online; accessed 7-March-2019]. URL: https://en.wikipedia.org/w/index.php?title=Antenna_gain&oldid=876776674.
- [64] Wikipedia contributors. Electromagnetic spectrum — Wikipedia, the free encyclopedia. 2019. [Online; accessed 14-February-2019]. URL: https://en.wikipedia.org/w/index.php?title=Electromagnetic_spectrum&oldid=882410353.
- [65] Wikipedia contributors. Magnetic core — Wikipedia, the free encyclopedia. 2018. [Online; accessed 3-January-2019]. URL: https://en.wikipedia.org/w/index.php?title=Magnetic_core&oldid=872148801.
- [66] Wikipedia contributors. Magnetometer — Wikipedia, the free encyclopedia. 2019. [Online; accessed 18-April-2019]. URL: <https://en.wikipedia.org/w/index.php?title=Magnetometer&oldid=891846955>.
- [67] Wikipedia contributors. Radio direction finder — Wikipedia, the free encyclopedia. 2019. [Online; accessed 24-May-2019]. URL: https://en.wikipedia.org/w/index.php?title=Radio_direction_finder&oldid=897173877.
- [68] Wikipedia contributors. Radio spectrum — Wikipedia, the free encyclopedia. 2019. [Online; accessed 28-February-2019]. URL: https://en.wikipedia.org/w/index.php?title=Radio_spectrum&oldid=884481320.
- [69] Wikipedia contributors. Real-time locating system — Wikipedia, the free encyclopedia. 2019. [Online; accessed 28-February-2019]. URL: https://en.wikipedia.org/w/index.php?title=Real-time_locating_system&oldid=878335872.
- [70] Z. Zhang, B. Zhang, and J. Wang. Optimal design of quadrature-shaped pickup for omnidirectional wireless power transfer. *IEEE Transactions on Magnetics*, 54(11):1–5, Nov 2018.
- [71] Z. Zhang, H. Pang, A. Georgiadis, and C. Cecati. Wireless power transfer—an overview. *IEEE Transactions on Industrial Electronics*, 66(2):1044–1058, Feb 2019. doi:10.1109/TIE.2018.2835378.